

NASA TECHNICAL MEMORANDUM

(NASA-TM-82483) A BIVARIATE GAMMA
PROBABILITY DISTRIBUTION WITH APPLICATION TO
GUST MODELING (NASA) 101 p HC A06/MP A01

CSSL 12A

N82-29094

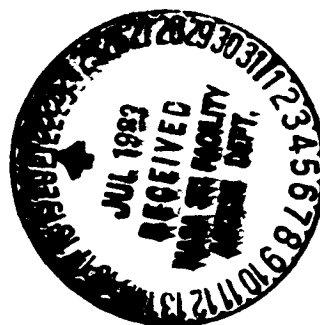
G3/65 Unclass
28399

NASA TM-82483

A BIVARIATE GAMMA PROBABILITY DISTRIBUTION WITH
APPLICATION TO GUST MODELING

By O. E. Smith, S. I. Adelfang, and J. D. Tubbs
Space Sciences Laboratory

July 1982



NASA

*George C. Marshall Space Flight Center
Marshall Space Flight Center, Alabama*

1. REPORT NO. NASA TM-82483	2. GOVERNMENT ACCESSION NO.	3. RECIPIENT'S CATALOG NO.
4. TITLE AND SUBTITLE A Bivariate Gamma Probability Distribution with Application to Gust Modeling		5. REPORT DATE July 1982
		6. PERFORMING ORGANIZATION CODE
7. AUTHOR(S) O. E. Smith, S. I. Adelfang,* and J. D. Tubbs**		8. PERFORMING ORGANIZATION REPORT #
9. PERFORMING ORGANIZATION NAME AND ADDRESS George C. Marshall Space Flight Center Marshall Space Flight Center, Alabama 35812		10. WORK UNIT NO.
		11. CONTRACT OR GRANT NO.
12. SPONSORING AGENCY NAME AND ADDRESS National Aeronautics and Space Administration Washington, D.C. 20546		13. TYPE OF REPORT & PERIOD COVERED Technical Memorandum
		14. SPONSORING AGENCY CODE
15. SUPPLEMENTARY NOTES *Computer Sciences Corporation, 300 Sparkman Drive, Huntsville, Alabama 35805 **University of Arkansas, Fayetteville, Arkansas 72701 Prepared by Space Sciences Laboratory, Science and Engineering Directorate		
16. ABSTRACT A five-parameter gamma distribution (BGD) having two shape parameters, two location parameters, and a correlation parameter is investigated. This general BGD is expressed as a double series and as a single series of the modified Bessel function. This general BGD reduces to the known special case for equal shape parameters. Practical functions for computer evaluations for the general BGD and for special cases are presented. Applications of the general BGD are to be found in reliability theory, signal noise, and meteorology. In this paper, applications to wind gust modeling for the ascent flight of the Space Shuttle are illustrated.		
17. KEY WORDS 5 Parameter Special cases Properties Computing Gust modeling		18. DISTRIBUTION STATEMENT <i>O.E. Smith</i> Unclassified Unlimited
19. SECURITY CLASSIF. (of this report) Unclassified	20. SECURITY CLASSIF. (of this page) Unclassified	21. NO. OF PAGES 99
		22. PRICE NTIS

PRECEDING PAGE BLANK NOT FILMED

TABLE OF CONTENTS

1.	Introduction	2
2.	Summary of Functions	4
2.1	Bivariate Gamma Density Function	4
2.2	Bivariate Probability Distribution Functions	7
2.3	Sector Probabilities	9
2.4	Probability in Triangles	14
2.5	Properties of the Conditional Distribution	21
2.6	Illustrations and Properties of the Bivariate Gamma Distribution	25
3.	Application	40
3.1	Data	40
3.2	Results	41
4.	Concluding Remarks	56
	Bibliography	58
	Appendix - Graphic Illustrations	A-1

LIST OF ILLUSTRATIONS

<u>Figure</u>		<u>Page</u>
1	Probability in a Rectangle.	7
2	Probability in a Sector	10
3	Probability in a Right Triangle	15
4	Probability in an Equilateral Right Triangle .	19
5a,b 6a,b 7a,b	Contours of Equal Probability Density (Schematics)	26
8a	Density Contours for $\gamma = 2$, $\rho = 0.25$	29
8b	Density Contours for $\gamma = 2$, $\rho = 0.50$	30
8c	Density Contours for $\gamma = 2$, $\rho = 0.75$	31
9a	Density Contours for $\gamma = 3$, $\rho = 0.25$	32
9b	Density Contours for $\gamma = 3$, $\rho = 0.50$	33
9c	Density Contours for $\gamma = 3$, $\rho = 0.75$	34
10	Mode, Z , Versus γ for Correlations, ρ	38
11	Density Mode Versus γ for Correlations, ρ . . .	39
12	Band-Pass Profiles Derived from a Jimsphere Wind Profile at Cape Canaveral, Florida (2/23/71, 1445 GMT)	42
13	Schematic Definition of Gust	43
14	Gamma and Observed PDF of Gust Component Amplitude, $ u' $, from 90-420m, 420-2470m, 2470-6000m Wavelength Band Filters at 12km Altitude, February, Cape Canaveral, Florida .	45
15	Gamma and Observed PDF of Gust Length, L_u , from 90-420m, 420-2470m, 2470-6000m Wavelength Band Filters at 12km Altitude, February, Cape Canaveral, Florida	46

LIST OF ILLUSTRATIONS (Cont'd.)

<u>Figure</u>		<u>Page</u>
16	Gamma PDF of Gust Component Amplitude $ u' $, from 420-2470m Wavelength Band Filter at 4, 6, ..., 14km Altitudes, February, Cape Canaveral, Florida	47
17	PDF of Gust Component Amplitude, $ u' $, from 420-2470m Wavelength Band at 12km Altitude for February, July, October, Cape Canaveral, Florida	48
18	Conditional PDF of Gust Component Amplitude, $ u' $, Given Gust Length, L_u , from 420-2470m Wavelength Band Filter at 12km Altitude, February, Cape Canaveral, Florida	50
19	Percentiles of Conditional Gust Component Amplitudes, $ u' $, Given Gust Length, L_u , from 420-2470m Wavelength Band Filter at 12km Altitude, February, Cape Canaveral, Florida .	51
20	Observed Non-Dimensional Gust Variables T_1 and T_2	53

LIST OF TABLES

<u>Table</u>		<u>Page</u>
1	Results of Testing the Hypothesis That the Samples of u and v Component Absolute Gust Length are Drawn from Gamma Distributed Populations	49
2	Observed and Expected Number of Occurrences within 2x2 Cells for Nondimensional Variables T_1 and T_2 Calculated from Absolute u Compo- nent Gust and Gust Length, L_u , at 12 km . .	54
3	Sector Probabilities for Equal Area Sectors (Calculated from Equation 2.14), $\gamma_1 = 2$. . .	55

A BIVARIATE GAMMA PROBABILITY DISTRIBUTION
WITH APPLICATION TO GUST MODELING

by

O. E. Smith
Space Sciences Laboratory
National Aeronautics and Space Administration
George C. Marshall Space Flight Center
Marshall Space Flight Center, Alabama 35812

S. I. Adelfang
Applied Technology Division
Computer Sciences Corporation
Huntsville, Alabama 35805

J. D. Tubbs
Department of Mathematics
University of Arkansas
Fayetteville, Arkansas 72701

ABSTRACT

A five-parameter gamma distribution (BGD) having two shape parameters, two location parameters, and a correlation parameter is investigated. This general BGD is expressed as a double series and as a single series of the modified Bessel function. This general BGD reduces to the known special case for equal shape parameters. Practical functions for computer evaluations for the general BGD and for special cases are presented. Applications of the general BGD are to be found in reliability theory, signal noise, and meteorology. In this paper, applications to wind gust modeling for the ascent flight of the Space Shuttle are illustrated.

This report is from a draft manuscript prepared to meet the requirements for a presentation at the American Statistical Association (ASA) National Annual Meeting, August 16-19, 1982, at Cincinnati, Ohio. The paper for the ASA meeting was accepted and will be presented. A version of this report will be submitted to the ASA for consideration for publication.

1. INTRODUCTION

Gunst and Webster (1973) discussed the need for a practical method of dealing with dependent chi-square variates. They stated that most of the known results discussing the bivariate chi-square and related bivariate F-distributions were too prohibitive for practical use in that they either involved mathematical functions such as Laguerre polynomials and convoluted sums or that they were too restrictive in the number of parameters. While Gunst and Webster were primarily concerned with dependent chi-square variates, it is obvious that the same is true for practical use of dependent gamma variates. For example, earlier work by authors such as Kibble (1941), Krishnamoorthy and Parthasarathy (1951), and Downton (1970) were restricted to the bivariate gamma with equal shape parameters. Jensen (1970) and Jensen and Howe (1968) were able to consider the unequal shape distributions; however, their results are computationally restrictive. Recently, McAllister, Lee, and Holland (1981) have been able to give efficient methods for computing probabilities from Jensen's joint bivariate F-distribution; however, this method is still difficult to use.

In this paper the results given by Gunst and Webster have been investigated as a computational model for the bivariate gamma distribution with unequal shape parameters.

Several functions, such as the conditional distributions and probabilities in different geometric regions, are also considered. Each of these expressions were of interest in considering applications to wind gust modeling for the ascent flight of the Space Shuttle.

Section 2 summarizes the results for the five-parameter bivariate density function and considers some special properties of the density function. Expressions are derived for probabilities over different geometrically shaped regions. Some properties of the conditional distribution functions are also presented. Section 3 presents an application of the bivariate gamma probability functions for wind gust modeling.

2. SUMMARY OF FUNCTIONS

2.1 Bivariate Gamma Probability Density Function

2.1.1 A Five-Parameter Bivariate Gamma Density Function

In this section, the results given by Gunst and Webster (1970) for the bivariate chi-square are extended to the bivariate gamma distribution with unequal shape parameters $\gamma_1 < \gamma_2$ given by

$$f(t_1, t_2; \gamma_1, \gamma_2, \eta) = \frac{t_1^{\gamma_1-1} t_2^{\gamma_2-1} \exp - \{(t_1+t_2)/(1-\eta)\}}{(1-\eta)^{\gamma_1} \Gamma(\gamma_1) \Gamma(\gamma_2-\gamma_1)} \\ \times \sum_{k=0}^{\infty} \sum_{j=0}^{\infty} \frac{\eta^{j+k}}{(1-\eta)^{2j+k}} \frac{\Gamma(\gamma_2-\gamma_1+k)}{\Gamma(\gamma_2+j+k)} \frac{(t_1 \cdot t_2)^j t_2^k}{j! k!} \quad (2.1)$$

Where $t_1 = \beta_1 x$, $t_2 = \beta_2 y$, β_1 and β_2 are known scale parameters

and $\eta = \rho \sqrt{\gamma_2/\gamma_1}$ where ρ is the correlation coefficient

between the variables x and y .

Due to the method of construction by Gunst and Webster, the above bivariate gamma density function has five parameters; namely, β_1 , β_2 , γ_1 , γ_2 , and η . However, the model is not completely general in that the correlation between the

ORIGINAL PAGE IS
OF POOR QUALITY

variables x and y , denoted by ρ is restricted to

$$0 \leq \rho \leq \left(\frac{\gamma_1}{\gamma_2} \right)^{\frac{1}{2}} \eta \quad (2.2)$$

Thus, the model is very restrictive whenever $\gamma_2 \gg \gamma_1$ and ρ is large. To the authors' knowledge, Moran (1969) has an expression for the general five-parameter gamma distribution. However, his expression for the density function is computationally unfeasible for most practical applications.

The above function (2.1) can be expressed as a single series in terms of the modified Bessel function of the first kind, $I_\nu(z)$ as:

$$f(t_1, t_2; \gamma_1, \gamma_2, \eta) = \frac{t_1^{\gamma_1-1} t_2^{\gamma_2-1} \exp -\{(t_1+t_2)/(1-\eta)\}}{(1-\eta)^{\gamma_1} \Gamma(\gamma_1) \Gamma(\gamma_2-\gamma_1)} \\ \times \sum_{k=0}^{\infty} \frac{\eta^k \Gamma(\gamma_2-\gamma_1+k) t_2^k}{k! (\eta t_1 t_2)^{k/2}} I_{\gamma_2+k-1} \left\{ \frac{2(\eta t_1 t_2)^{\frac{1}{2}}}{1-\eta} \right\} \quad (2.3)$$

2.1.2 The Four-Parameter Bivariate Gamma Density Function

For equal shape parameters, $\gamma_1 = \gamma_2 = \gamma$, $\eta = \rho$, and 2.1 becomes:

$$f(t_1, t_2; \gamma, \rho) = \frac{(t_1 \cdot t_2)^{\gamma-1} \exp -\{(t_1+t_2)/(1-\rho)\}}{(1-\rho)^\gamma \Gamma(\gamma)} \\ \times \sum_{j=0}^{\infty} \frac{\rho^j (t_1 \cdot t_2)^j}{(1-\rho)^{2j} \Gamma(\gamma+j) j!} \quad (2.4)$$

This function can also be expressed in terms of the Bessel function, as:

$$f(t_1, t_2; \gamma, \rho) = \frac{(t_1 \cdot t_2)^{(\gamma-1)/2} \exp -\{(t_1+t_2)/(1-\rho)\}}{\rho^{(\gamma-1)/2} (1-\rho) \Gamma(\gamma)} \\ \times I_{\gamma-1} \left\{ \frac{2(\rho t_1 \cdot t_2)^{1/2}}{(1-\rho)} \right\} \quad (2.5)$$

This is the form of the four-parameter bivariate gamma density function as derived by Kibble (1941) and reported by Downton (1970). Although no claim can be made that equation 2.1 is a completely generalized five-parameter bivariate gamma density function, it is satisfying to see that 2.1 reduces to the known special case.

Because the four-parameter bivariate gamma density function (2.4) is symmetrical with respect to the line $t_1 = t_2$, a transformation of the coordinates can be made to take advantage of this symmetry as was done by Adelfang and Smith (1981).

ORIGINAL PAGE IS
OF POOR QUALITY

The expressions to give the finite number of terms sufficiently large to ensure convergence to an assigned accuracy of these infinite series expressions for computational evaluations can be established.

2.2 Bivariate Probability Distribution Functions (PDF)

2.2.1 For the five-parameter density function (2.1) the PDF is defined (see Figure 1) as:

$$\int_0^{t_1^*} \int_0^{t_2^*} f(t_1, t_2; \gamma_1, \gamma_2, \eta) dt_2 dt_1$$

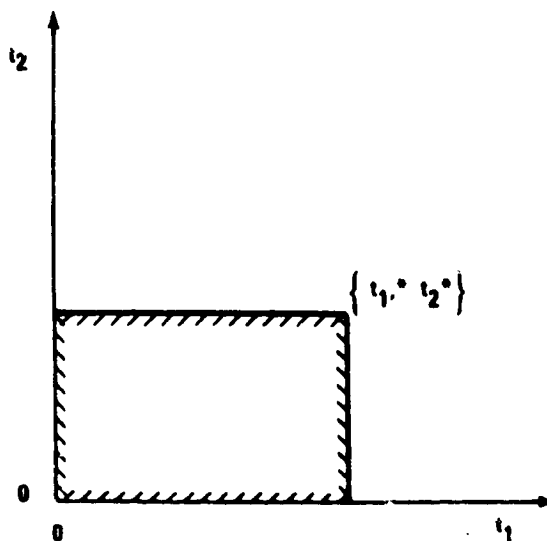


FIG. 1 PROBABILITY IN A RECTANGLE

$$Pr \{t_1 \leq t_1^*, t_2 \leq t_2^*\}$$

ORIGINAL PAGE IS
OF POOR QUALITY

After performing the indicated integration gives:

$$\begin{aligned}
 F[t_1 \leq t_1^*, t_2 \leq t_2^*] &= \Pr\{t_1 \leq t_1^*, t_2 \leq t_2^*\} \\
 &= \frac{(1-\eta)^\gamma}{\Gamma(\gamma_1) \Gamma(\gamma_2 - \gamma_1)} \sum_{k=0}^{\infty} \sum_{j=0}^{\infty} \frac{\eta^{j+k} \Gamma(\gamma_2 - \gamma_1 + k)}{j! k! \Gamma(\gamma_2 + j + k)} \\
 &\quad \times \gamma(\gamma_1 + j, \frac{t_1^*}{1-\eta}) \gamma(\gamma_2 + j + k, \frac{t_2^*}{1-\eta}) .
 \end{aligned} \tag{2.6}$$

Where $\gamma(a, x)$ is the incomplete gamma function which is defined as:

$$\gamma(a, x) = \int_0^x t^{a-1} e^{-t} dt . \tag{2.7}$$

This expression can be expanded in several ways; namely,

$$\gamma(a, x) = \sum_{n=0}^{\infty} \frac{(-1)^n x^{a+n}}{n! (a+n)} , \tag{2.8}$$

$$\gamma(a, x) = a^{-1} \Gamma(1+a) e^{-x} \sum_{n=0}^{\infty} \frac{x^{a+n}}{\Gamma(1+a+n)} , \tag{2.9}$$

and

$$P(a, x) = \gamma(a, x) / \Gamma(a) . \tag{2.10}$$

ORIGINAL PAGE IS
OF POOR QUALITY

The expression 2.9 is of particular usefulness in obtaining the required integration for sector probabilities of Section 2.3.

2.2.2 For the four-parameter function (2.4), the PDF is:

$$\Pr\{t_1 \leq t_1^*, t_2 \leq t_2^*\} = \frac{(1-\rho)^\gamma}{\Gamma(\gamma)}$$
$$\sum_{j=0}^{\infty} \frac{\rho^j}{j!} \frac{\gamma(\gamma+j, t_1^*/(1-\rho)) \gamma(\gamma+j, t_2^*/(1-\rho))}{\Gamma(\gamma+j)} \quad (2.11)$$

Computer programs were developed to evaluate the PDF's using the series expressions and by double numerical integration of the density functions expressed in terms of the Bessel function. Although both methods gave high precision results, the evaluations of the PDF expressed as series were far more efficient in computational time.

2.3 Sector Probabilities

Two expressions are given to determine the probability contained in a sector for both the five-parameter function (2.1) and the four-parameter function (2.4).

2.3.1(a) For the five-parameter function, the probability contained in a sector (see Figure 2, Condition a) is defined as:

$$P_{(\alpha, \infty)} = \int_0^{t_1=\infty} \int_0^{t_2=\alpha t_1} f(t_1, t_2; \gamma_1, \gamma_2, n) dt_2 dt_1 \quad (2.12)$$

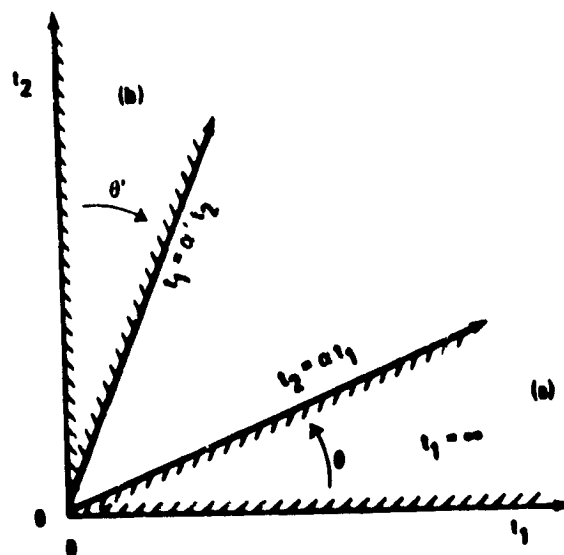


FIG. 2 PROBABILITY IN A SECTOR

(a) $Pr \{t_1 < \infty, t_2 \leq \alpha t_1\}$ (b) $Pr \{t_1 \leq \alpha t_2, t_2 < \infty\}$

ORIGINAL PAGE IS
OF POOR QUALITY

The series expression for the integration of Equation 2.12
is:

$$P_{(\alpha, \infty)} = \frac{\alpha^{\gamma_2} (1-\eta)^{\gamma_2}}{(1+\alpha)^{\gamma_1+\gamma_2} \Gamma(\gamma_1) \Gamma(\gamma_2-\gamma_1)} \\ \times \sum_{k=0}^{\infty} \sum_{j=0}^{\infty} \sum_{n=0}^{\infty} \frac{\eta^{j+k}}{j!k!} \frac{\Gamma(\gamma_2-\gamma_1+k) \Gamma(\gamma_1+\gamma_2+2j+k+n) \alpha^{j+k+n}}{\Gamma(1+\gamma_2+j+k+n) (1+\alpha)^{2j+k+n}}, (2.13)$$

where $\alpha > 0$. $\alpha = \tan^{-1} (t_2^*/t_1^*)$ or $\alpha = \tan \theta$.

For the independent case $\eta = 0$ in 2.12, the sector
probability for 2.13 becomes:

$$P_{(\alpha, \infty)} = \frac{\alpha^{\gamma_2}}{(1+\alpha)^{\gamma_1+\gamma_2} \Gamma(\gamma_1)} \sum_{n=0}^{\infty} \frac{\Gamma(\gamma_1+\gamma_2+n)}{\Gamma(1+\gamma_2+n)} \frac{\alpha^n}{(1+\alpha)^n} \quad (2.14)$$

A special case of interest for computer program checkout is to set $\gamma_1 = 1$ in 2.14 and obtain

$$P_{(\alpha, \infty)} = [\alpha/(1+\alpha)]^{\gamma_2} . \quad (2.15)$$

In addition, by letting $\alpha = \tan\theta$ in 2.14 gives

$$P(\theta, \infty) = [1 + \cot\theta]^{-\gamma_2} \quad (2.16)$$

Further, for $\gamma_1 = 2, 3, 4 \dots$, the series in 2.14 can also be obtained in closed form.

2.3.1(b) For large α expression 2.12 converges slowly. By changing the order of integration of 2.1.2, the probability contained in a sector (condition b in Figure 2) is defined by:

$$P_{(\alpha', \infty)} = \int_0^\infty \int_0^{t_1 = \alpha' t_2} f(t_1, t_2; \gamma_1, \gamma_2, n) dt_1 dt_2 , \quad (2.17)$$

and the sector probability is obtained as

$$P_{(\alpha', \infty)} = \frac{\alpha'^{\gamma_1} (1-\eta)^{\gamma_2}}{(1+\alpha')^{\gamma_1 + \gamma_2} \Gamma(\gamma_1) \Gamma(\gamma_2 - \gamma_1)} \\ \times \sum_{k=0}^{\infty} \sum_{j=0}^{\infty} \sum_{n=0}^{\infty} \frac{\eta^{j+k} \Gamma(\gamma_2 - \gamma_1 + k) \Gamma(\gamma_1 + j) \Gamma(\gamma_1 + \gamma_2 + 2j + k + n) \alpha'^{j+n}}{j! k! \Gamma(\gamma_2 + j + k) \Gamma(1 + \gamma_1 + j + n) (1 + \alpha')^{2j+k+n}} , \quad (2.18)$$

where $\alpha' = \tan^{-1} \frac{t_1^*}{t_2^*}$

or $\alpha' = \tan \theta'$ and $\theta' = (90 - \theta)$.

For the independent case, $\eta = 0$, equation 2.18 becomes

$$P(\alpha', \infty) = \frac{\alpha'^{\gamma_1}}{(1+\alpha')^{\gamma_1+\gamma_2} \Gamma(\gamma_2)} \sum_{n=0}^{\infty} \frac{\Gamma(\gamma_1+\gamma_2+n)}{\Gamma(1+\gamma_1+n)} \frac{\alpha'^n}{(1+\alpha')^n} \quad (2.19)$$

Note for the special cases, $\eta = 0$; comparing 2.19 with 2.13 it is seen that the subscripts to the shape parameters are interchanged and that α is replaced by α' .

2.3.2 Sector Probability for the Four-Parameter Function

2.3.2(a) For equal shape parameters, $\gamma_1 \equiv \gamma_2 = \gamma$ (see Figure 2, condition a), the probability in a sector is:

$$P(\alpha, \infty) = \frac{\alpha^\gamma}{(1+\alpha)^{2\gamma}} \frac{(1-\rho)^\gamma}{\Gamma(\gamma)} \sum_{j=0}^{\infty} \sum_{n=0}^{\infty} \frac{\rho^j}{j!} \frac{\Gamma(2\gamma+2j+n)}{\Gamma(1+\gamma+j+n)} \frac{\alpha^{j+n}}{(1+\alpha)^{2j+n}} \quad (2.20)$$

and for $\rho = 0$ Equation 2.20 becomes:

$$P(\alpha, \infty) = \frac{\alpha^\gamma}{(1-\alpha)^{2\gamma}} \sum_{n=0}^{\infty} \frac{\Gamma(2\gamma+n) \alpha^n}{\Gamma(1+\gamma+n) (1+\alpha)^n} \quad (2.21)$$

2.3.2(b) For equal shape parameters, $\gamma_1 \equiv \gamma_2 = \gamma$, the sector probability for condition b shown in Figure 2 is:

$$P(\alpha', \infty) = \frac{\alpha'^\gamma (1-\rho)^\gamma}{(1+\alpha')^{2\gamma} \Gamma(\gamma)} \times \sum_{j=0}^{\infty} \sum_{n=0}^{\infty} \frac{\rho^j \Gamma(2\gamma+2j+n) \alpha'^{j+n}}{j! \Gamma(1+\gamma+j+n) (1+\alpha')^{2j+n}} \quad (2.22)$$

2.4 Probability in Triangles

This section presents expressions to obtain the probability contained in a right triangle for two conditions, a and b, and for an equilateral right triangle.

2.4.1 The Probability in a Right Triangle for the Five-Parameter Function

2.4.1.1(a) The probability contained in a right triangle shown as condition a in Figure 3 is obtained by taking the definite integral for the second integration of Equation 2.12.

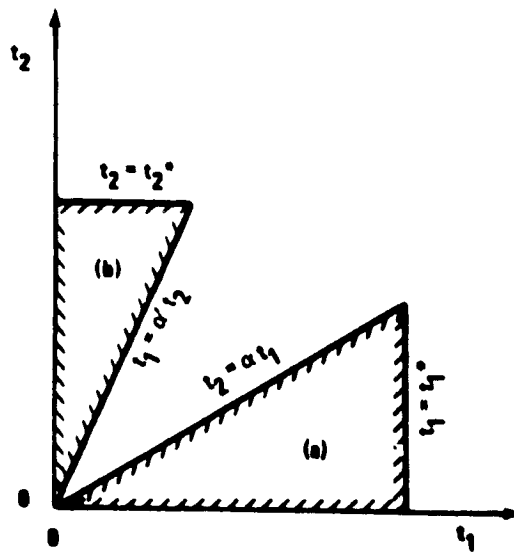


FIG. 3 PROBABILITY IN A RIGHT TRIANGLE

(a) $\Pr \{t_1 \leq t_1^0, t_2 \leq \alpha t_1^0\}$ (b) $\Pr \{t_1 \leq \alpha t_2^0, t_2 \leq t_2^0\}$

This results in

$$\begin{aligned}
 P_{RT} &= \frac{\alpha^{\gamma_2} (1-\eta)^{\gamma_2}}{(1+\alpha)^{\gamma_1+\gamma_2} \Gamma(\gamma_1) \Gamma(\gamma_2-\gamma_1)} \\
 &\times \sum_{k=0}^{\infty} \sum_{j=0}^{\infty} \sum_{n=0}^{\infty} \frac{\eta^{j+k}}{j!k!} \frac{\Gamma(\gamma_2-\gamma_1+k)}{\Gamma(1+\gamma_2+j+k+n)} \frac{\alpha^{j+k+n}}{(1+\alpha)^{2j+k+n}} \\
 &\times \gamma(\gamma_1+\gamma_2+2j+k+n, \left(\frac{1+\alpha}{1-\eta}\right) t_1^*) \quad . \quad (2.23)
 \end{aligned}$$

For $\eta = 0$ Equation 2.23 becomes:

$$P_{RT} = \frac{\alpha^{\gamma_2}}{(1+\alpha)^{\gamma_1+\gamma_2} \Gamma(\gamma_1)} \sum_{n=0}^{\infty} \frac{\alpha^n}{(1+\alpha)^n} \frac{\gamma(\gamma_1+\gamma_2+n, (1+\alpha)t_1^*)}{\Gamma(1+\gamma_2+n)} \quad . \quad (2.24)$$

2.4.1.1(b) The probability contained in a right triangle shown as condition b in Figure 3 is obtained by taking the definite integral for the second integration of Equation 2.17. The result is:

ORIGINAL PAGE IS
OF POOR QUALITY

$$\begin{aligned}
 P_{RT} &= \frac{\alpha'^{\gamma_1} (1-\eta)^{\gamma_2}}{(1+\alpha')^{\gamma_1+\gamma_2} \Gamma(\gamma_1) \Gamma(\gamma_2-\gamma_1)} \\
 &\times \sum_{k=0}^{\infty} \sum_{j=0}^{\infty} \sum_{n=0}^{\infty} \frac{\eta^{j+k} \Gamma(\gamma_2-\gamma_1+k) \Gamma(\gamma_1+j) \alpha'^{j+k+n}}{j! k! \Gamma(\gamma_2+j+k) \Gamma(1+\gamma_1+j+n) (1+\alpha')^{2j+k+n}} \\
 &\times \gamma\left(\gamma_1+\gamma_2+2j+k+n, \left(\frac{1+\alpha}{1-\eta}\right) t_2^*\right) . \quad (2.25)
 \end{aligned}$$

For $\eta = 0$ Equation 2.25 becomes:

$$\begin{aligned}
 P_{RT} &= \frac{\alpha'^{\gamma_1}}{(1+\alpha')^{\gamma_1+\gamma_2}} \sum_{n=0}^{\infty} \frac{\gamma(\gamma_1+\gamma_2+n, (1+\alpha') t_2^*)}{\Gamma(1+\gamma_1+n)} \\
 &\times \frac{\alpha'^n}{(1+\alpha')^n} . \quad (2.26)
 \end{aligned}$$

2.4.1.2 The Probability in a Right Triangle for the Four-Parameter Function

2.4.1.2(a) The probability contained in a right triangle for the equal shape parameter bivariate gamma function for condition a shown in Figure 3 is:

For $\gamma_1 \equiv \gamma_2 = \gamma$ Equation 2.23 reduces to:

ORIGINAL PAGE IS
OF POOR QUALITY

$$P_{RT} = \frac{\alpha^\gamma (1-\rho)^\gamma}{(1+\alpha)^{2\gamma} \Gamma(\gamma)} \sum_{j=0}^{\infty} \sum_{n=0}^{\infty} \frac{\rho^j}{j!} \frac{\alpha^{j+n}}{\Gamma(1+\gamma+j+n) (1+\alpha)^{2j+n}} \\ \times \gamma(2\gamma+2j+n, \left(\frac{1+\alpha}{1-\rho}\right) t_1^*) \quad (2.27)$$

and for $\rho = 0$ Equation 2.27 becomes:

$$P_{RT} = \frac{\alpha^\gamma}{(1+\alpha)^{2\gamma} \Gamma(\gamma)} \sum_{n=0}^{\infty} \frac{\gamma(2\gamma+n, (1+\alpha) t_1^*) \alpha^n}{\Gamma(1+\gamma) (1+\alpha)^n} \quad (2.28)$$

4.4.1.2(b) For condition b shown in Figure 3, the probability in a right triangle is:

For $\gamma_1 \equiv \gamma_2 = \gamma$

$$P_{RT} = \frac{\alpha'^\gamma (1-\rho)^{\gamma_2}}{(1+\alpha')^{2\gamma} \Gamma(\gamma)} \sum_{j=0}^{\infty} \sum_{n=0}^{\infty} \frac{\rho^j}{j! \Gamma(1+\gamma+j+n)} \\ \times \frac{\alpha'^{j+n}}{(1+\alpha')^{2j+n}} \gamma(2\gamma+2j+n, \left(\frac{1+\alpha'}{1-\rho}\right) t_2^*) \quad (2.29)$$

and for $\rho = 0$ Equation 2.29 becomes

$$P_{RT} = \frac{\alpha'^\gamma}{(1+\alpha')^{2\gamma} \Gamma(\gamma)} \sum_{n=0}^{\infty} \frac{\gamma(2\gamma+n, (1+\alpha') t_2^*)}{\Gamma(1+\gamma+n)} \times \frac{\alpha'^n}{(1+\alpha')^n} \quad (2.30)$$

2.4.2 For Equilateral Right Triangle

2.4.2.1 For the Five-Parameter Function

The probability contained in an equilateral right triangle shown in Figure 4 for the five-parameter function is obtained from (2.31).

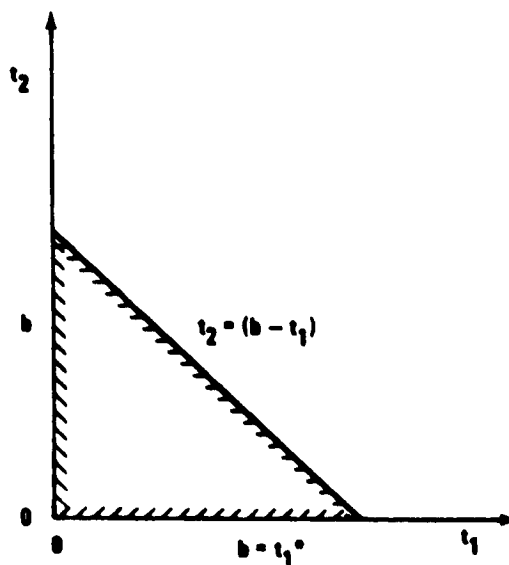


FIG. 4. PROBABILITY IN AN EQUILATERAL RIGHT TRIANGLE
 $Pr \{t_1 \leq t_1^*, t_2 \leq (b - t_1)\}$

$$P_{ERT} = \int_0^{t_1=b=t_1^*} \int_0^{t_2=(b-t_1)} f(t_1, t_2; \gamma_1, \gamma_2, \eta) dt_2 dt_1 \quad (2.31)$$

The indicated integrations of 2.31 yield:

$$P_{ERT} = \frac{t_1^{*\gamma_1+\gamma_2} \exp \{-t_1^*/(1-\eta)\}}{(1-\eta)^{\gamma_1} \Gamma(\gamma_2-\gamma_1) \Gamma(\gamma_1)} \\ \times \sum_{k=0}^{\infty} \sum_{j=0}^{\infty} \sum_{n=0}^{\infty} \frac{\eta^{j+k} \Gamma(\gamma_2-\gamma_1+k) \Gamma(\gamma_1+j) \Gamma(1+\gamma_2+j+k+n) t_1^{*2j+k+n}}{(1-\eta)^{2j+k+n} j! k! \Gamma(1+\gamma_1+\gamma_2+2j+k+n)} \quad (2.32)$$

For $\eta = 0$ Equation 2.32 reduces to:

$$P_{ERT} = t_1^{*\gamma_1+\gamma_2} e^{-t_1^*} \sum_{n=0}^{\infty} \frac{\Gamma(1+\gamma_2+n) t_1^{*n}}{\Gamma(1+\gamma_1+\gamma_2+n)} \quad (2.33)$$

2.4.2.2 For the Four-Parameter Function

For equal shape parameters, Equation 2.32 reduces to:

ORIGINAL PAGE IS
OF POOR QUALITY

For $\gamma_1 = \gamma_2 = \gamma$

$$P_{ERT} = \frac{t_1^{*2\gamma} \exp \{-t_1^*/(1-\rho)\}}{(1-\rho)^\gamma \Gamma(\gamma)} \times \sum_{j=0}^{\infty} \sum_{n=0}^{\infty} \frac{\rho^j \Gamma(\gamma+j) \Gamma(1+\gamma+j+n) t_1^{*2j+n}}{(1-\rho)^{2j+n} j! \Gamma(1+2\gamma+2j+n)}, \quad (2.34)$$

and for $\rho = 0$, Equation 2.34 becomes:

$$P_{ERT} = t_1^{*2} \exp\{-t_1^*\} \sum_{n=0}^{\infty} \frac{\Gamma(1+\gamma+n) t_1^{*n}}{\Gamma(1+2\gamma+n)}. \quad (2.35)$$

2.5 Properties of the Conditional Distribution

2.5.1 Conditional Probabilities

Because the five-parameter gamma function 2.1 is not a symmetrical function, there are two expressions for the conditional distribution. They are for $(t_1 | t_2)$ and $(t_2 | t_1)$ given by 2.36 and 2.38.

$$\Pr\{t_1 \leq \hat{t}_1 \mid t_2 = t_2^*; \gamma_1, \gamma_2, n\} =$$

$$\frac{\Gamma(\gamma_2)}{\Gamma(\gamma_1) \Gamma(\gamma_2 - \gamma_1)} \exp\left\{-\frac{n t_2^*}{1-n}\right\} \left[\sum_{j=0}^{\infty} \left(\frac{n t_2^*}{1-n}\right)^j \frac{\gamma(\gamma_1 + j, \hat{t}_1/(1-n))}{j!} \right. \\ \left. \times \sum_{k=0}^{\infty} \left(\frac{n t_2}{1-n}\right)^k \frac{\Gamma(\gamma_2 - \gamma_1 + k)}{\Gamma(\gamma_2 + j + k) k!} \right] . \quad (2.36)$$

By taking the limit of the given value in 2.36 as $t_2 \rightarrow 0$ produces:

$$\Pr\{t_1 \leq \hat{t}_1 \mid t_2 \rightarrow 0\} = \frac{\gamma(\gamma_1, \hat{t}_1/(1-n))}{\Gamma(\gamma_1)} \quad (2.37)$$

$$\Pr\{t_2 \leq \hat{t}_2 \mid t_1 = t_1^*; \gamma_1, \gamma_2, n\}$$

$$= \frac{(1-n)^{\gamma_2 - \gamma_1} \exp\left\{-\frac{n t_1^*}{1-n}\right\}}{\Gamma(\gamma_2 - \gamma_1)} \left[\sum_{j=0}^{\infty} \left(\frac{n t_1^*}{1-n}\right)^j \frac{1}{j!} \right. \\ \left. \times \sum_{k=0}^{\infty} \frac{n^k}{k!} \frac{\Gamma(\gamma_2 - \gamma_1 + k)}{\Gamma(\gamma_2 + j + k)} \gamma(\gamma_2 + j + k, \hat{t}_2/(1-n)) \right] . \quad (2.38)$$

and upon taking the limit as $t_1 \rightarrow 0$ in 2.38 gives

$$\begin{aligned} \Pr\{t_2 \leq \hat{t}_2 \mid t_1 \rightarrow 0\} &= \frac{(1-\eta)^{\gamma_2-1}}{\Gamma(\gamma_2-\gamma_1)} \\ &\times \sum_{k=0}^{\infty} \frac{\eta^k}{k!} \frac{\Gamma(\gamma_2-\gamma_1+k)}{\Gamma(\gamma_2+k)} \gamma(\gamma_2+k, \hat{t}_2/(1-\eta)) . \end{aligned} \quad (2.39)$$

For the equal shape parameter bivariate gamma function, the conditional PDF is

$$\begin{aligned} \Pr\{t_2 \leq \hat{t}_2 \mid t_1 = t_1^*; \gamma, \rho\} &= \exp - \left\{ \frac{\rho t_1^*}{1-\rho} \right\} \\ &\times \sum_{k=0}^{\infty} \frac{\rho^k}{(1-\rho)^k} \frac{t_1^*}{k!} \gamma(\gamma+k, \hat{t}_2/(1-\rho)) , \end{aligned} \quad (2.40)$$

and for the limit as $t_1^* \rightarrow 0$

$$\begin{aligned} \Pr\{t_2 \leq \hat{t}_2 \mid t_1 \rightarrow 0; \gamma, \rho\} &= \frac{\hat{t}_2^{\gamma-1}}{(1-\rho)^{\gamma} \Gamma(\gamma)} \\ &\times \exp - \{ \hat{t}_2/(1-\rho) \} . \end{aligned} \quad (2.41)$$

Because this is a symmetrical function, the conditional distribution for $\{t_1 \mid t_2\}$ can be obtained by interchanging the subscripts in Equations 2.40 and 2.41.

Equations 2.37, 2.39, and 2.41 are interesting results. This is because the original bivariate gamma functions (2.1 and 2.4) are bounded at the origin and yet the conditional functions are not bounded at the origin as the limit of the given values approaches zero. This property of the conditional functions must be reasoned with when they are used as models for physical data.

2.5.2 Moments of the Conditional Function

For the four-parameter (equal shape parameter) bivariate gamma density, $f(t_1, t_2; \gamma, \rho)$, the conditional moments are sufficiently simple to be derived. For this case, the non-central conditional moments are expressed as

$$\begin{aligned} \mu_j^* (t_2 \mid t_1 = t_1^*) &= \frac{\Gamma(\gamma+j)(1-\rho)^j}{\Gamma(\gamma)} e^{-(\rho t_1^*)/(1-\rho)} \\ &\times {}_1F_1(\gamma+j; \gamma; (\rho t_1^*)/(1-\rho)) \quad , \end{aligned} \quad (2.42)$$

where ${}_1F_1(a; c; z)$ is the confluent hypergeometric function of Kummer's function as defined by W. Magnus et al (1966).

From 2.42 the conditional mean and variance are given by

$$E(t_2 \mid t_1 = t_1^*) = 1-\rho \{ \gamma + \rho t_1^* / (1-\rho) \} \quad (2.43)$$

$$\text{Var}(t_2 \mid t_1 = t_1^*) = (1-\rho)^2 [\gamma + 2\rho t_1^*/(1-\rho)] \quad (2.44)$$

Note that the conditional moments exist when the given value t_1^* approaches zero in Equations 2.43 and 2.44. Also, it is observed from 2.43 and 2.44 that the regression of t_2 on t_1 is not homogeneous over t_1 .

2.6 Illustrations and Properties of the Bivariate Gamma Distribution

This section presents graphical displays of the bivariate gamma density function to illustrate some of the properties of this function.

Figures 5a, 5b, 6a, 6b, 7a, and 7b are schematic illustrations of the contours of equal probability density to show the variations with the shape parameter, γ , and the correlation coefficient, ρ , for the four-parameter function, $f(t_1, t_2; \gamma, \rho)$, Equation 2.4. In all Figures 5a-7b, the density contours are symmetrical with respect to the line $t_1 = t_2$.

For $\gamma < 1$, Figures 5a and 5b, the density is a maximum for small values of t_1 and t_2 and becomes undefined at $t_1 = t_2 = 0$.

For $\gamma = 1$, Figures 6a and 6b, which is the bivariate exponential density function, the maximum density is at

ORIGINAL PAGE IS
OF POOR QUALITY

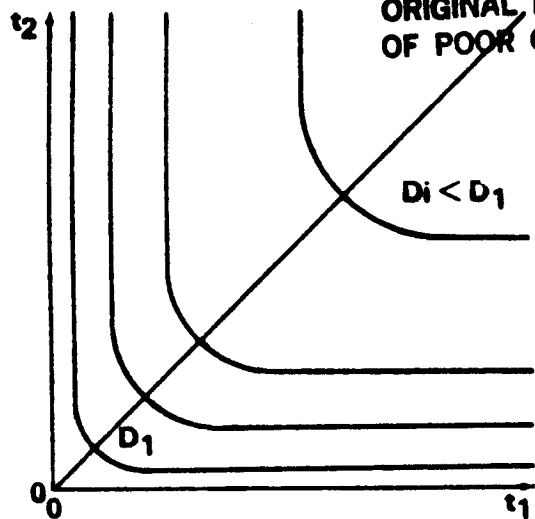


FIG. 5a. $f(t_1, t_2; \gamma = \gamma < 1, \rho = 0)$

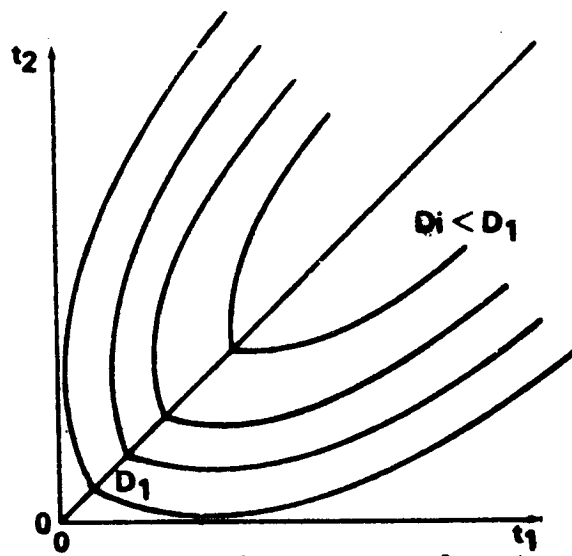


FIG. 5b. $f(t_1, t_2; \gamma = \gamma < 1, \rho)$

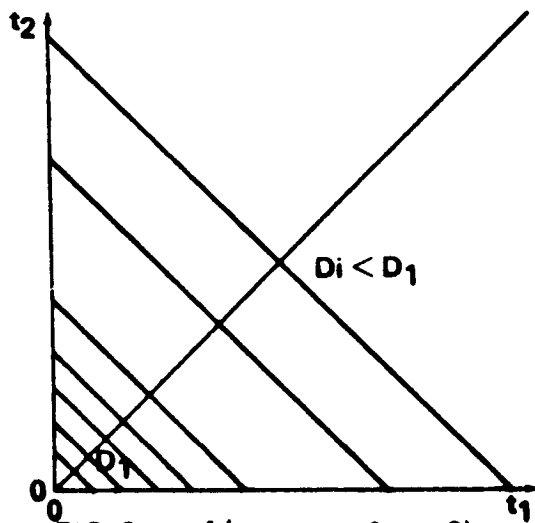


FIG. 6a. $f(t_1, t_2; \gamma = 1, \rho = 0)$

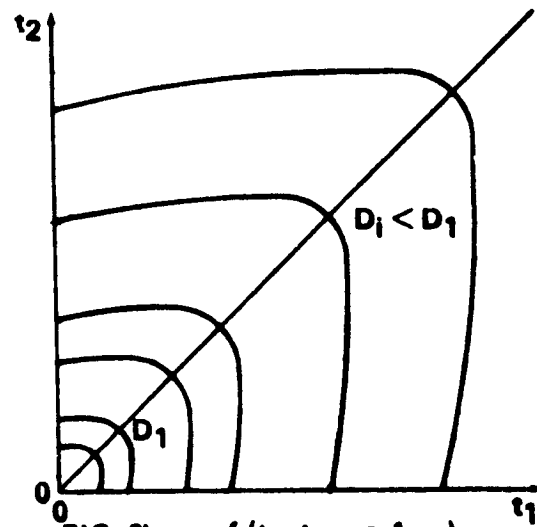


FIG. 6b. $f(t_1, t_2; \gamma = 1, \rho)$

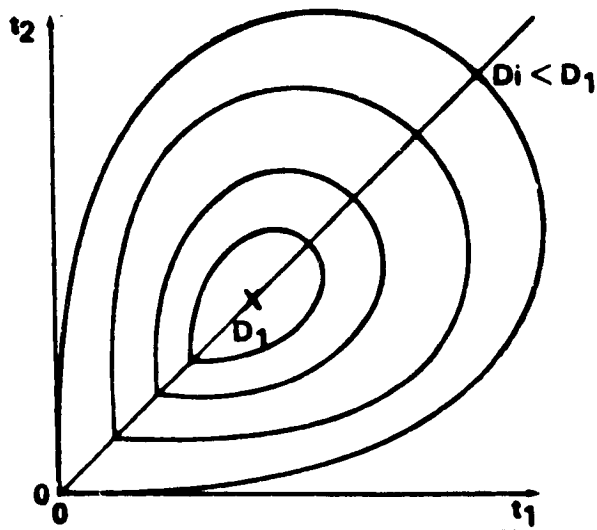


FIG. 7a. $f(t_1, t_2; \gamma = \gamma > 1, \rho = 0)$

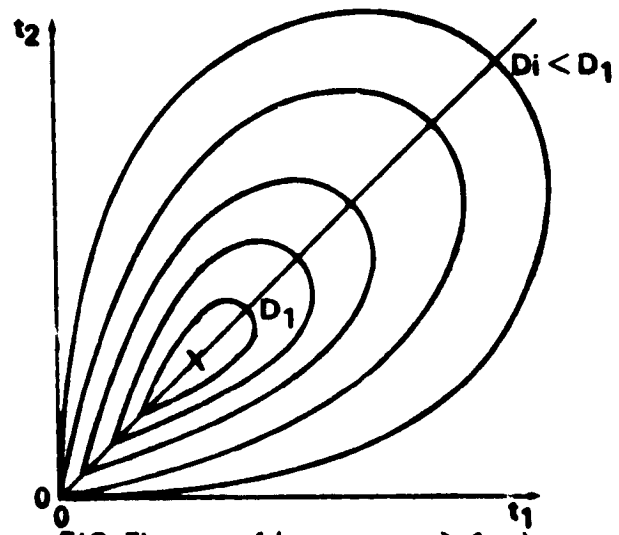


FIG. 7b. $f(t_1, t_2; \gamma = \gamma > 1, \rho)$

CONTOURS OF EQUAL PROBABILITY DENSITY(SCHEMATICS)

$t_1 = t_2 = 0$. For $\gamma = 1$, $\rho = 0$ (Figure 6a), the contours for equal probability density form straight lines normal to the line $t_1 = t_2$.

For $\gamma > 1$ (Figures 7a and 7b), the mode exists and lies on the line $t_1 = t_2$. (Additional characteristics of the mode and the density of the mode are shown in Figures 10 and 11.)

Because the equal shape parameter bivariate gamma density function 2.1 is symmetrical with respect to the line $t_1 = t_2$, there is some analytical advantage in expressing this function in a coordinate system rotated by 45 degrees. In terms of the Bessel function, Equation 2.5 in the rotated coordinate system is

$$f(z_1, z_2; \gamma, \rho) = \frac{(z_1^2 - z_2^2)^{\frac{\gamma-1}{2}}}{(1-\rho)(2\rho)^{(\gamma-1)/2} \Gamma(\gamma)} \times \exp - \{ \sqrt{2} z_1 / (1-\rho) \} I_{\gamma-1} \frac{\sqrt{2\rho} (z_1^2 - z_2^2)^{\frac{1}{2}}}{(1-\rho)}, \quad (2.45)$$

where $z_1 = \frac{\sqrt{2}}{2} (\beta_x x + \beta_y y)$, $z_2 = \frac{\sqrt{2}}{2} (\beta_y y - \beta_x x)$

and $z_1 \geq 0$, $z_2 \geq 0$, $z_1 > z_2$; $\gamma > 0$ and $0 < \rho < 1$.

This Bessel function is available as a computer subroutine to aid in evaluating 2.45.

Computer graphics for the evaluation of 2.45 for contours of equal probability density are shown in Figures 8a, 8b, and 8c for $\gamma = 2$ with $\rho = 0.25, 0.50$, and 0.75 ; and in Figures 9a, 9b, and 9c for $\gamma = 3$ with $\rho = 0.25, 0.50$, and 0.75 . The density contours were obtained by the following steps:

1. Iterative evaluations of 2.45 with $z_2 = 0$ to obtain the model value, \tilde{z}_1 .
2. Dividing the \tilde{z}_1 into 11 increments, Δz_1 , and evaluation of 2.45 with $z_2 = 0$ and Δz_1 to obtain the 11 density values to be contoured.
3. The contouring for the 11 density values was by iterative evaluations of 2.45 for the valid range of z_1 and z_2 for each contour.

Interesting special cases of 2.45 can be expressed. One is for $\gamma = 1.5$. For $\gamma = 1.5$, the Bessel function reduces to a hyperbolic function and the PDF becomes:

$$f(z_1, z_2; \gamma = 1.5, \rho) = \frac{2}{\pi[\rho(1-\rho)]^{\frac{1}{2}}} \times \exp - \left\{ \frac{\sqrt{2} z_1}{1-\rho} \right\} \sinh \left\{ \frac{\sqrt{2\rho} (z_1^2 - z_2^2)^{\frac{1}{2}}}{(1-\rho)} \right\} . \quad (2.46)$$

ORIGINAL PAGE IS
OF POOR QUALITY

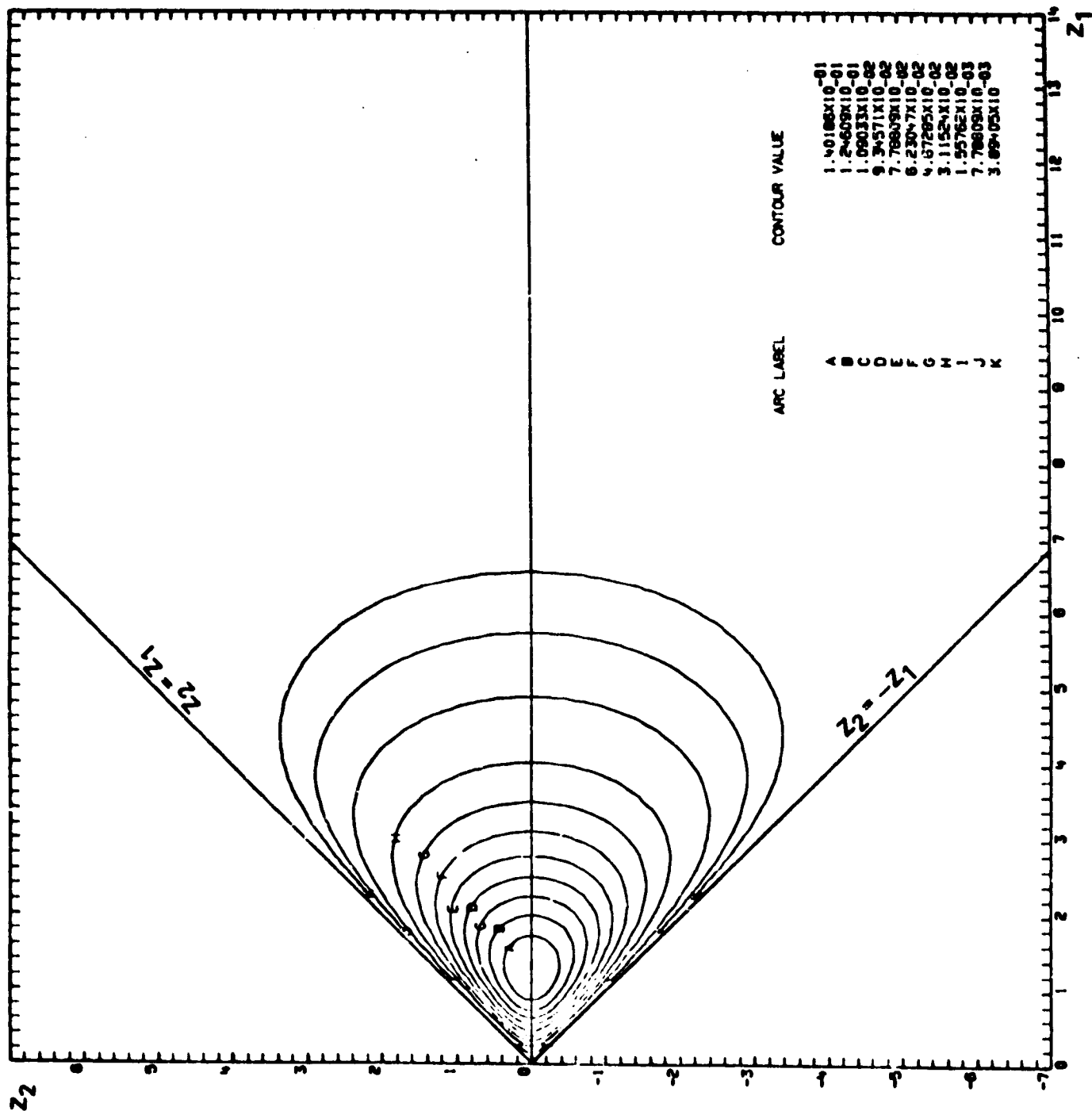


FIGURE 8a. DENSITY CONTOURS FOR $\gamma = 2$, $\rho = 0.25$

ORIGINAL PAGE IS
OF POOR QUALITY

JOB NO 1HE58134C900 PAGE 18

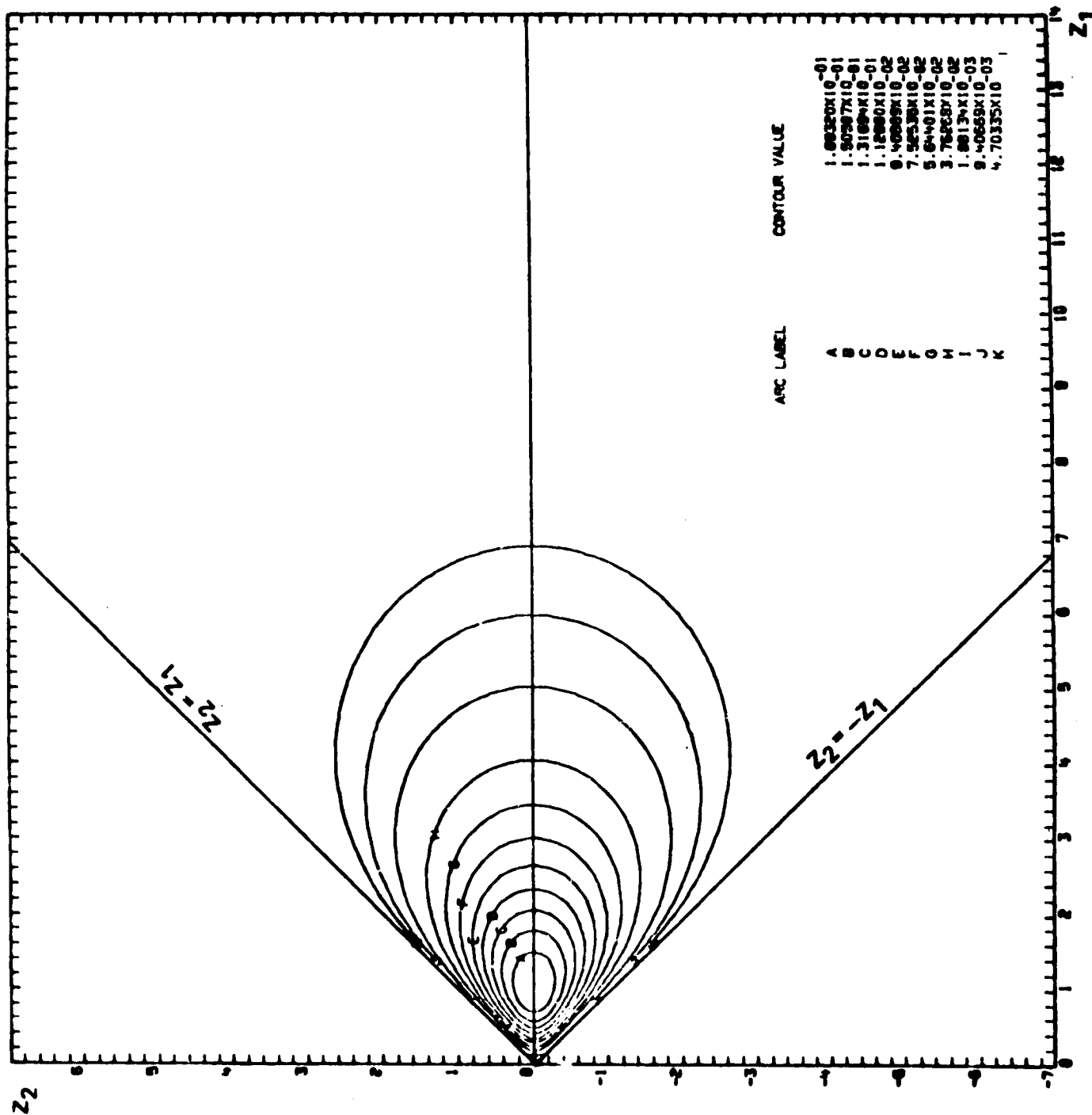


FIGURE 8b. DENSITY CONTOURS FOR $\gamma = 2$, $\rho = 0.50$

ORIGINAL PAGE IS
OF POOR QUALITY

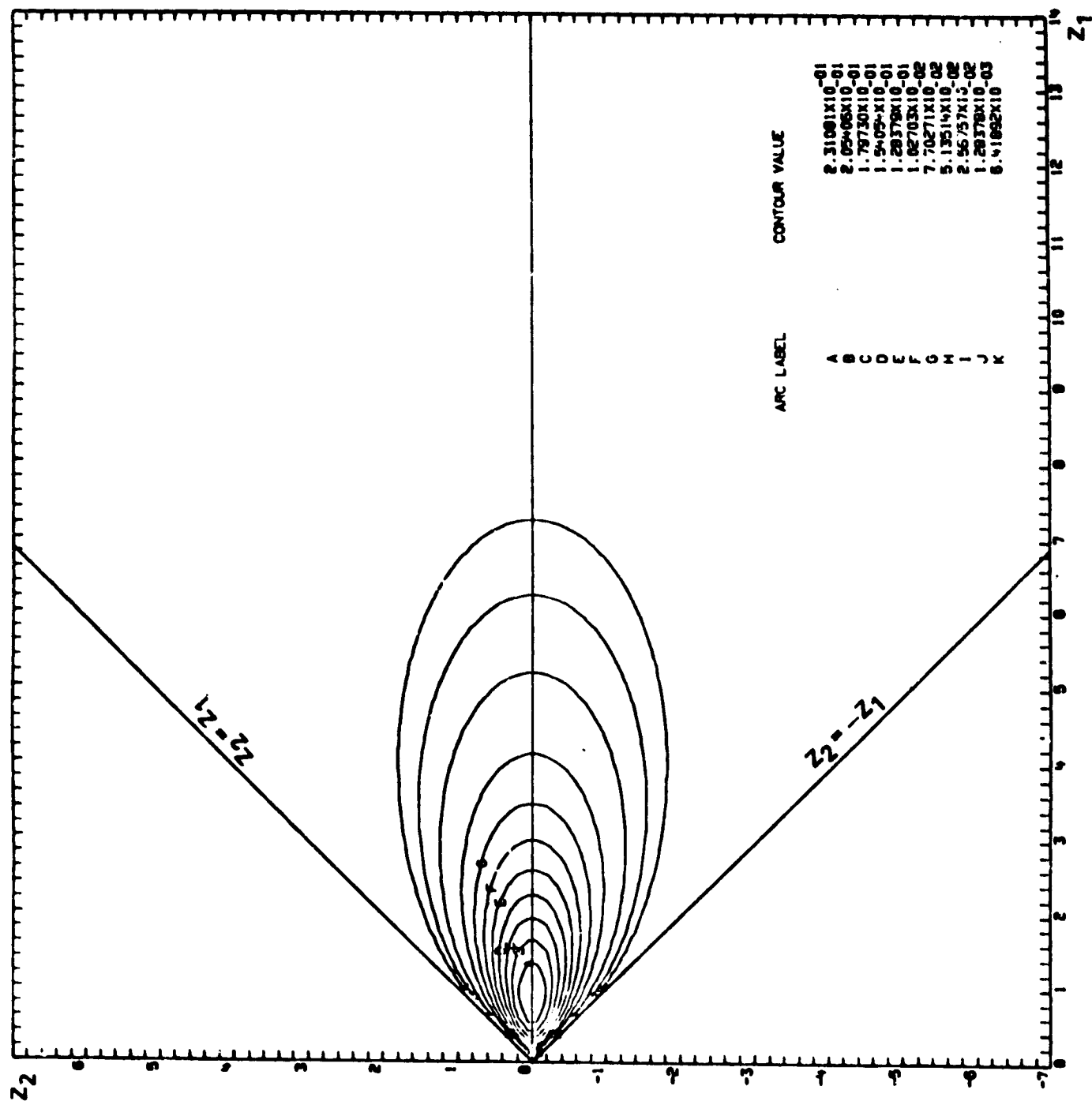


FIGURE 8c. DENSITY CONTOURS FOR $\gamma = 2$, $\rho = 0.75$

ORIGINAL PAGE IS
OF POOR QUALITY

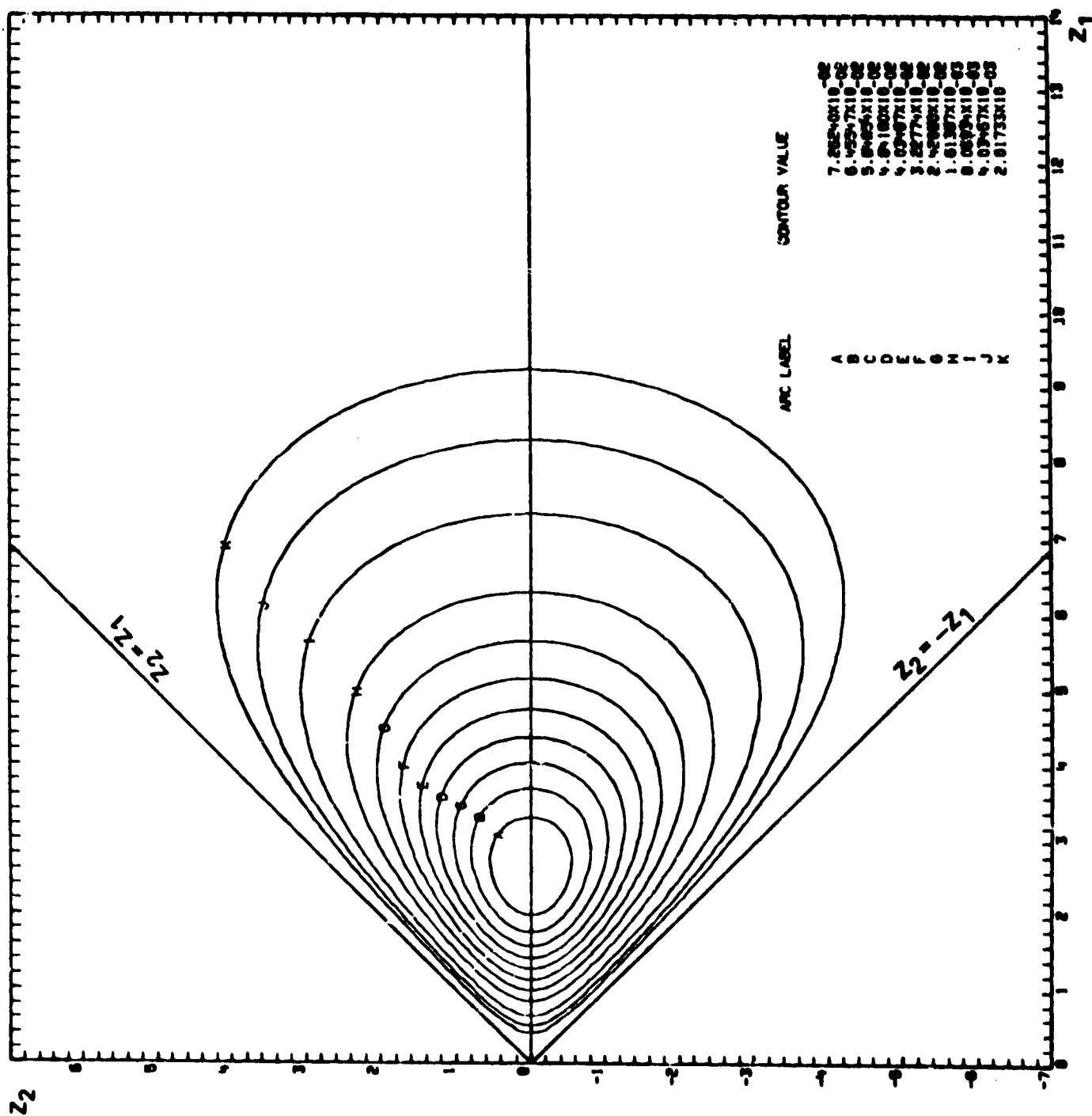


FIGURE 9a. DENSITY CONTOURS FOR $\gamma = 3$, $\rho = 0.25$

ORIGINAL PAGE IS
OF POOR QUALITY

PAGE 24

JOB NO 14ESB13-0900

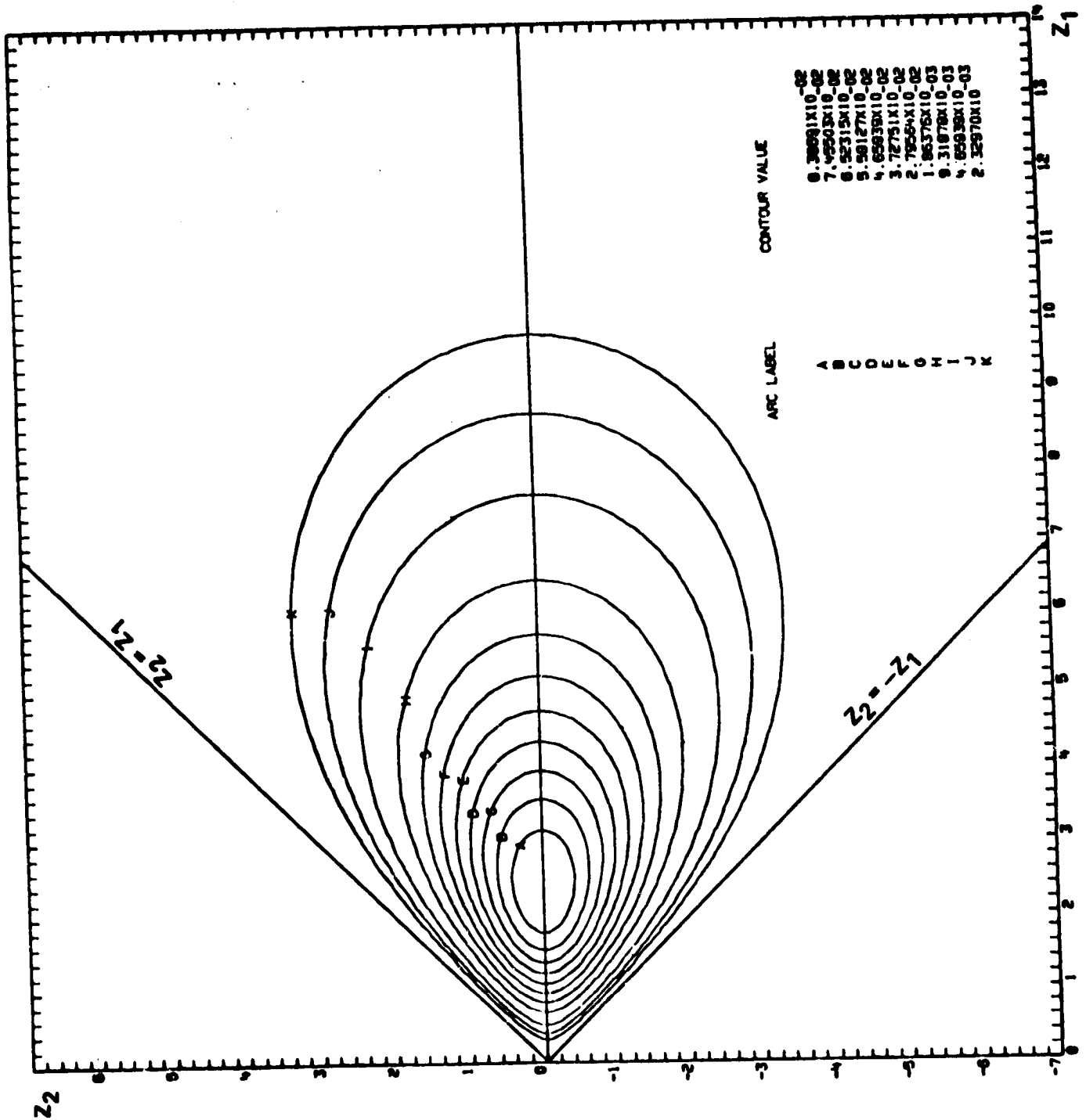


FIGURE 9b. DENSITY CONTOURS FOR $\gamma = 3$, $\rho = 0.50$

ORIGINAL PAGE IS
OF POOR QUALITY

PAGE 26

JOB NO 1145813-10900

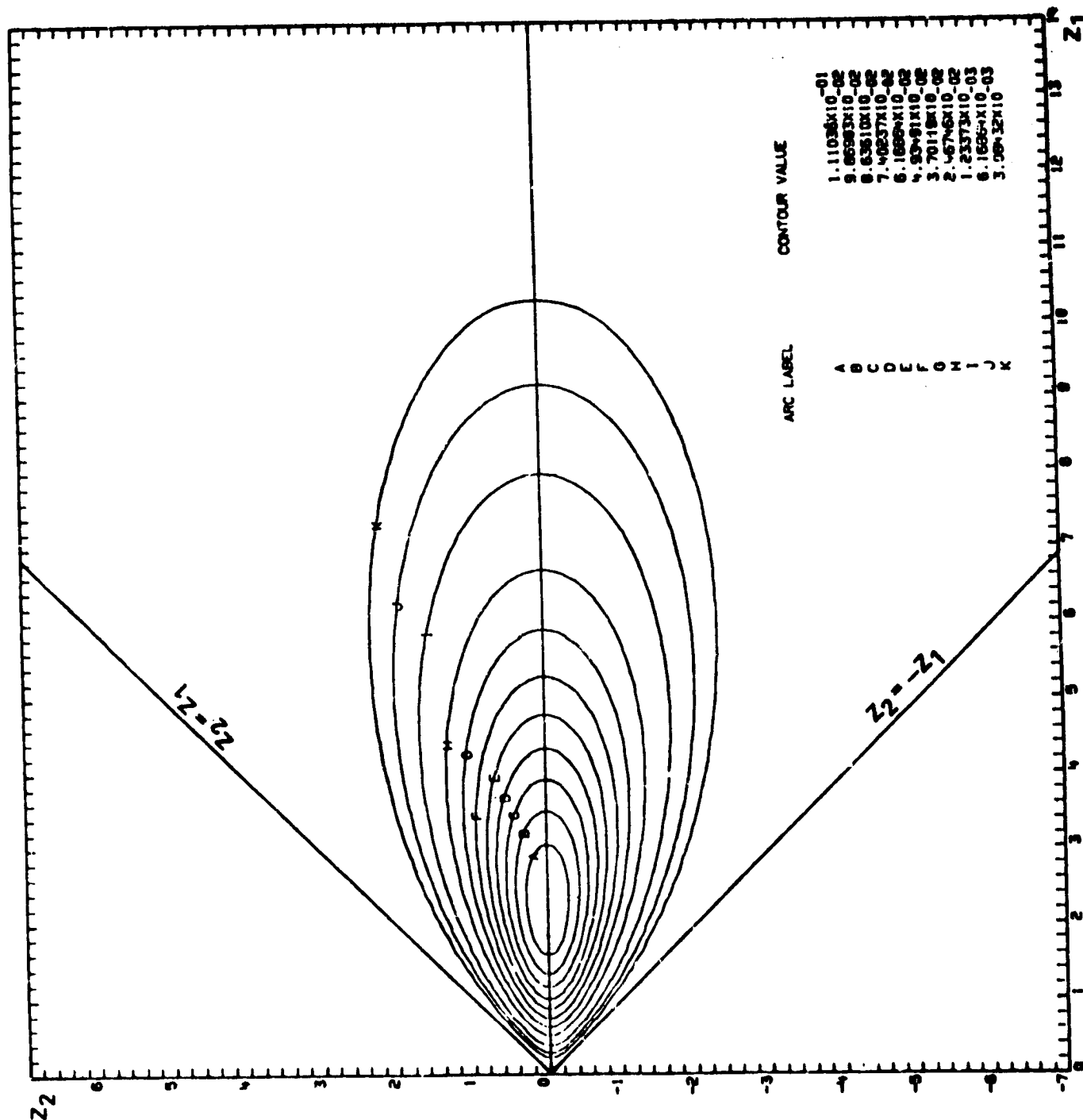


FIGURE 9c. DENSITY CONTOURS FOR $\gamma = 3, \rho = 0.75$

from which the mode, \tilde{z}_1 , is

$$\tilde{z}_1 = \frac{(1-\rho)}{\sqrt{2\rho}} \tanh^{-1} \{\sqrt{\rho}\} \quad (2.47)$$

and the modal density, D , is obtained in closed form as:

$$\tilde{D} = \frac{2 \exp \left\{ -\frac{\sqrt{2}}{(1-\rho)} z_1 \right\}}{\pi \sqrt{\rho(1-\rho)}} \sinh \left\{ \frac{\sqrt{2\rho}}{(1-\rho)} \tilde{z}_1 \right\} \quad (2.48)$$

The values of z_2 as a function of z_1 , for ρ fixed and density, $D = \text{constant}$, is expressed as:

$$z_2^2 = z_1^2 - \frac{(1-\rho)^2}{2\rho} \left[\sinh^{-1} \left[\frac{\pi}{2} \sqrt{\rho(1-\rho)} \cdot D \cdot \exp \left\{ \frac{\sqrt{2}}{(1-\rho)} z_1 \right\} \right] \right]^2 \quad (2.49)$$

By using the identity for the inverse hyperbolic sine function, 2.49 becomes

$$z_2^2 = z_1^2 - \frac{(1-\rho)^2}{2\rho} \left[\ln \left\{ \xi + \sqrt{\xi^2 + 1} \right\} \right]^2 \quad (2.50)$$

$$\text{where } \xi = \frac{\pi}{2} \sqrt{\rho(1-\rho)} \cdot D \cdot \exp \left\{ \frac{\sqrt{2}}{(1-\rho)} z_1 \right\} \quad (2.51)$$

$$\text{Then } z_2 = \pm \sqrt{z_2^2} \quad (2.52)$$

ORIGINAL PAGE IS
OF POOR QUALITY

Equation 2.49 or 2.50 can be used as a special case to compute contours of equal probability density.

Another special case is to let $\rho = 0$ and for $\gamma > 1$ in 2.45 to get

$$f(z_1, z_2; \gamma > 1, \rho = 0) = \frac{(z_1^2 - z_2^2)^{\gamma-1} \exp - \{\sqrt{2} z_1\}}{2^{\gamma-1} [\Gamma(\gamma)]^2} \quad (2.53)$$

and

$$f(z_1, z_2 = 0, \gamma > 1, \rho = 0) = \frac{z_1^{2(\gamma-1)} \exp - \{\sqrt{2} z_1\}}{2^{\gamma-1} [\Gamma(\gamma)]^2} \quad (2.54)$$

from which the mode is

$$\tilde{z}_1 = \sqrt{2} (\gamma-1) \quad (2.55)$$

and density at the mode is

$$\tilde{D} = \frac{(\gamma-1)^{2(\gamma-1)}}{[\Gamma(\gamma)]^2} \exp - \{2(\gamma-1)\} \quad (2.56)$$

Then z_2 as a function of z_1 and fixed density, D , is

$$z_2^2 = z_1^2 - \left[2^{\gamma-1} [\Gamma(\gamma)]^2 \cdot D \cdot \exp \{\sqrt{2} z_1\} \right]^{\frac{1}{\gamma-1}} \quad (2.57)$$

The location of the mode and the density value at the mode are informative properties of skewed and usually bounded probability distributions.

For the four-parameter gamma probability function (2.45), the location of the mode, \tilde{z}_1 , versus γ for correlations, ρ , is shown in Figure 10. Here it is observed that the mode, \tilde{z}_1 , increases with increasing γ and decreases for increasing ρ . The value of the density at the mode (Figure 11) decreases with increasing γ and increases with increasing ρ .

Three-dimensional computer graphics are shown in Appendix A for equal and unequal shape parameter gamma densities as the correlation varies. Also illustrated are contours for equal probability densities. Although the abscissa and ordinate scales are unequal, it can be seen that more density is above the line, $t_1=t_2$, than below this line for $\gamma_2 > \gamma_1$.

Within Section 2 there are elements on the properties of the bivariate gamma probability distribution which are believed to be original contributions to the better understanding of this function. Just as it is important to understand the characteristics of a data sample to make statistical inferences and to model the sample by a probability function, it is also important to understand the properties of the probability function in the selection of other alternatives as a model for the sample data.

ORIGINAL PAGE IS
OF POOR QUALITY

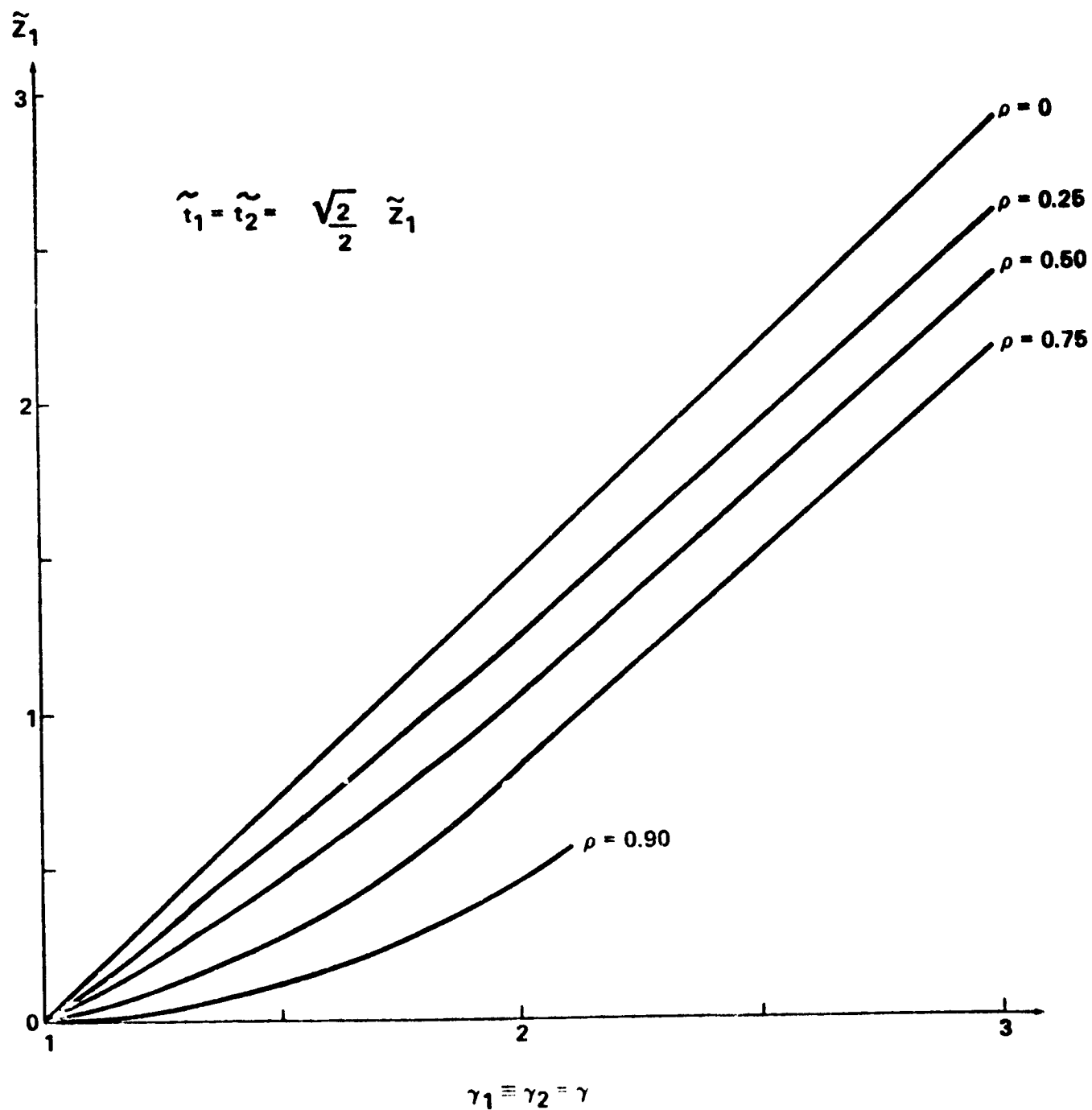


FIGURE 10. MODE, \tilde{Z} , VERSUS γ FOR CORRELATIONS, ρ

ORIGINAL PAGE IS
OF POOR QUALITY

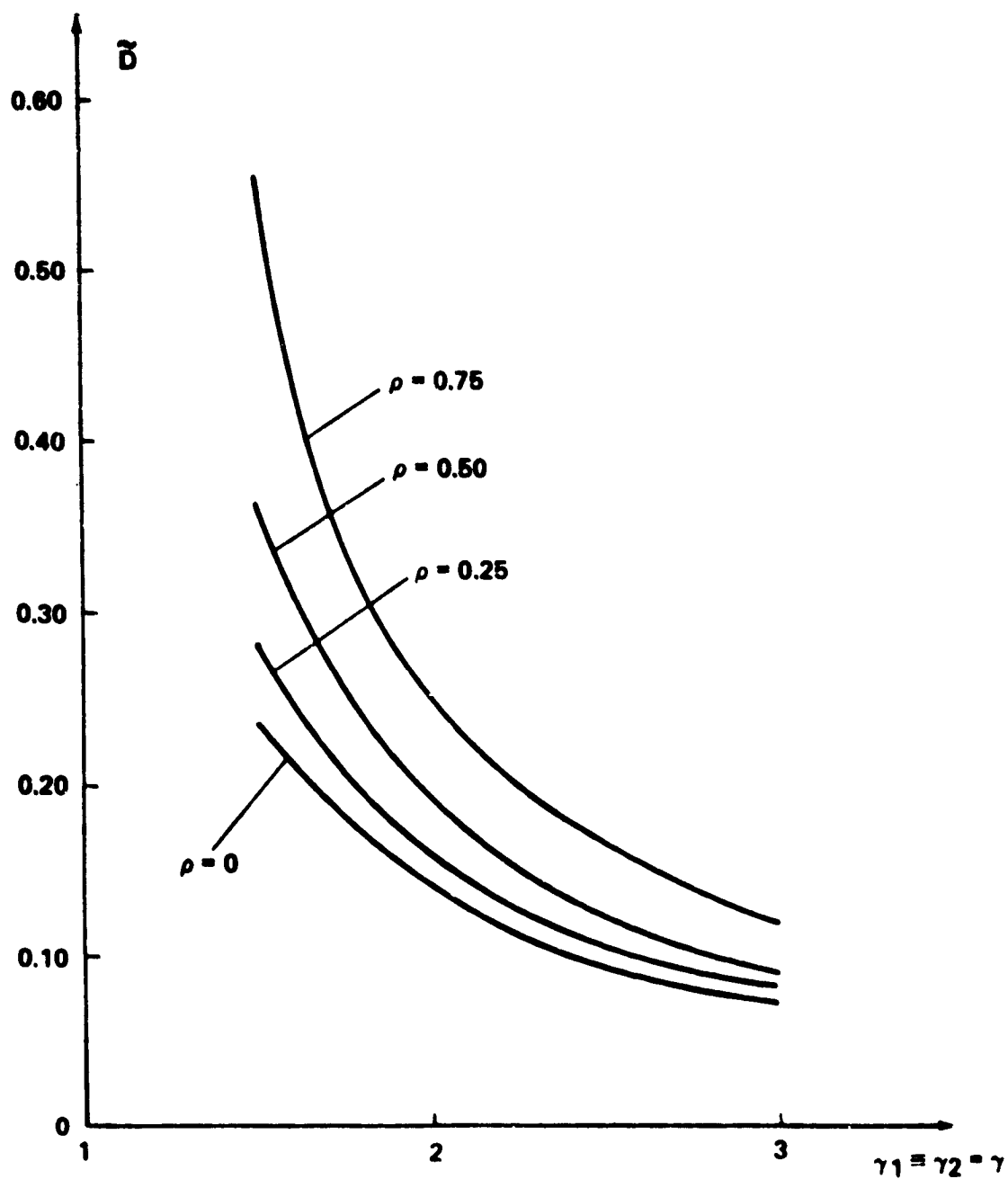


FIG. 11 DENSITY MODE VERSUS γ FOR CORRELATIONS, ρ

3. APPLICATION

Aerospace launch vehicles experience structural loads that are imposed by wind variability along the vehicle trajectory. The largest loads are often associated with a discrete gust that stands out above the general disturbance level (Jones, 1971). To ensure a margin of safety, information about the amplitude and length scale of discrete gusts and how they vary with altitude and season is required. A previous discrete gust model used in aerospace engineering applications proposes a gust with a quasi-square wave shape, a variable length scale, and constant amplitude (Daniels, 1973). Other studies (Adelfang, 1970; Fichtl and Perlmutter, 1976) based on analysis of detailed Jimsphere wind profiles between the surface and 16 km have concluded that gust amplitude increases with altitude above 9 km. A new model described herein treats gust amplitude and length scale as the variables of a bivariate gamma distribution. Parameters of the model at various altitudes are estimated from samples of gust data derived from wind profiles.

3.1 Data

Detailed wind profiles at Cape Canaveral, Florida, measured from the earth's surface to 18 km at 25-meter altitude intervals with the Jimsphere FPS-16 measurement system (Camp, 1971) were used. The sample consists of 150 profiles per

month for the months of February, April, and July. Data suitable for analysis were derived from these profiles by application of three band-pass Martin-Graham digital filters (DeMandel and Krivo, 1971). The filtered profiles defined here as residual profiles contain wavelengths within the 90-420, 420-2470, and 2470-6000 meter bands. A set of zonal wind component, u' , residual profiles calculated from a Jimsphere profile at Cape Canaveral (2/23/71, 1445 GMT) is illustrated in Figure 12.

The definition of gust used in this study satisfies the objective to provide data suitable for detailed analysis of singularities or discrete perturbations that are often observed in Jimsphere wind profiles. According to the conventional approach, all the amplitudes in the filtered profile would be defined as gusts. In this study, only the largest residual with equivalent sign to the residual at reference height, H_0 , is defined as a gust; as illustrated in Figure 13, the gust, u' , occurs between successive zero crossings at H_1 and H_2 ; L_u , is defined as the gust length.

3.2 Results

3.2.1 Marginal and Conditional Distributions

Examples of expected (gamma) and observed PDF's for absolute gust component amplitude, $|u'|$, and associated gust length,

ORIGINAL PAGE IS
OF POOR QUALITY

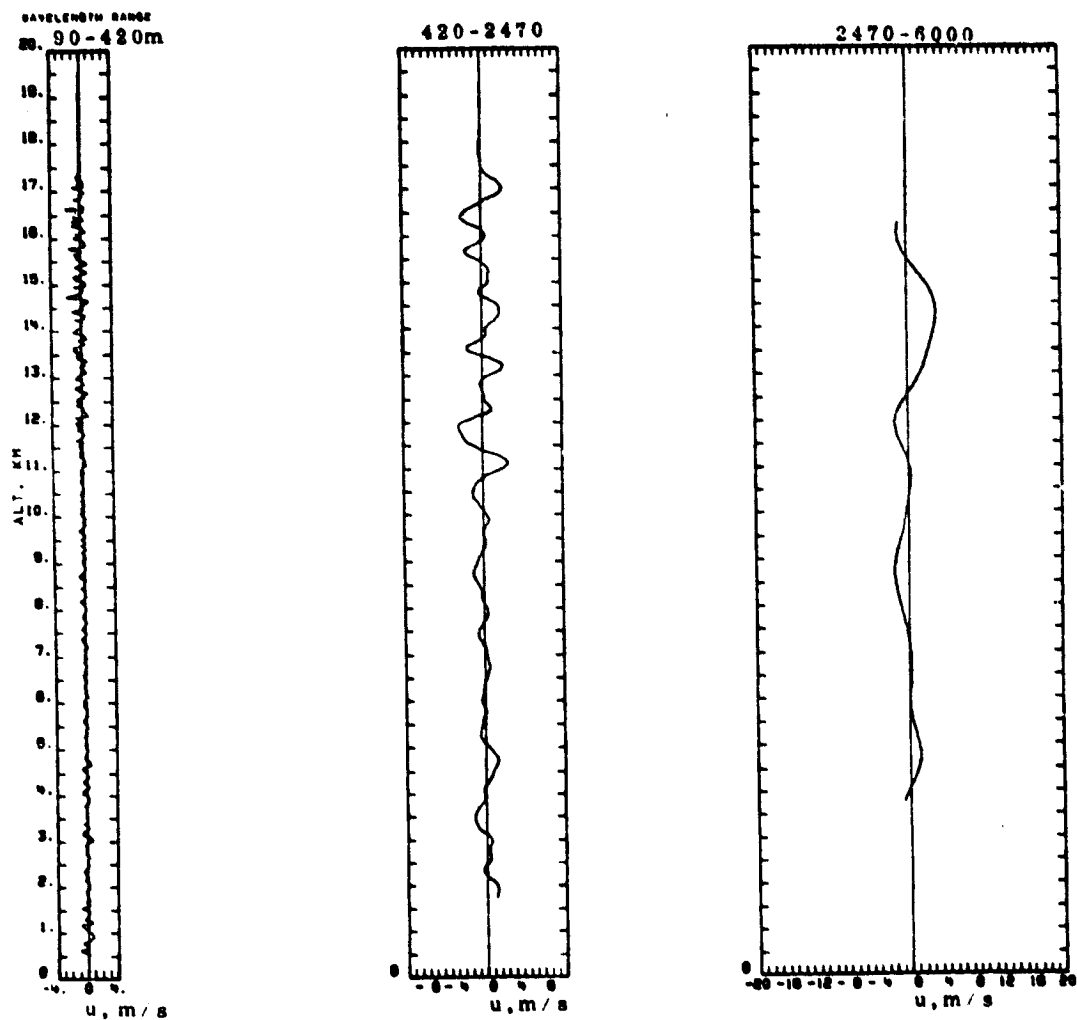


Figure 12. Band-Pass Profiles Derived from a Jimsphere
Wind Profile at Cape Canaveral, Florida
(2/23/71, 1445 GMT)

ORIGINAL PAGE IS
OF POOR QUALITY

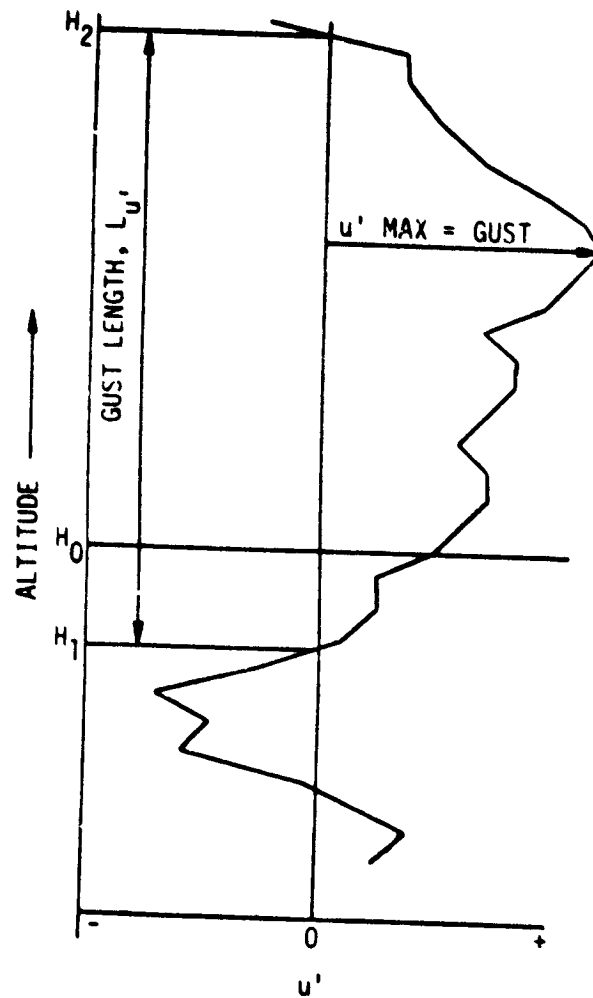


Figure 13. Schematic Definition of Gust

L_u , are illustrated in Figures 14 and 15; the gamma PDF's, illustrated with solid lines, were calculated from sample estimates of the parameters γ and β listed in the figure insets. The relatively small gust amplitudes in the 90-420 meter wavelength band and the good agreement between gamma and observed PDF's are clearly indicated.

A further indication of goodness of fit was obtained from calculations of the χ^2 statistic from expected and observed populations. Although the outcome can be affected by the arbitrary choice of the size and number of class intervals, the results to date have supported the conclusion that the marginal distributions are gamma distributed. A partial summary of the results is illustrated in Table 1. Results for other months and other wavelength bands have yielded a similar conclusion.

The variation of gust component amplitude with altitude and season is an important consideration in aerospace design and operations. Illustrations of how the univariate gamma distribution is used to describe this variability are given in Figures 16 and 17. During February at Cape Canaveral, u component gust amplitude increases with altitude between 4 and 12 km; the variation is relatively small between 4 and 8 km and large between 10 and 12 km (Figure 16). As indicated in Figure 17, gust amplitude is much smaller in summer (July) and early fall (October) than in Winter (February).

ORIGINAL PAGE IS
OF POOR QUALITY

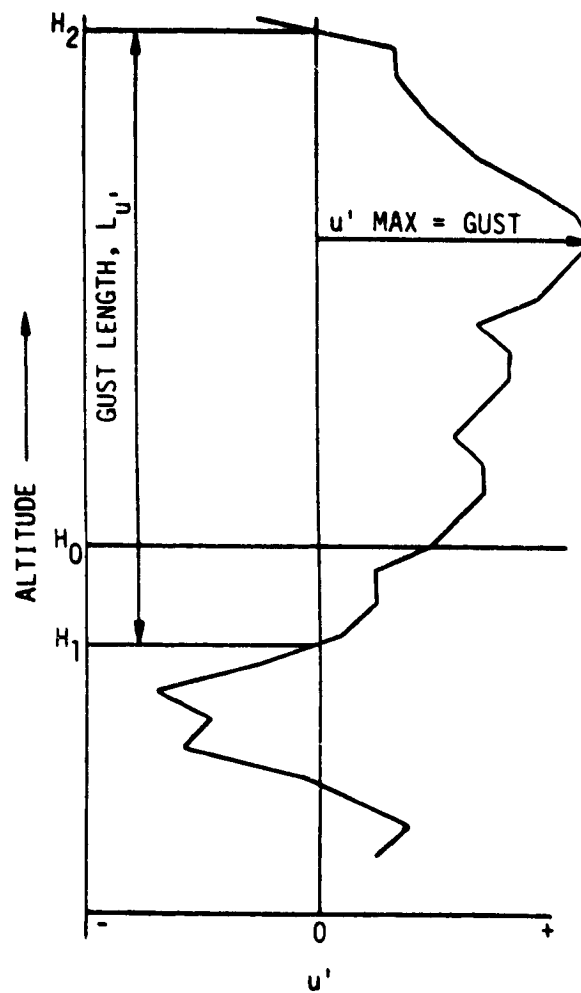


Figure 13. Schematic Definition of Gust

L_u , are illustrated in Figures 14 and 15; the gamma PDF's, illustrated with solid lines, were calculated from sample estimates of the parameters γ and β listed in the figure insets. The relatively small gust amplitudes in the 90-420 meter wavelength band and the good agreement between gamma and observed PDF's are clearly indicated.

A further indication of goodness of fit was obtained from calculations of the χ^2 statistic from expected and observed populations. Although the outcome can be affected by the arbitrary choice of the size and number of class intervals, the results to date have supported the conclusion that the marginal distributions are gamma distributed. A partial summary of the results is illustrated in Table 1. Results for other months and other wavelength bands have yielded a similar conclusion.

The variation of gust component amplitude with altitude and season is an important consideration in aerospace design and operations. Illustrations of how the univariate gamma distribution is used to describe this variability are given in Figures 16 and 17. During February at Cape Canaveral, u component gust amplitude increases with altitude between 4 and 12 km; the variation is relatively small between 4 and 8 km and large between 10 and 12 km (Figure 16). As indicated in Figure 17, gust amplitude is much smaller in summer (July) and early fall (October) than in Winter (February).

ORIGINAL PAGE IS
OF POOR QUALITY

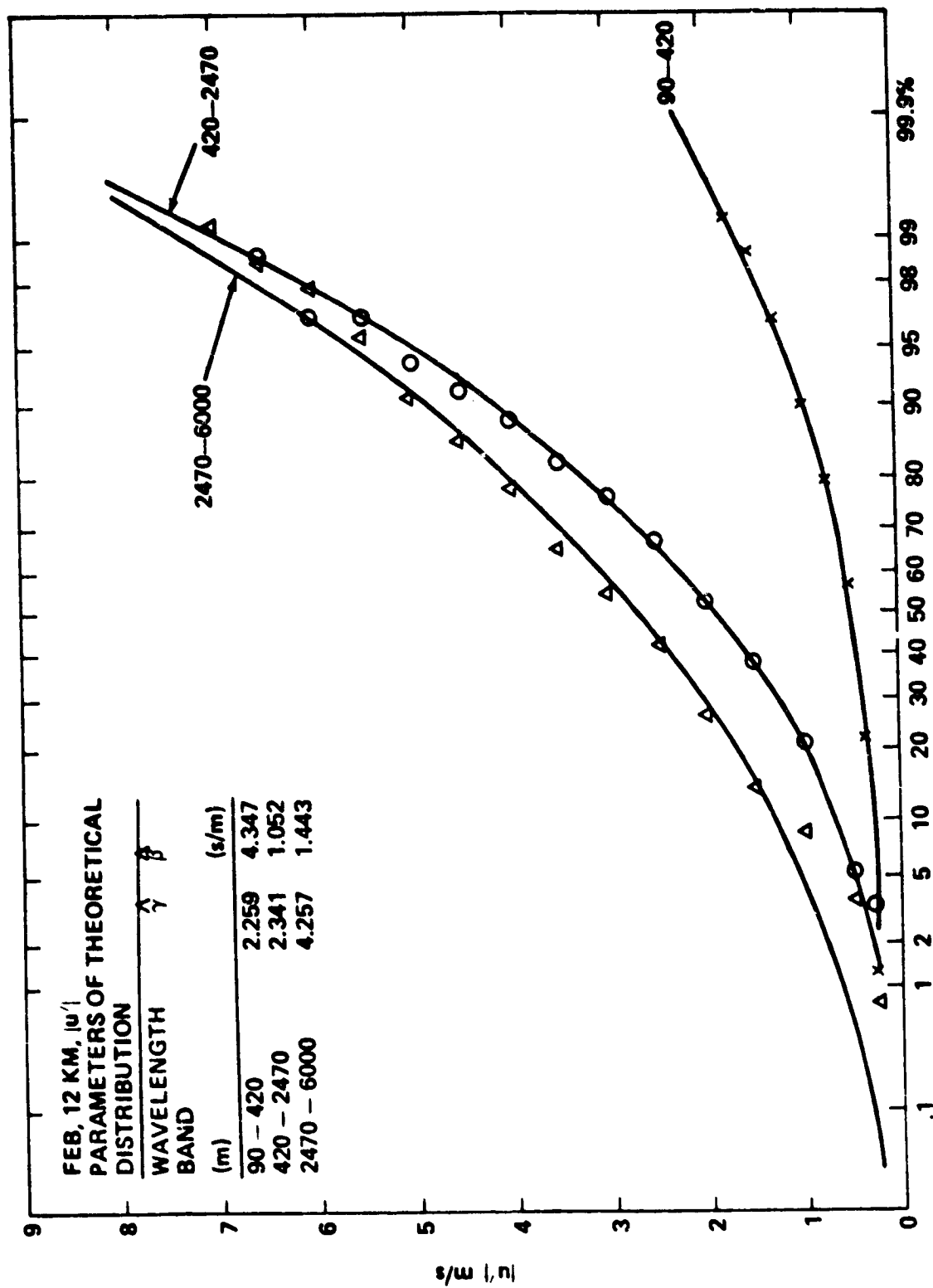


FIGURE 14. GAMMA AND OBSERVED PDF OF GUST COMPONENT AMPLITUDE, $|u'|$, FROM
90-420m, 420-2470m, 2470-6000m WAVELENGTH BAND FILTERS AT 12km ALTITUDE, FEBRUARY,
CAPE CANAVERAL, FLORIDA

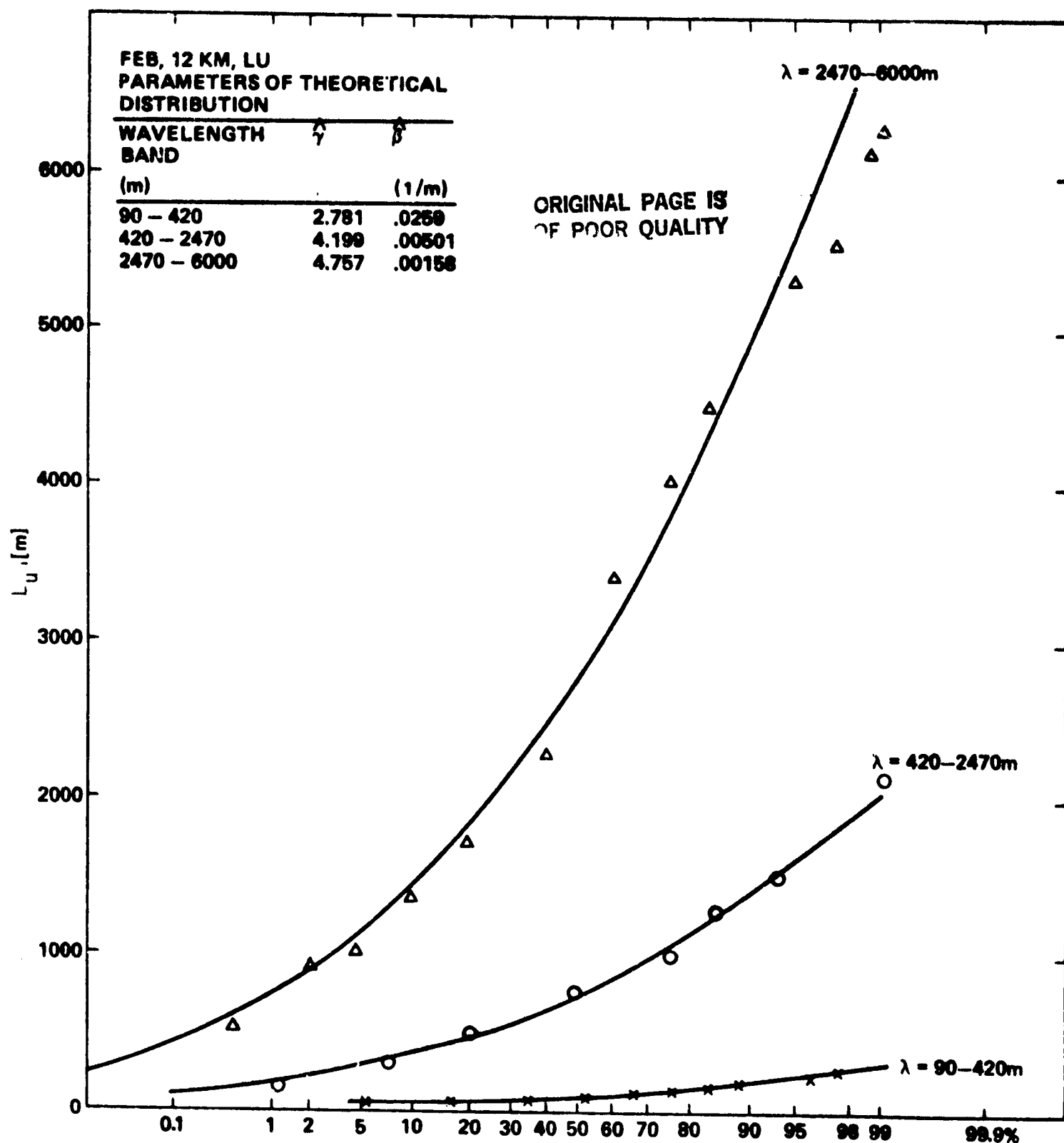


FIGURE 15. GAMMA AND OBSERVED PDF OF GUST LENGTH, L_U , FROM 90-420m, 420-2470m, 2470-6000m WAVELENGTH BAND FILTERS AT 12km ALTITUDE, FEBRUARY, CAPE CANAVERAL, FLORIDA

ORIGINAL PAGE IS
OF POOR QUALITY

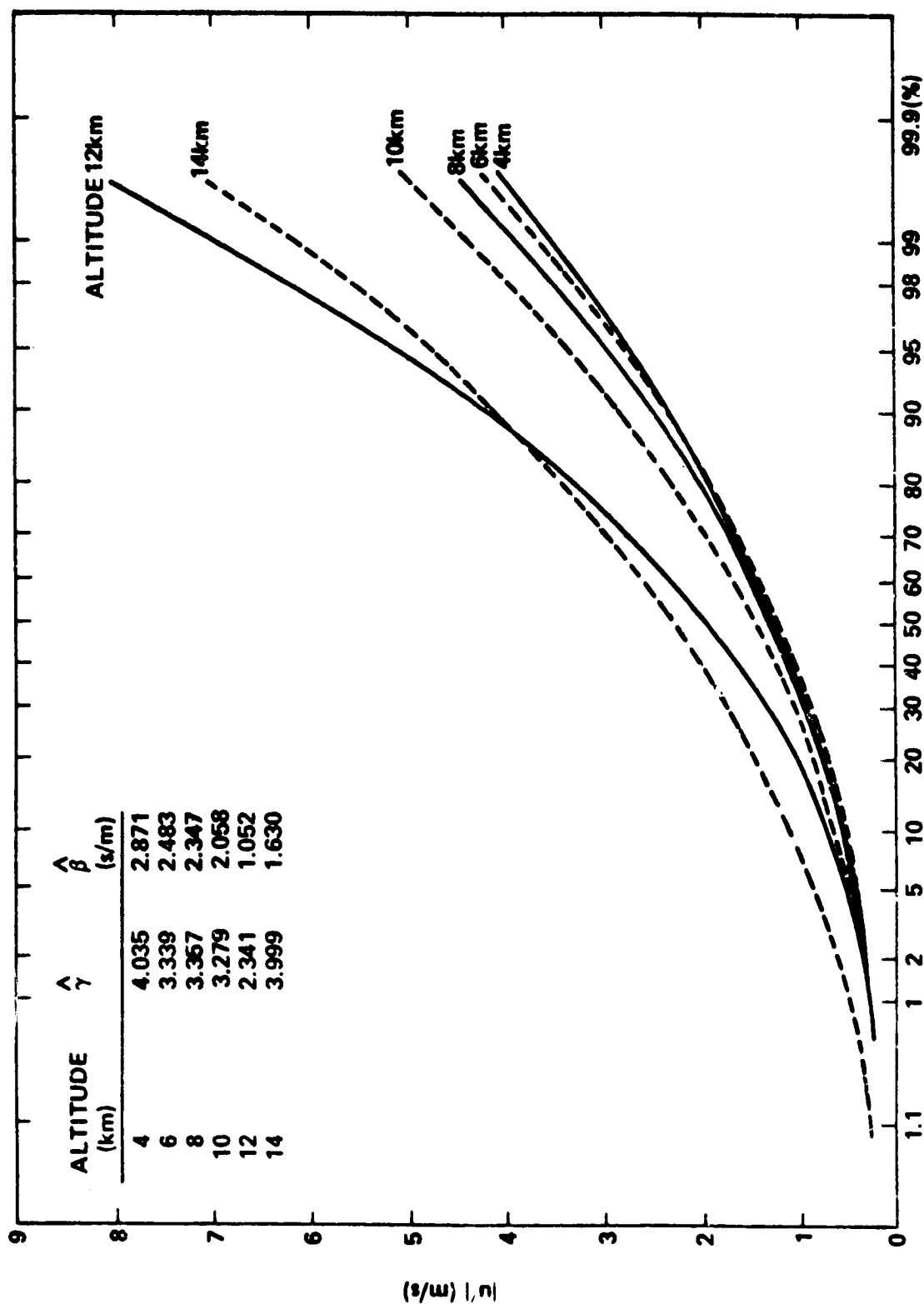


FIGURE 16. GAMMA PDF OF GUST COMPONENT AMPLITUDE $|u'|$, FROM 420-2470 m WAVELENGTH BAND FILTER AT 4, 6, 8, 10, 12, 14 km ALTITUDES, FEBRUARY, CAPE CANAVERAL, FLORIDA

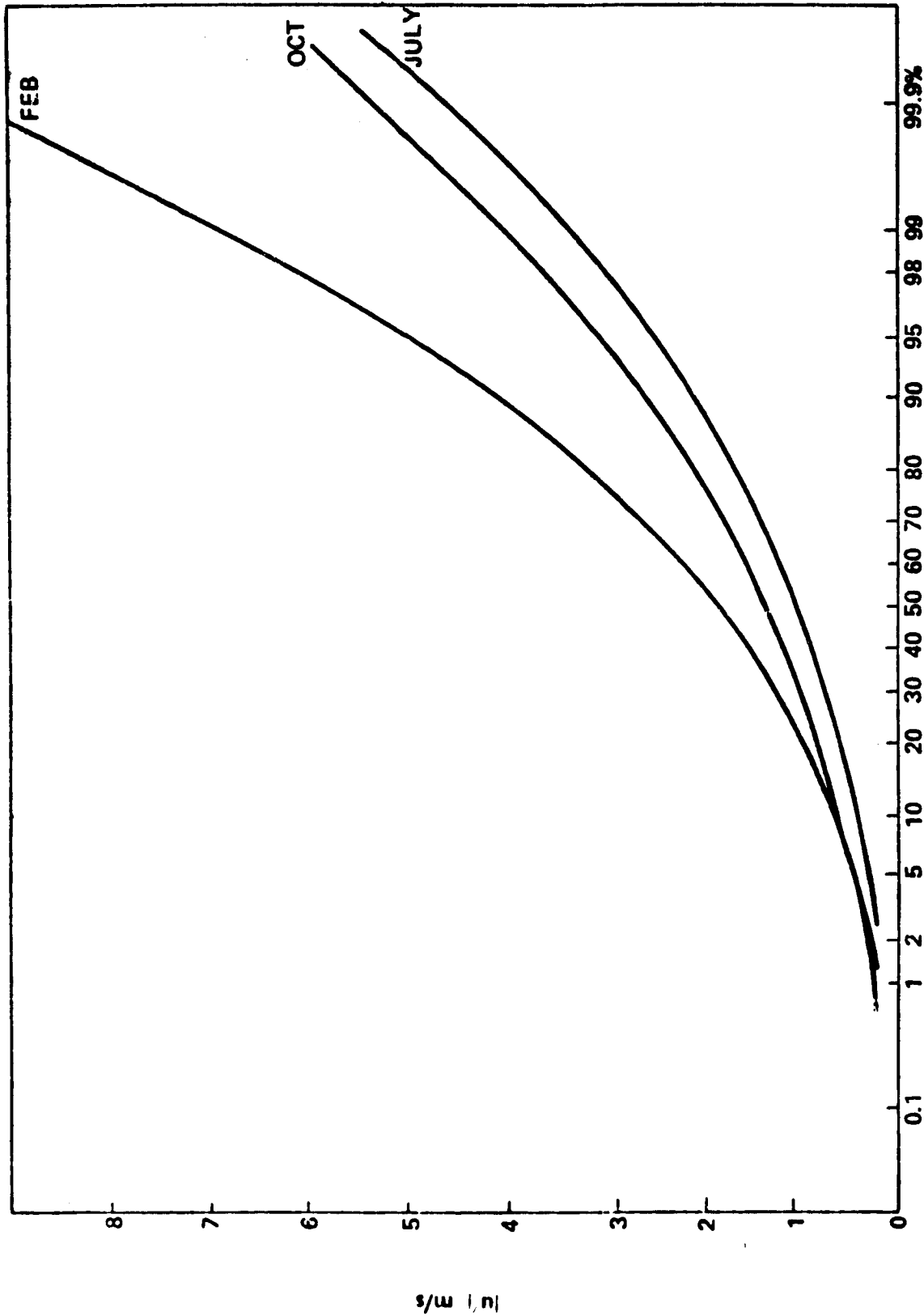


FIGURE 17. PDF OF GUST COMPONENT AMPLITUDE, $|u'|$, FROM 420-2470m WAVELENGTH BAND AT 12km ALTITUDE FOR FEBRUARY, JULY, OCTOBER, CAPE CANAVERAL, FLORIDA.

Table 1. Results of Testing the Hypothesis that the Samples¹ of u and v Component Absolute Gust and Gust Length are Drawn from Gamma Distributed Populations

Wavelength Band (m)	A/R ²				
	u'	v'	L _u '	L _v '	All Variables
90-420	4/2	6/0	5/1	5/1	20/4
420-2470	5/1	6/0	6/0	6/0	23/1
2470-6000 ³	4/1	5/0	4/1	4/1	17/3
All Filters	13/4	17/0	15/2	15/2	40/8

¹Samples for month of February at six altitudes (4, 6, ..., 14 km) for Cape Canaveral, Florida.

²Ratio of cases accepted to cases rejected utilizing the χ^2 test at the .05 level of significance.

³Five altitudes (6, 8, ..., 14 km)

Aerospace vehicle control systems can respond critically to large wind perturbations at certain wavelengths. The conditional PDF of gust component amplitude, $|u'|$, given a gust length, L_u , for various altitudes and months is useful in vehicle design. Conditional PDF's calculated from Equation 2.36 using sample estimates of the parameters from Cape Canaveral band pass (420-2470) gust data at 12 km are illustrated in Figure 18. Percentiles of the conditional PDF plotted as a function of the given gust length are illustrated in Figure 19. It is indicated that each percentile can be approximated by an empirical linear function of L_u , for this example.

ORIGINAL PAGE IS
OF POOR QUALITY

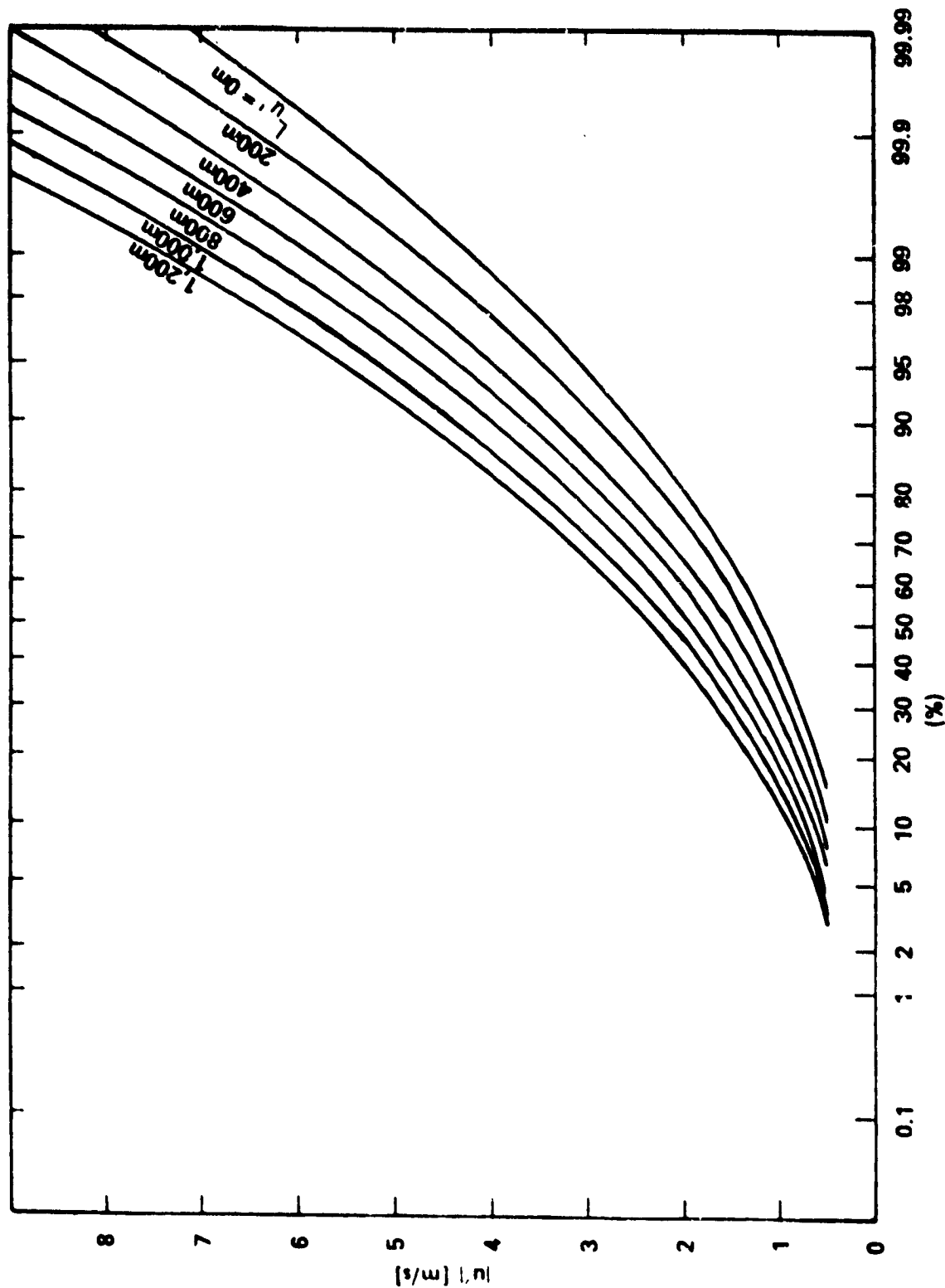


FIGURE 18. CONDITIONAL PDF OF GUST COMPONENT AMPLITUDE $|u'|$, GIVEN GUST LENGTH, L_u , FROM 420 - 2470m WAVELENGTH BAND FILTER AT 12km ALTITUDE FEBRUARY, CAPE CANAVERAL, FLORIDA.

ORIGINAL PAGE IS
OF POOR QUALITY

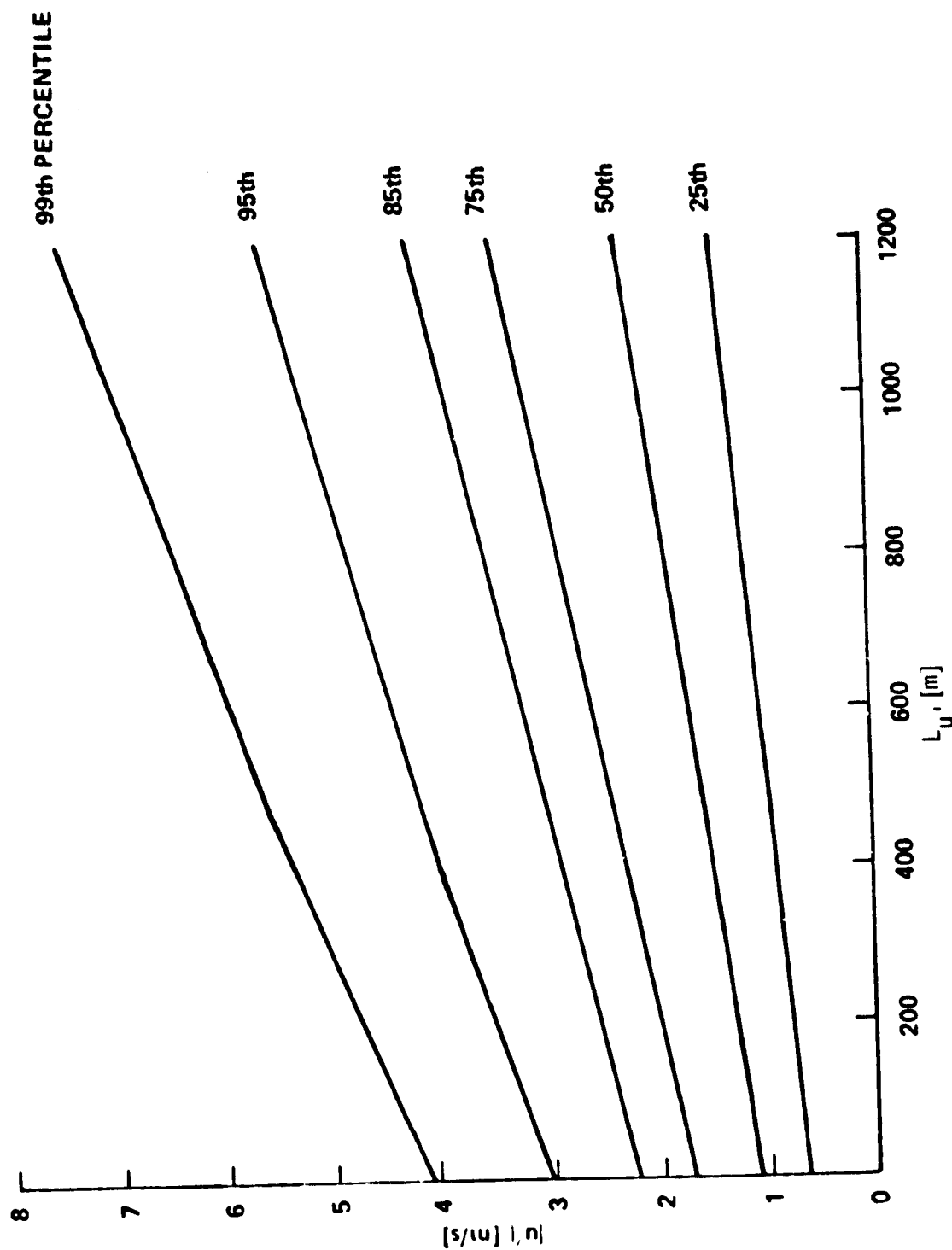


FIGURE 19. PERCENTILES OF CONDITIONAL GUST COMPONENT AMPLITUDE, $|u'|$, GIVEN GUST LENGTH, L_u' , FROM 420 - 2470m WAVELENGTH BAND FILTER AT 12km ALTITUDE FEBRUARY, CAPE CANAVERAL, FLORIDA

3.2.2 Bivariate Distributions

An observed bivariate distribution of gust variables is illustrated in Figure 20. The nondimensional variables T_1 and T_2 are calculated from u component absolute gust, $|u'|$, and associated gust length, L_u , data at 12 km over Cape Canaveral for a wavelength range of 420-2470 meters. The probability contained within rectangular domains was calculated according to Equation 2.6. Rectangular domains are well suited for preliminary evaluation of the goodness of fit of the model to the observed distribution. A comparison is given in Table 2 of the observed number of occurrences (counted within 2x2 cells in Figure 20) and the expected number if T_1 and T_2 are bivariate gamma distributed. There is good agreement between observed and expected cell counts.

The domain of bivariate gamma distributed variables can be divided into a number of equal-area sectors. The probability contained within each sector is obtained by calculating the difference in probability between two partially overlapping sector probabilities. For sectors of equal area, the variation of probability from sector to sector is a measure of the relationship between the shape parameters of the marginal distributions. Equivalence of shape parameters yields a symmetry in the variation of the sector probabilities; whereas, nonequivalence yields asymmetry. The change in symmetry is

ORIGINAL PAGE IS
OF POOR QUALITY

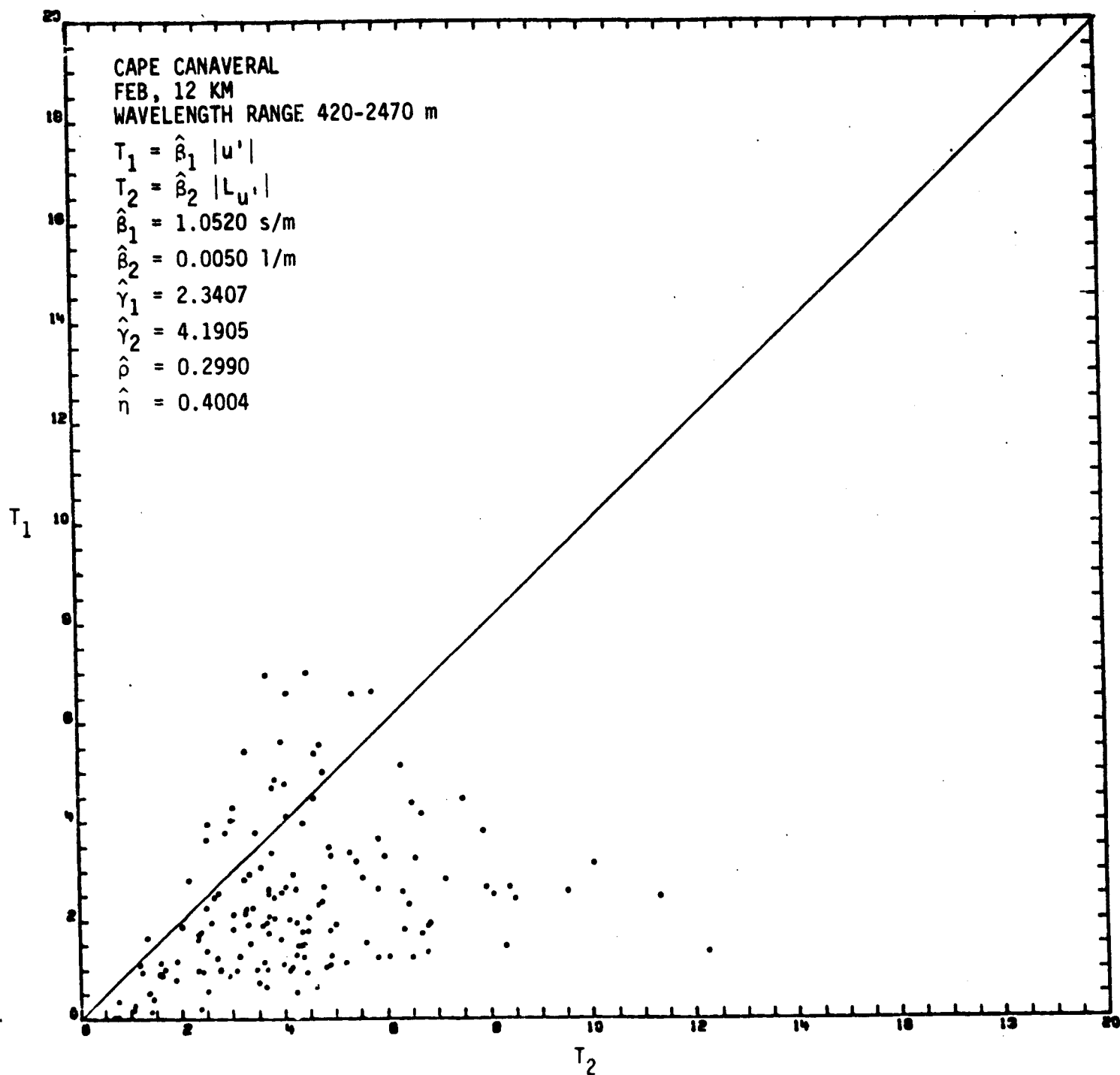


FIGURE 20. OBSERVED NON-DIMENSIONAL GUST VARIABLES
 T_1 AND T_2

Table 2. Observed¹ and Expected² Number of Occurrences within 2x2 Cells for Nondimensional Variables T_1 and T_2 Calculated³ from Absolute u Component Gust and Gust Length L_u , at 12 km

T_1	T_2						
	0-2	2-4	4-6	6-8	8-10	10-12	12-14
0-2	18 11.99	28 34.16	23 19.83	7 6.37	1 1.53	0 0.31	1 0.06
2-4	0 5.15	22 21.67	17 18.06	6 7.74	4 2.34	2 0.57	0 0.12
4-6	0 0.73	6 4.60	6 5.53	4 3.20	0 1.24	0 0.37	0 0.09
6-8	0 0.08	1 0.69	4 1.15	0 0.88	0 0.43	0 0.16	0 0.05
8-10	0 0.01	0 0.09	0 0.19	0 0.19	0 0.11	0 0.05	0 0.02

¹Cape Canaveral at 12 km during February for a wavelength range of 420-2470 meters; integer values in upper left of table entries for each cell.

²Expected for correlated bivariate gamma distributed variables; values in lower right of table entries (calculated from Equation 2.6).

³ $T_1 = \beta_1 |u'|$, $T_2 = \beta_2 L_u$; refer to Figure 20 caption for parameter estimates.

clearly indicated in Table 3. A case illustrating asymmetry in an observed distribution is illustrated in Figure 20; the significant difference in the sample estimates of the γ parameters (listed in the figure inset) is consistent with the asymmetry of the plotted data. Nearly 90 percent of the data are within the lower half of the domain illustrated in Figure 20.

Table 3. Sector Probabilities for Equal Area Sectors
(Calculated from Equation 2.14), $\gamma_1 = 2$

Sector Range Deg.	γ_2			
	2	3	4	5
0-15	.11510	.03177	.00829	.00208
15-30	.18875	.11054	.05518	.02531
30-45	.19615	.17020	.12403	.08198
45-60	.19615	.22211	.21056	.18047
60-75	.18875	.26696	.31588	.33770
75-90	.11510	.19843	.28606	.37245

4. CONCLUDING REMARKS

Although the main topics stated in the abstract and introduction have been investigated, there remains a need for further investigations to address such topics as parameter estimation and hypothesis testing for data samples taken from correlated bivariate gamma distributed variables.

Three commonly used procedures for estimating the parameters for the univariate gamma distribution are:

1. The moment method,
2. A maximum likelihood method by Thom (1966), and
3. A polynomial approximation given by Greenwood and Durand (1960).

Bury (1975) gives a detailed discussion on parameter estimation in the gamma distribution.

Very little can be found in the open literature concerning hypothesis testing for the parameters of the gamma distribution. In most cases, the results given in the literature assume that the shape parameters are known and tested for the scale parameter. In this report, a test for equality of shape parameters in the presence of correlation was needed. However, this problem has not been satisfactorily resolved

and remains unresolved to the best of our knowledge. That is, there is not a test for

$$H_0 : \gamma_x = \gamma_y$$

whenever $(x,y) \sim \Gamma(\gamma_x, \beta_x, \gamma_y, \beta_y, \rho)$ and $\rho \neq 0$. Moran (1969) has given an expression for the joint likelihood function and has indicated a procedure for testing $H_0 : \gamma_x = \gamma_y$.

Further discussions on the properties of the functions presented in Section 2 and additional examples in Section 3 may be helpful to those investigators who are interested in making applications of these distribution functions.

BIBLIOGRAPHY

- *ABRAMOWITZ, M., and STEGUN, I. A. (1964), Handbook of Mathematical Functions, National Bureau of Standards, Applied Mathematics Series #55.
- ADELFGANG, S. I. (1970), "Analysis of Jimsphere Wind Profiles Viewed in the Flight Time Domain of a Saturn Vehicle," Journal of Spacecraft and Rockets, 7, 9, 1146-1149.
- ADELFGANG, S. I., and SMITH, O. E. (1981), "Vector Wind Gust Model," NASA TM-82441.
- BURG, K. V. (1975), Statistical Models in Applied Science, John Wiley and Sons.
- CAMP, D. W. (1971), "NASA/Marshall Space Flight Center's FPS-16 Radar/Jimsphere Wind Profile Program," A.M.S. Bulletin, 52, 4, 253-254.
- DANIELS, G. E. (ed.) (1973), "Terrestrial Environment (Climatic) Criteria Guidelines for Use in Aerospace Vehicle Development," 1973 Rev., NASA TMX-64757.
- DEMANDEL, R. E., and KRIVO, S. J. (1971), "Selecting Digital Filters for Application to Detailed Wind Profiles," NASA CR-61325.
- DOWNTON, F. (1970), "Bivariate Exponential Distribution in Reliability Theory," J. of Royal Statistical Society B, 32, 408-417.
- *ERDE'LYI, A., et al (1954), Tables of Integral Transforms, Vols. I and II, McGraw-Hill Book Co.

*Not cited in text.

FICHTL, G. H., and PERLMUTTER, M. (1976), "Stochastic Simulation of Vertically Nonhomogeneous Gusts," AIAA Paper 76-389.

*GRADSHTEYN, I. S., and RYZHIK, I. M. (1965), Tables of Integrals, Series, and Products, Academic Press, New York and London.

GREENWOOD, J. A., and DURAND, D. (1960), "Aids for Fitting the Gamma Distribution by Maximum Likelihood," Technometrics, 2, 55-65.

GUNST, R. F., and WEBSTER, J. T. (1973), "Density Functions of the Bivariate Chi-Square Distribution," J. of Statistical Computations and Simulations, 2, 275-288.

JENSEN, D. R., and HOWE (1968), "The Joint Distribution of Quadratic Forms and Related Distributions," Australian Journal of Statistics, 12, 13-22.

_____ (1968), "Probability Content of Bivariate Chi-Square Distributions Over Rectangular Regions," Virginia Journal of Science, 19, 233-239.

*JOHNSON, N. L., and KOTZ, S. (1972), Distributions in Statistics: Continuous Multivariate Distributions, John Wiley and Sons, Inc.

JONES, J. C. (1971), "A Unified Gust and Power Spectrum Treatment of Atmospheric Turbulence," International Conference on Atmospheric Turbulence, London, England, May 1971.

KIBBLE, W. F. (1941), "A Two Variate Gamma Type Distribution," Sankhya A, 5, 137-150.

*Not cited in text.

ORIGINAL PAGE IS
OF POOR QUALITY

- *KRISHNAMOORTHY, A. S., and PARTHASARTHY, M. (1951), "A Multivariate Gamma Type Distribution," Annals of Mathematical Statistics, 22, 549-557.
- MAGNUS, W., OBERHETTINGER, F., and SONI, R. P. (1966), Formulas and Theorems for the Special Functions of Mathematical Physics, Vol. 52, Springer-Verlag New York, Inc.
- *MARDIA, K. V. (1965), Families of Bivariate Distributions, Hafner Publishing Co., Griffen Statistical Monographs #27.
- MCALLISTER, P. R., LEE, R., and HOLLAND, B. S. (1981), "Computation of Probabilities from Jensen's Bivariate F Distribution," Comm. in Statistics, B10(3), 249-263.
- MORAN, P. A. P. (1969), "Statistical Inference with the Bivariate Gamma Distribution," Biometrika, 56, 627-634.
- *RICE, S. O. (1945), "Mathematical Analysis of Random Noise," Bell Systems Technical Journal, Vol. 24, 46-156.
- *SLATEN, L. J. (1960), Confluent Hypergeometric Functions, Cambridge Univ. Press.
- *SMITH, O. E., and ADELFGANG, S. I. (1981), "Gust Model Based on the Bivariate Gamma Distribution," J. Spacecraft, Vol. 18, No. 6, 545-549.
- *SMITH, O. E., and AUSTIN, L. P. (1982), "Sensitivity Analysis of the Space Shuttle to Ascent Wind Profiles," NASA Technical Paper 1988.
- THOM, H. C. S. (1966), "Some Methods of Climatological Analysis," WMO Technical Note 81, WMO-MO 199.TP.103.

*Not cited in text.

APPENDIX
GRAPHIC ILLUSTRATIONS

This appendix presents three-dimensional computer graphics of bivariate gamma density (Figures A1-A17) and contours of equal probability density (Figures A18-A34) for equal shape parameters (2.4) and unequal shape parameters (2.1) as the correlation varies.

Bivariate Gamma Density

Figure Number	Parameters	
	$\gamma_1 = \gamma_2$	ρ
A1	1.5	0.0
A2	1.5	0.25
A3	1.5	0.50
A4	1.5	0.75
A5	3.0	0.0
A6	3.0	0.25
A7	3.0	0.50
A8	3.0	0.75
A9	3.0	0.90

Figure Number	Parameters		
	γ_1	γ_2	ρ
A10	1	3	0.0
A11	1	3	0.25
A12	1	3	0.50
A13	1	3	0.75
A14	2	3	0.0
A15	2	3	0.25
A16	2	3	0.50
A17	2	3	0.75

ORIGINAL PAGE IS
OF POOR QUALITY

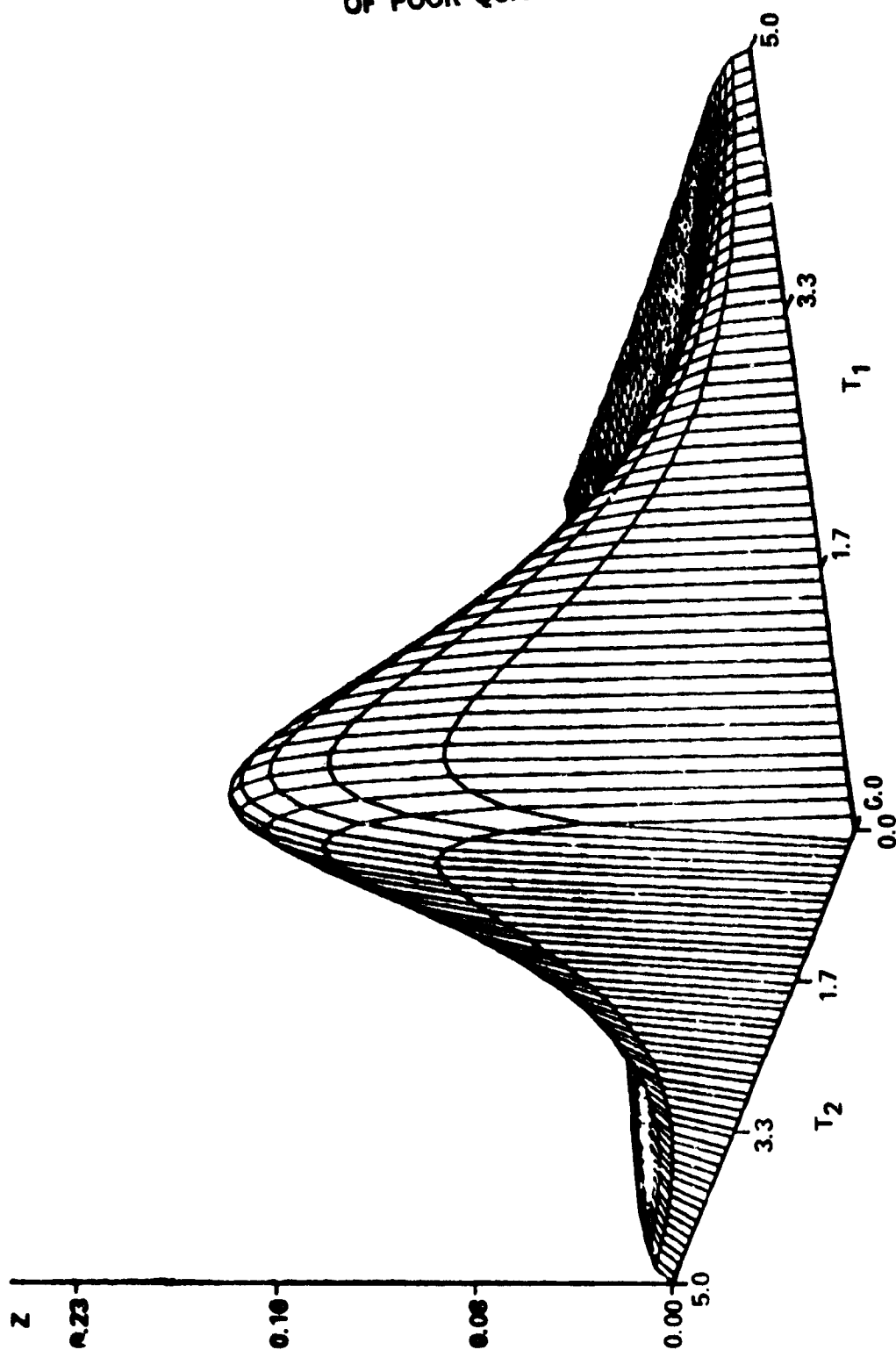


FIGURE A1. BIVARIATE GAMMA DENSITY, $\gamma_1 = \gamma_2 = 1.5$, $\rho = 0$

ORIGINAL PAGE IS
OF POOR QUALITY

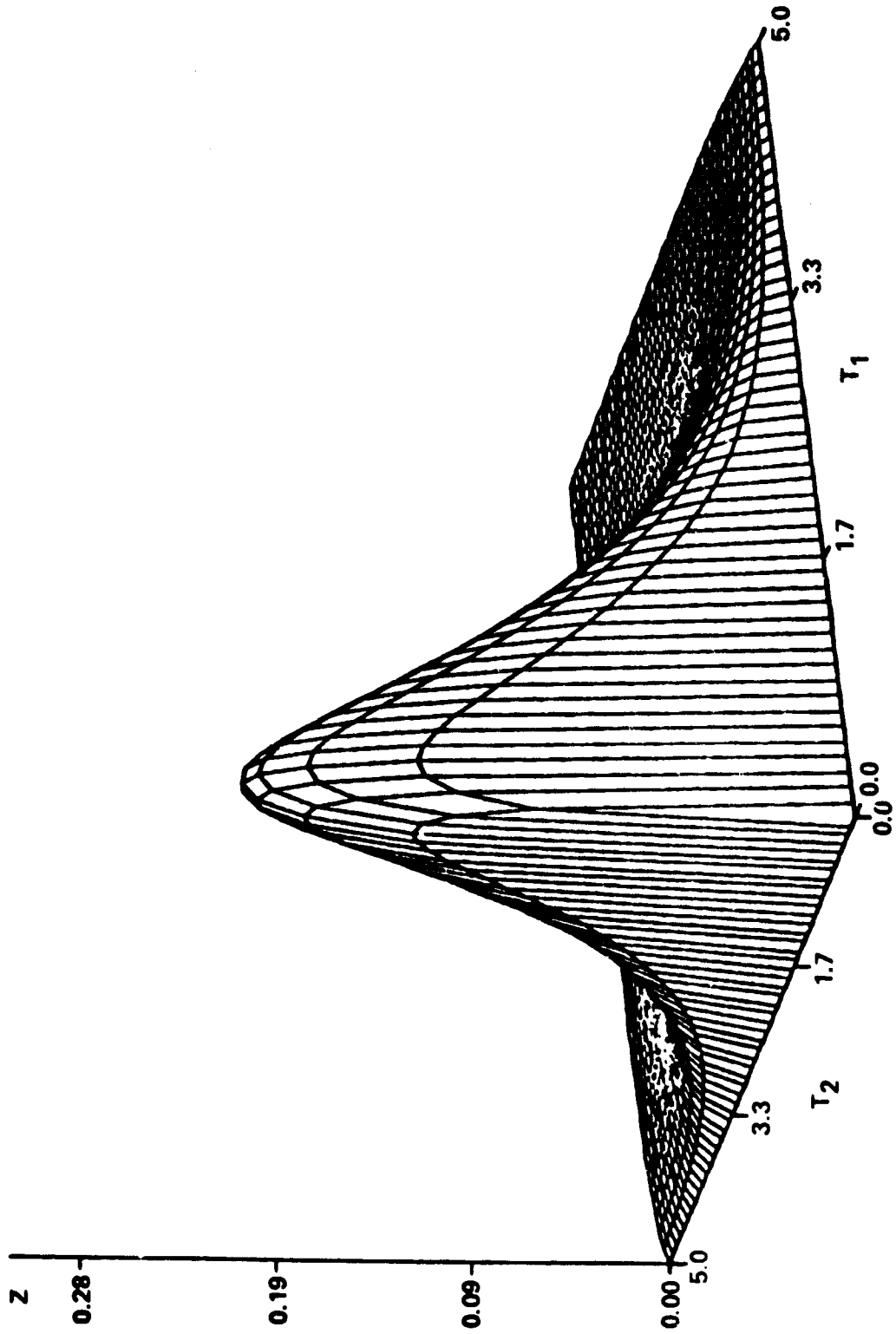


FIGURE A2 BIVARIATE GAMMA DENSITY, $\gamma = \gamma_2 = 1.5$, $\rho = 0.25$

ORIGINAL PAGE IS
OF POOR QUALITY

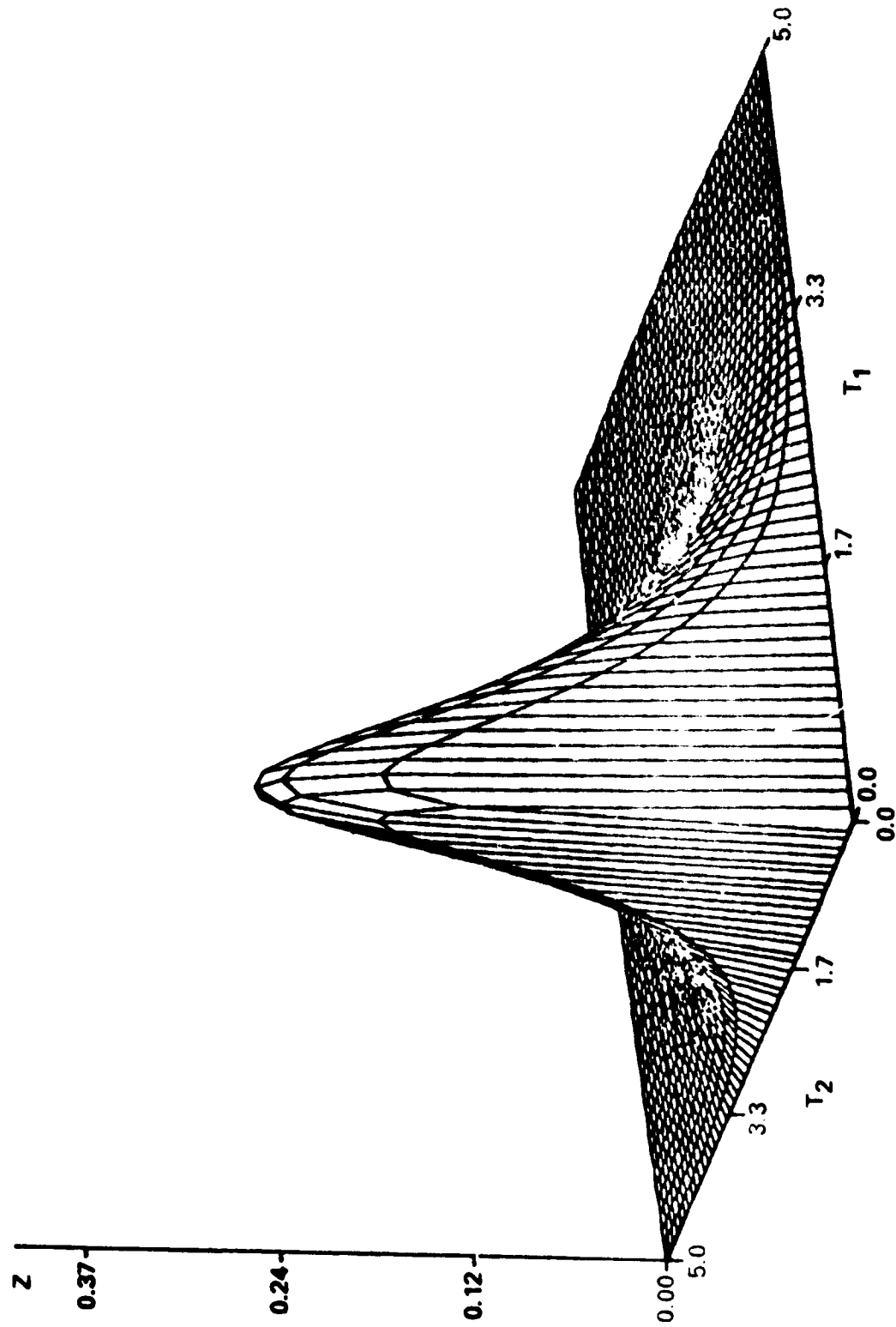


FIGURE A3. BIVARIATE GAMMA DENSITY, $\gamma = \gamma_2 = 1.5$, $\rho = 0.50$

ORIGINAL PAGE IS
OF POOR QUALITY

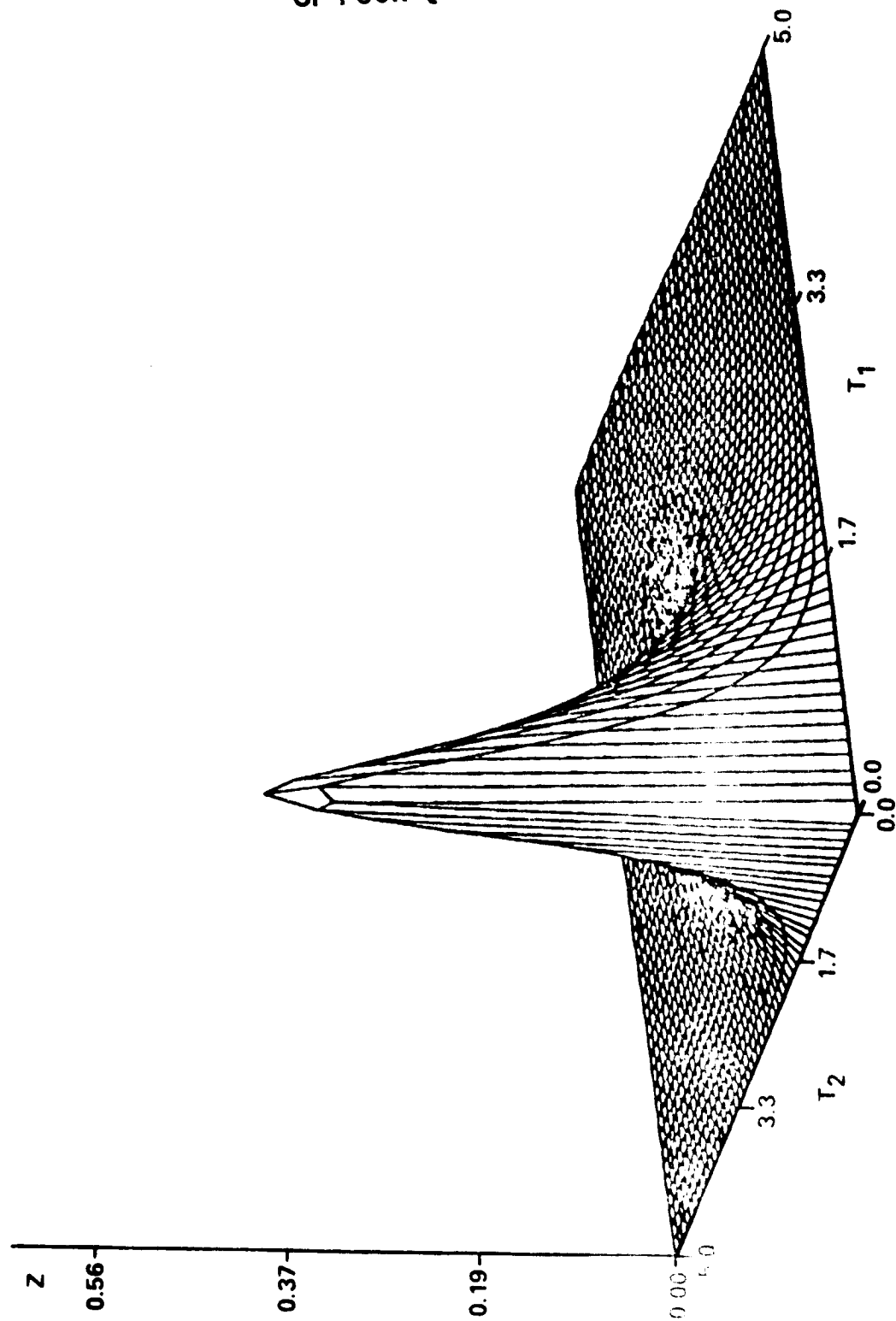


FIGURE A4. BIVARIATE GAMMA DENSITY, $\gamma_1 = \gamma_2 = 1.5$, $\rho = 0.75$

ORIGINAL PAGE IS
OF POOR QUALITY

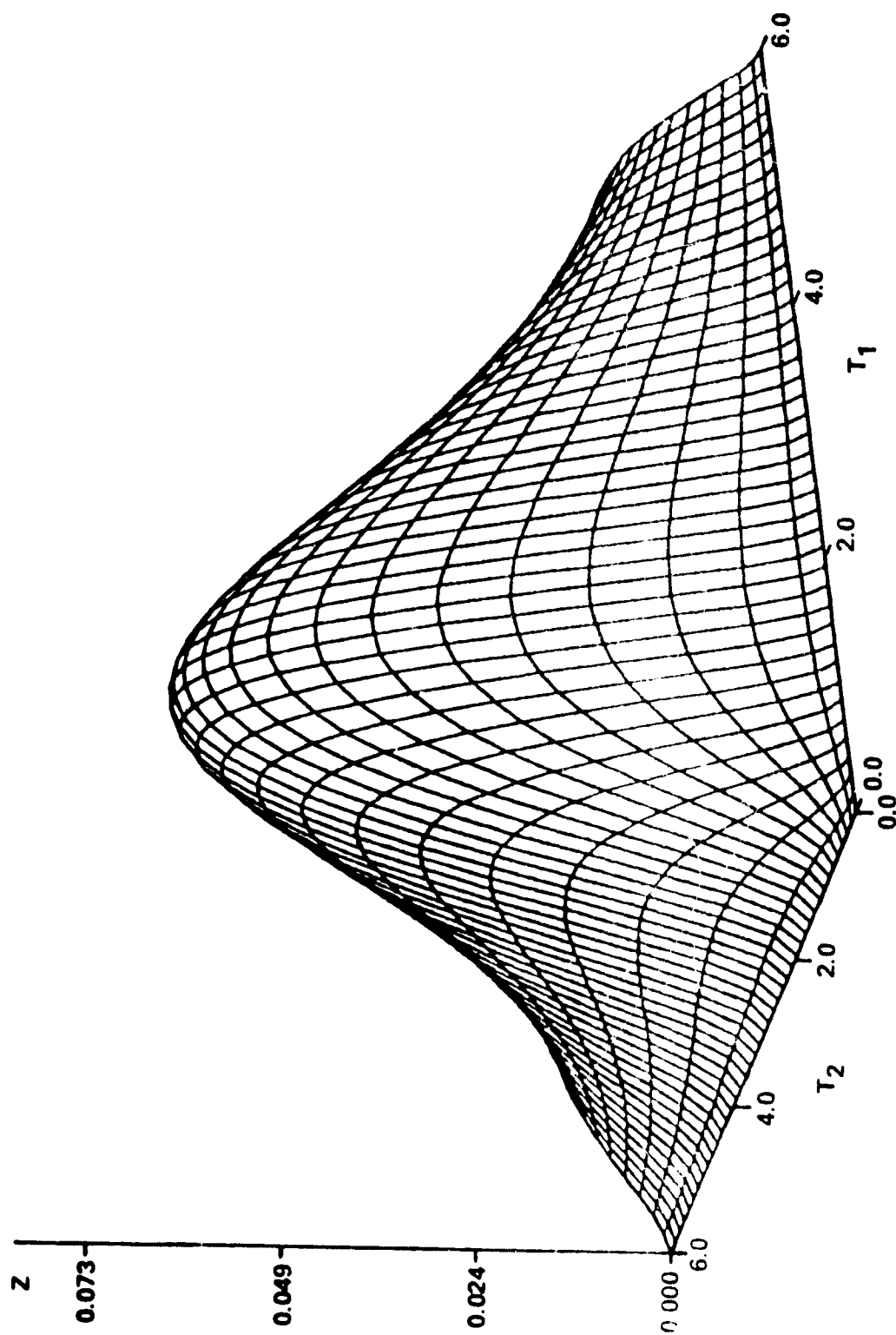


FIGURE A5. BIVARIATE GAMMA DENSITY, $\gamma_1 = \gamma_2 = 3.0$, $\rho = 0$

ORIGINAL PAGE IS
OF POOR QUALITY

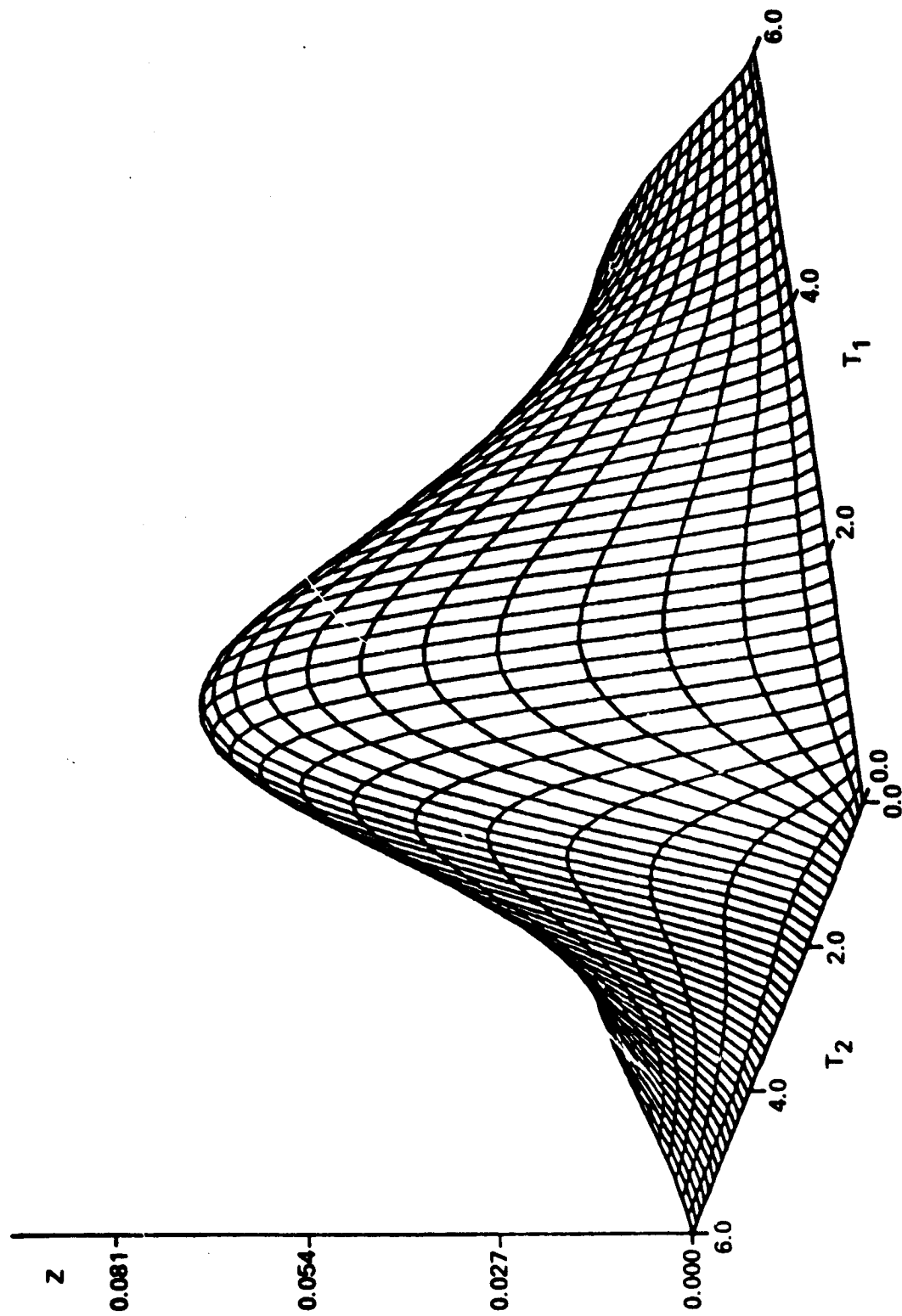


FIGURE A6. BIVARIATE GAMMA DENSITY, $\gamma_1 = \gamma_2 = 3.0$, $\rho = 0.25$

ORIGINAL PAGE IS
OF POOR QUALITY

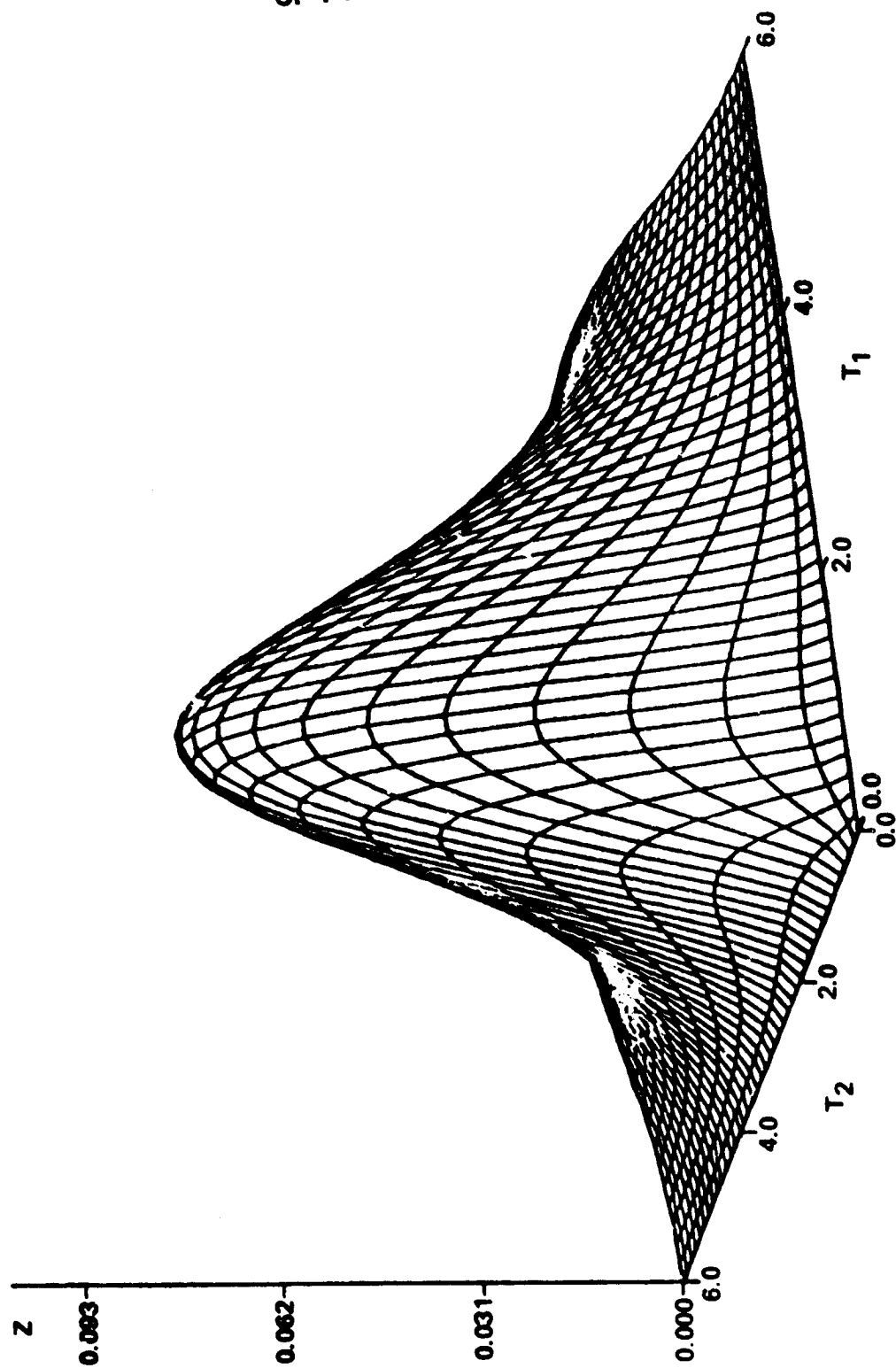


FIGURE A7. BIVARIATE GAMMA DENSITY, $\gamma_1 = \gamma_2 = 3.0$, $\rho = 0.50$

ORIGINAL PAGE IS
OF POOR QUALITY

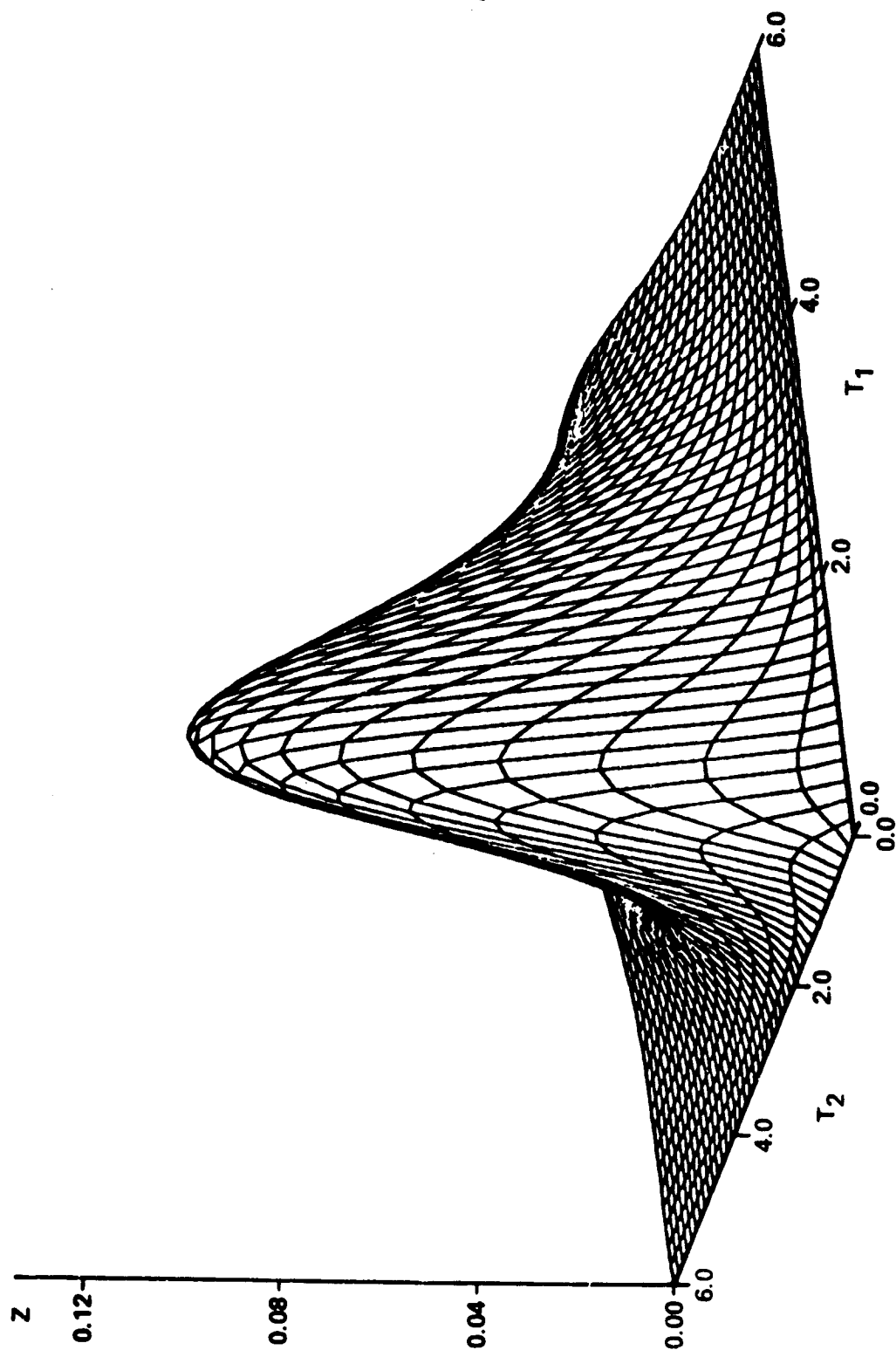


FIGURE A8. BIVARIATE GAMMA DENSITY, $\gamma_1 = \gamma_2 = 3.0$, $\rho = 0.75$

ORIGINAL PAGE IS
OF POOR QUALITY

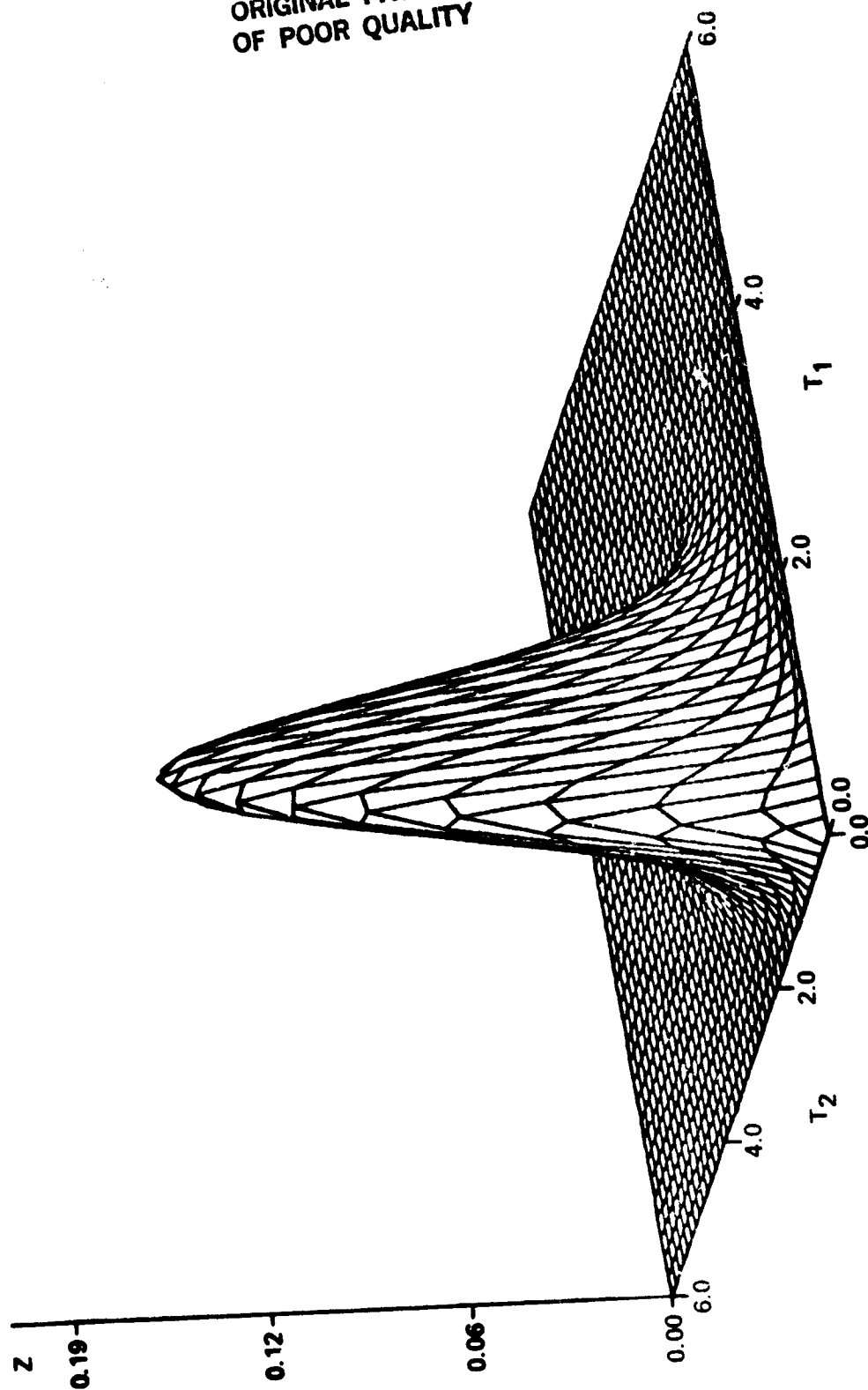


FIGURE A9. BIVARIATE GAMMA DENSITY, $\gamma_1 = \gamma_2 = 3.0$, $\rho = 0.90$

ORIGINAL PAGE IS
OF POOR QUALITY

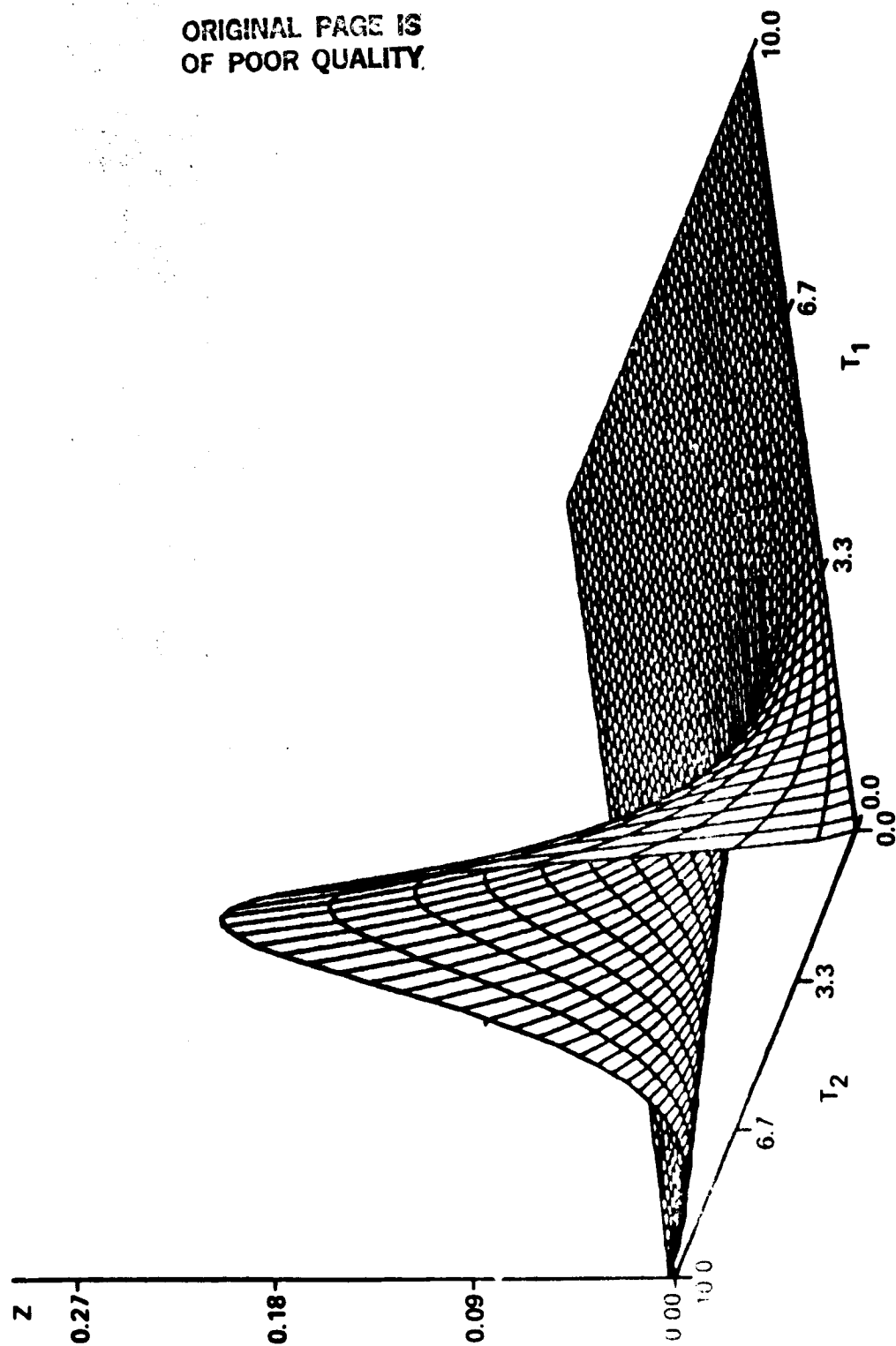


FIGURE A10. BIVARIATE GAMMA DENSITY, $\gamma_1 = 1.0$, $\gamma_2 = 3.0$, $\eta = 0$

ORIGINAL PAGE IS
OF POOR QUALITY

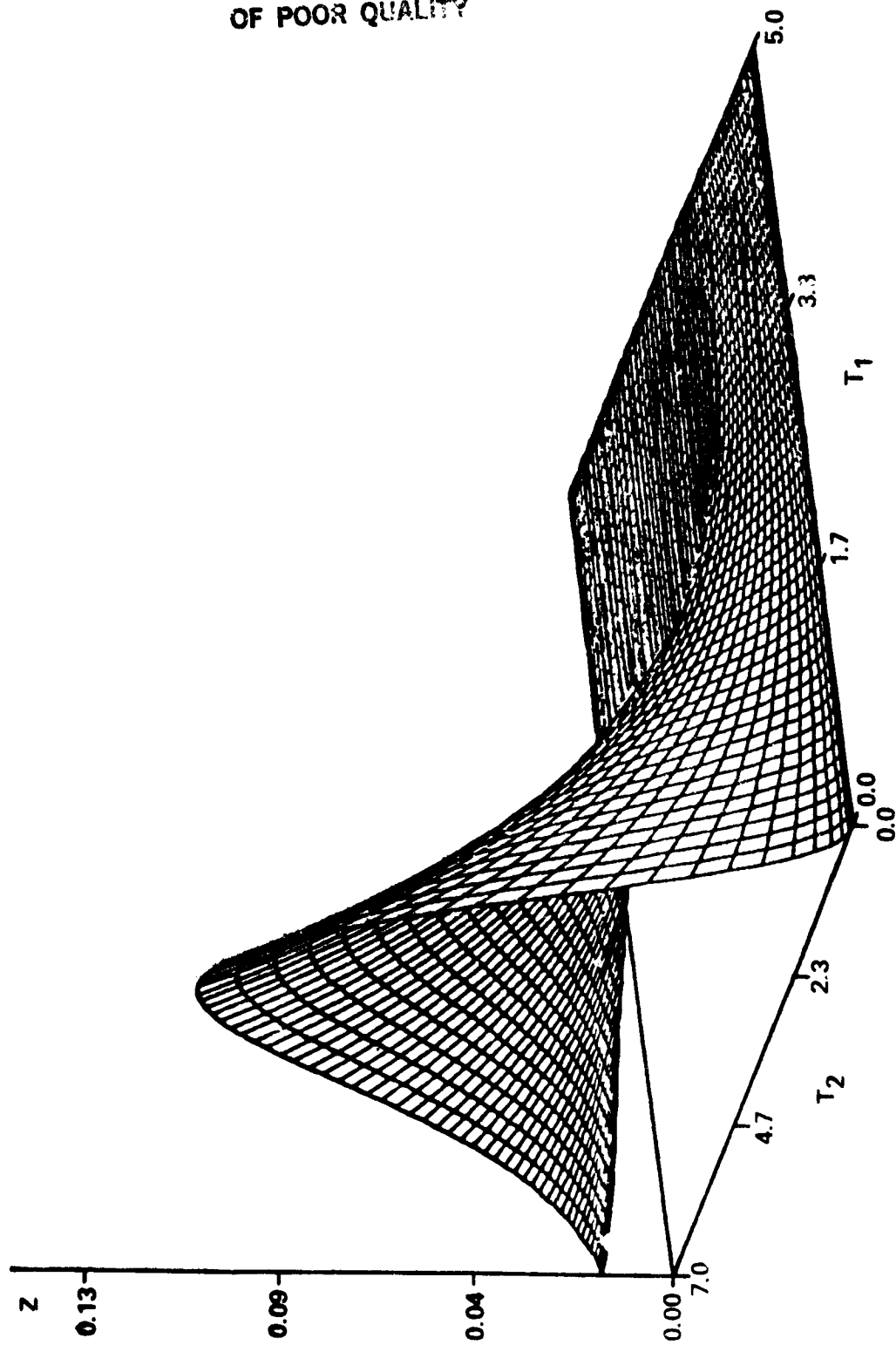


FIGURE A11. BIVARIATE GAMMA DENSITY, $\gamma_1 = 1.0$, $\gamma_2 = 3.0$, $\eta = 0.25$

ORIGINAL PAGE IS
OF POOR QUALITY

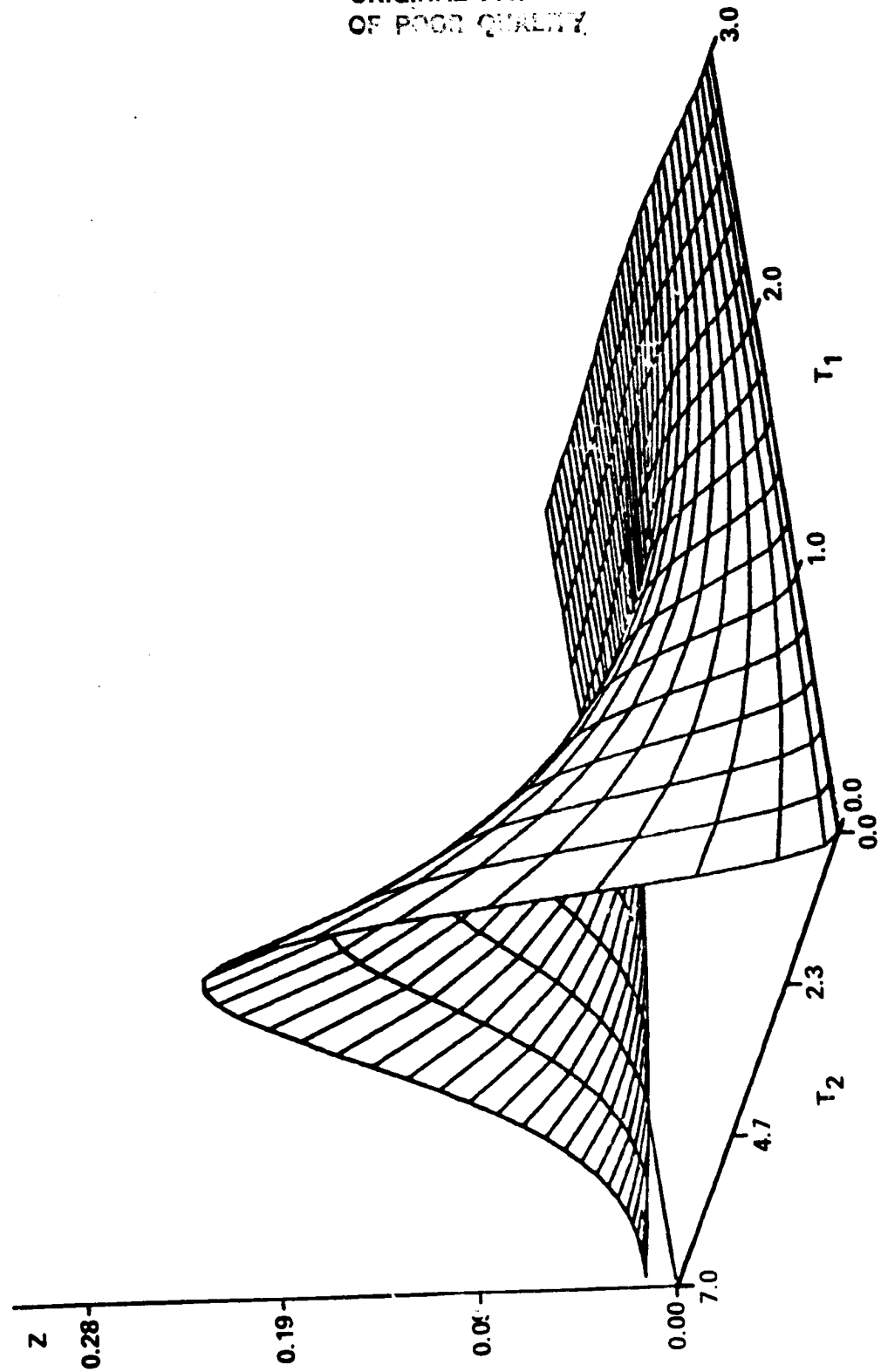


FIGURE A12 BIVARIATE GAMMA DENSITY, $\gamma_1 = 1.0$, $\gamma_2 = 3.0$, $\eta = 0.50$

ORIGINAL PAGE IS
OF POOR QUALITY

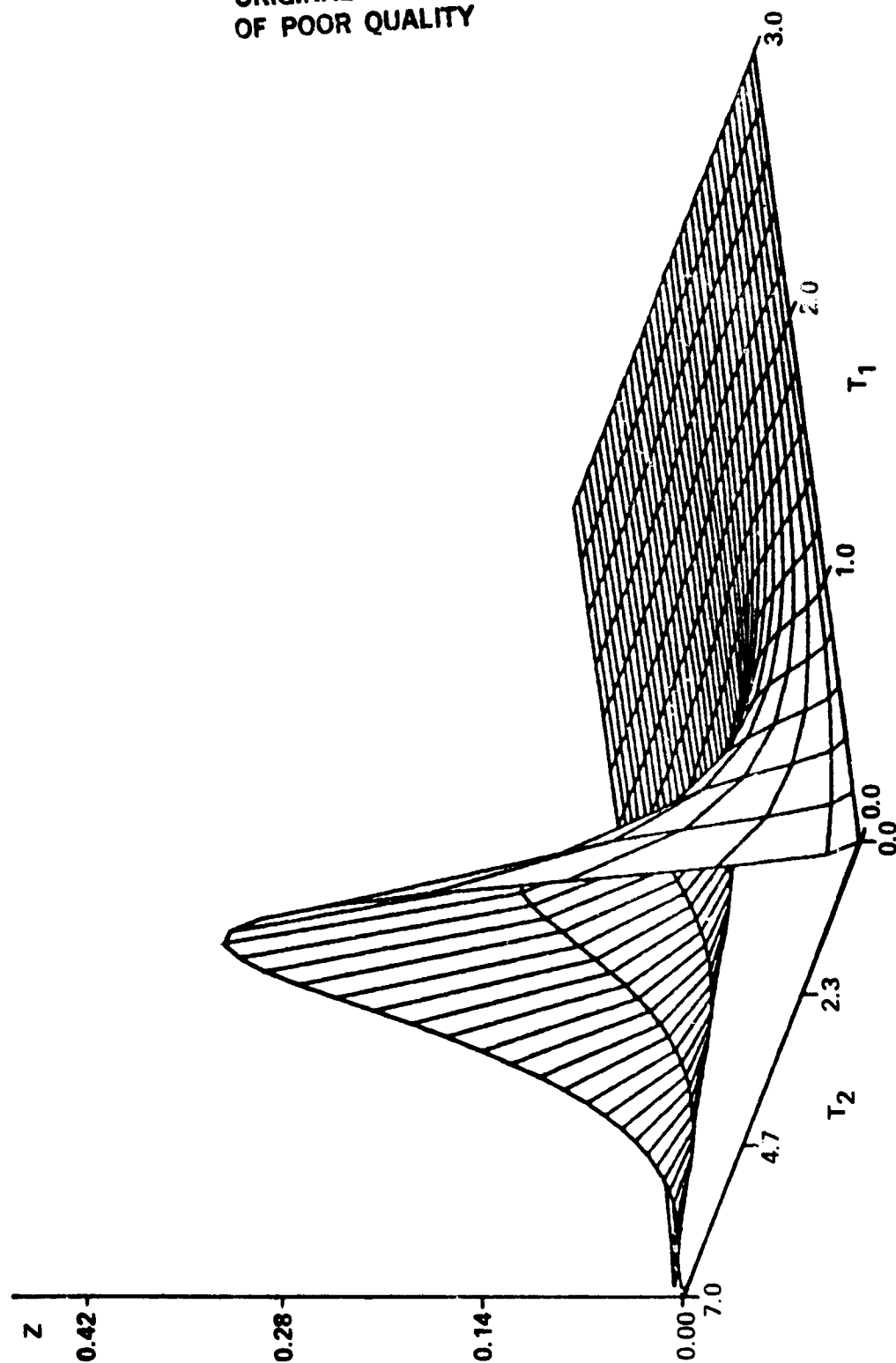


FIGURE A13. BIVARIATE GAMMA DENSITY, $\gamma_1 = 1.0$, $\gamma_2 = 3.0$, $\eta = 0.75$

ORIGINAL PAGE IS
OF POOR QUALITY

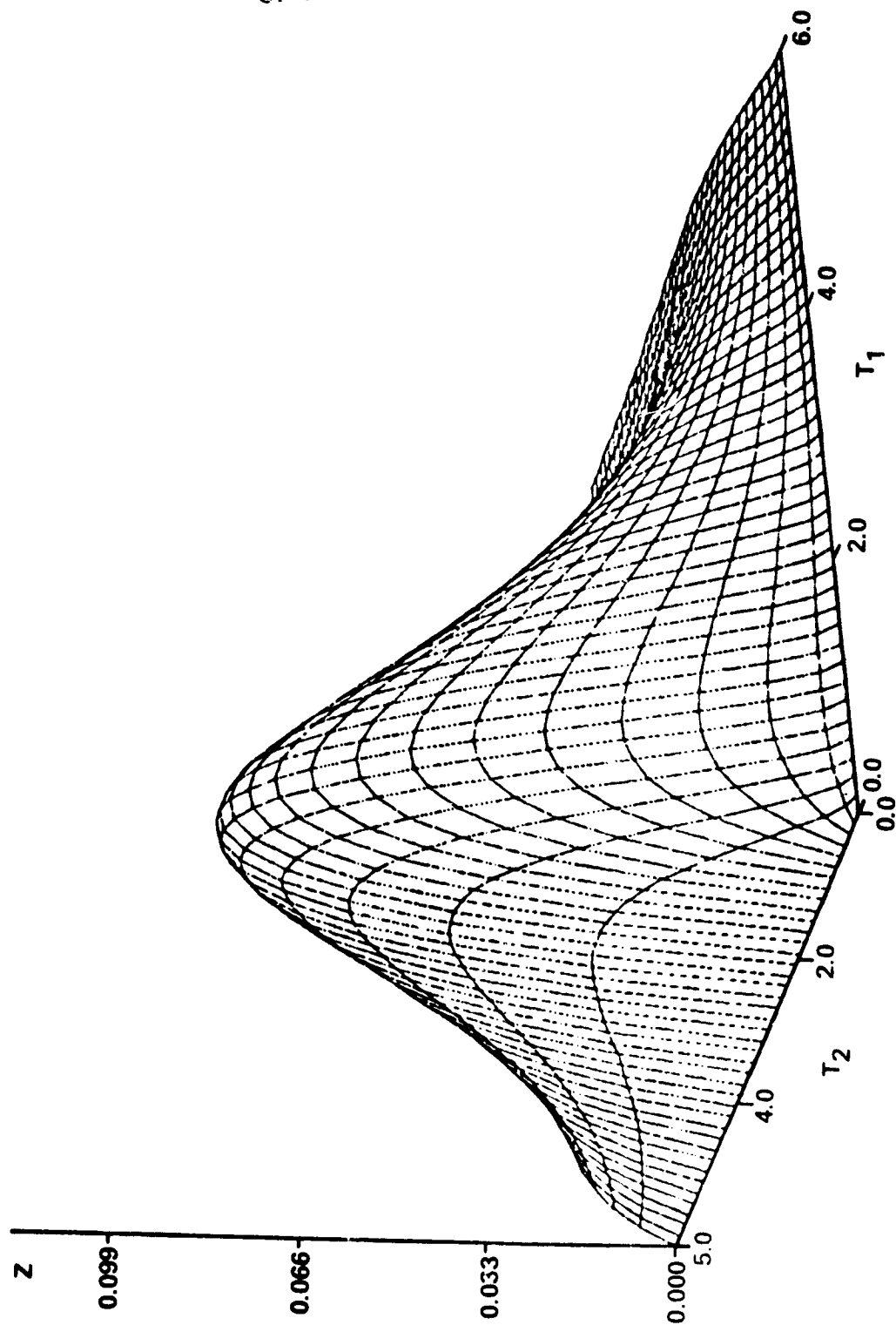


FIGURE A14. BIVARIATE GAMMA DENSITY, $\gamma_1 = 2.0$, $\gamma_2 = 3.0$, $\eta = 0$

ORIGINAL PAGE IS
OF POOR QUALITY

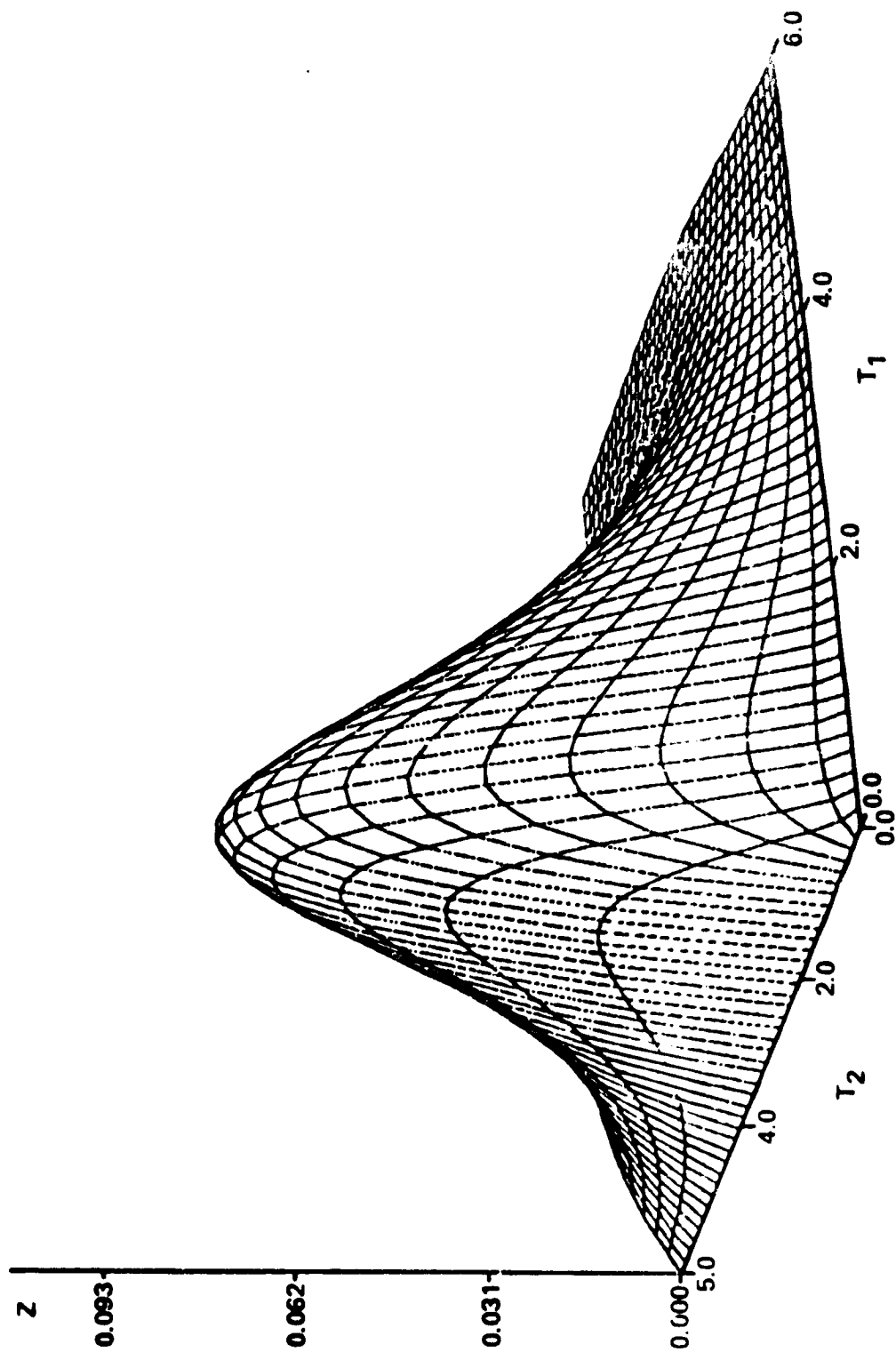


FIGURE A15. BIVARIATE GAMMA DENSITY, $\gamma_1 = 2.0$, $\gamma_2 = 3.0$, $\eta = 0.25$

ORIGINAL PAGE IS
OF POOR QUALITY

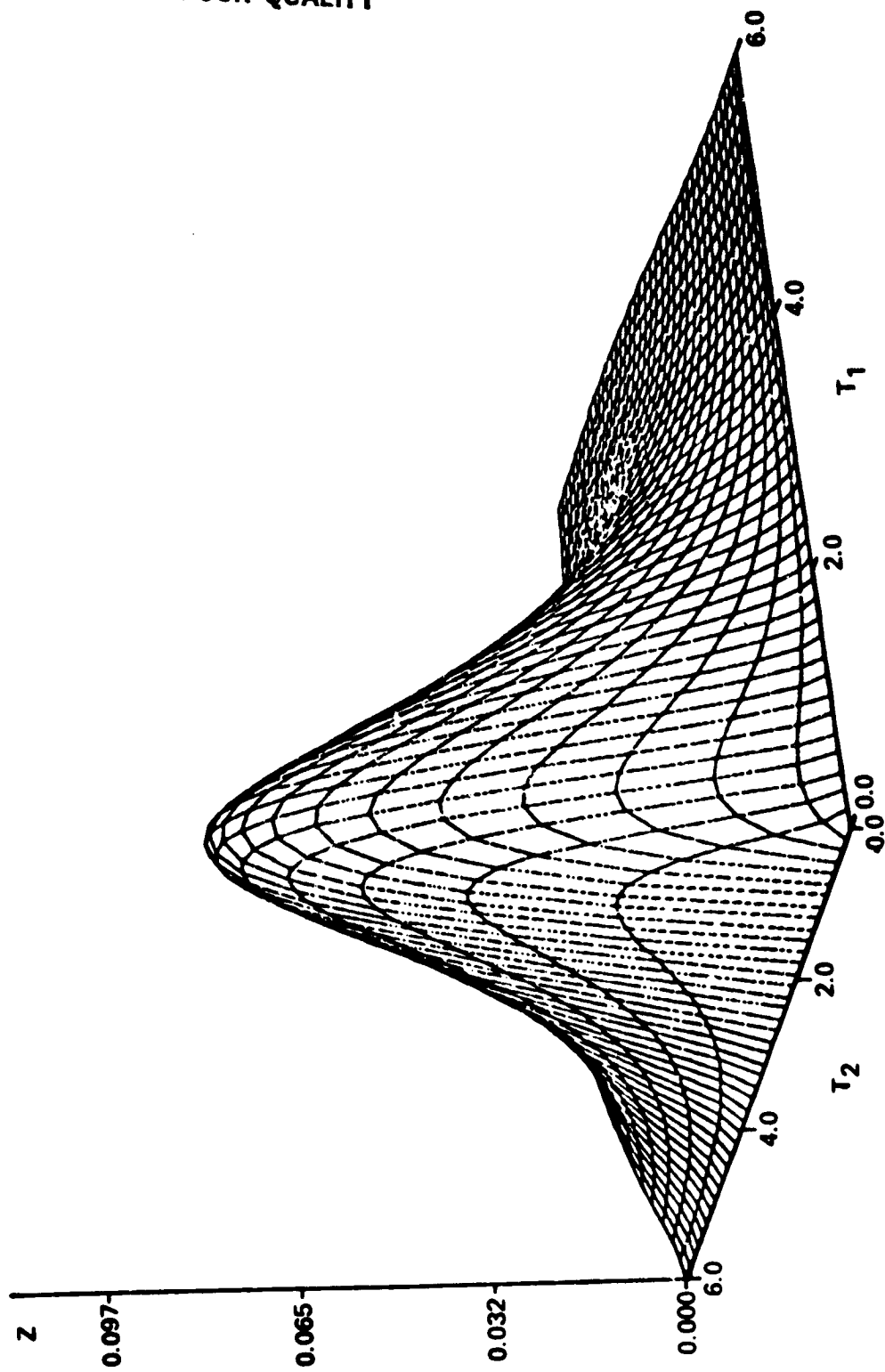


FIGURE A16. BIVARIATE GAMMA DENSITY, $\gamma_1 = 2$, $\gamma_2 = 3.0$, $\eta = 0.50$

ORIGINAL PAGE IS
OF POOR QUALITY

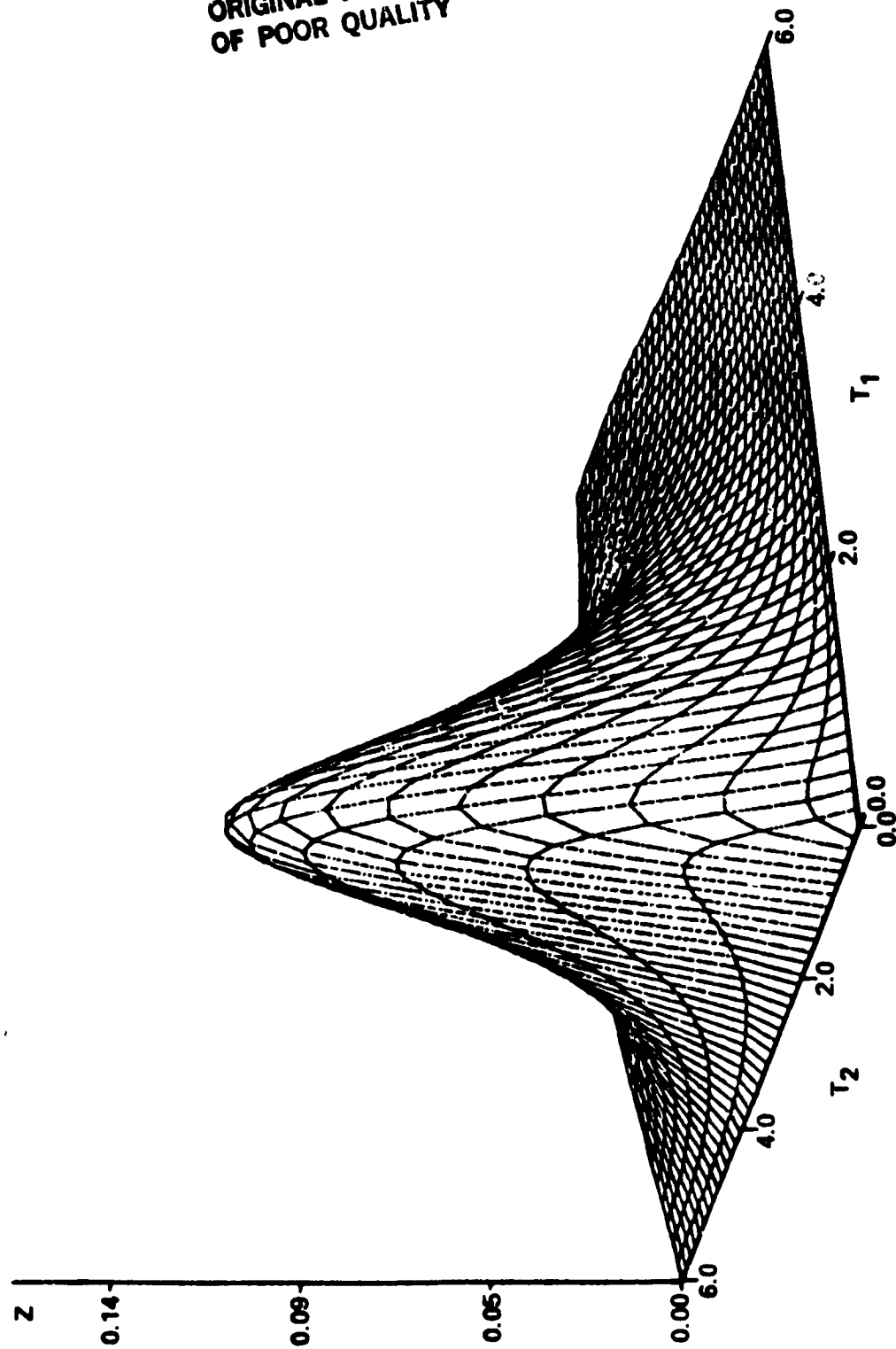


FIGURE A17. BIVARIATE GAMMA DENSITY, $\gamma_1 = 2.0$, $\gamma_2 = 3.0$, $\eta = 0.75$

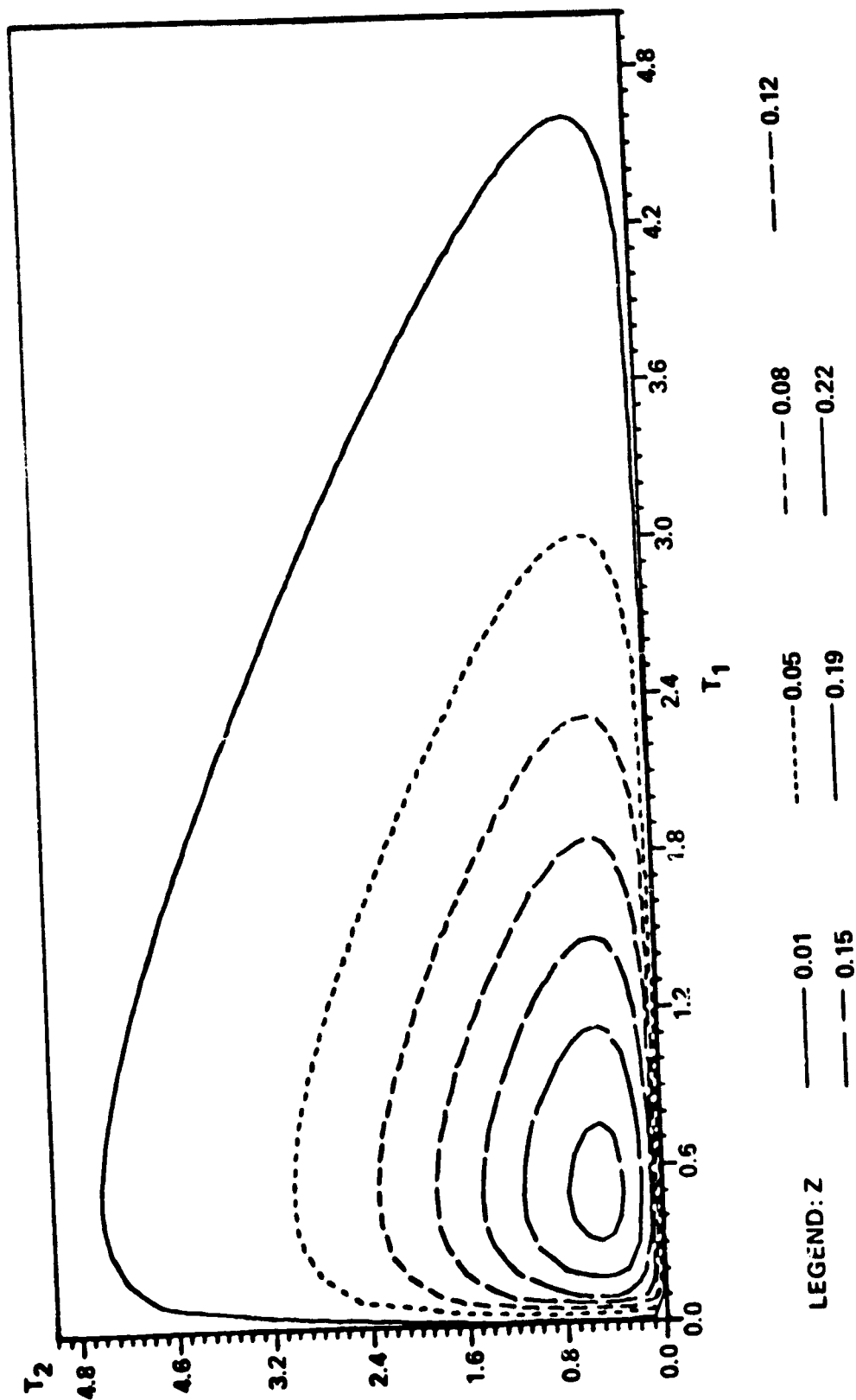


FIGURE A18. BIVARIATE GAMMA DENSITY CONTOURS, $\gamma_1 = \gamma_2 = 1.5$, $\rho = 0$

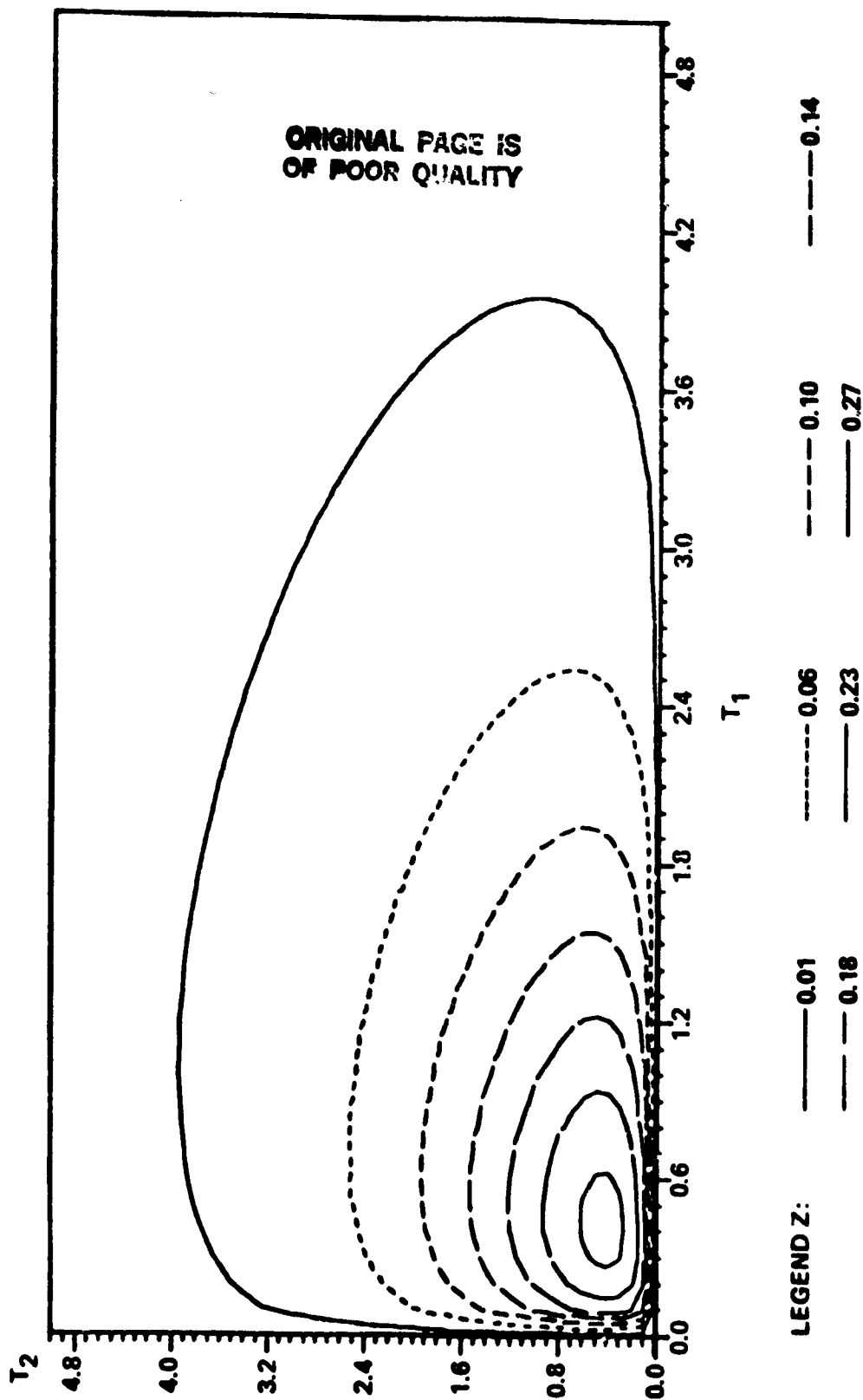


FIGURE A19. BIVARIATE GAMMA DENSITY CONTOURS, $\gamma_1 = 1.5$, $\rho = 0.25$

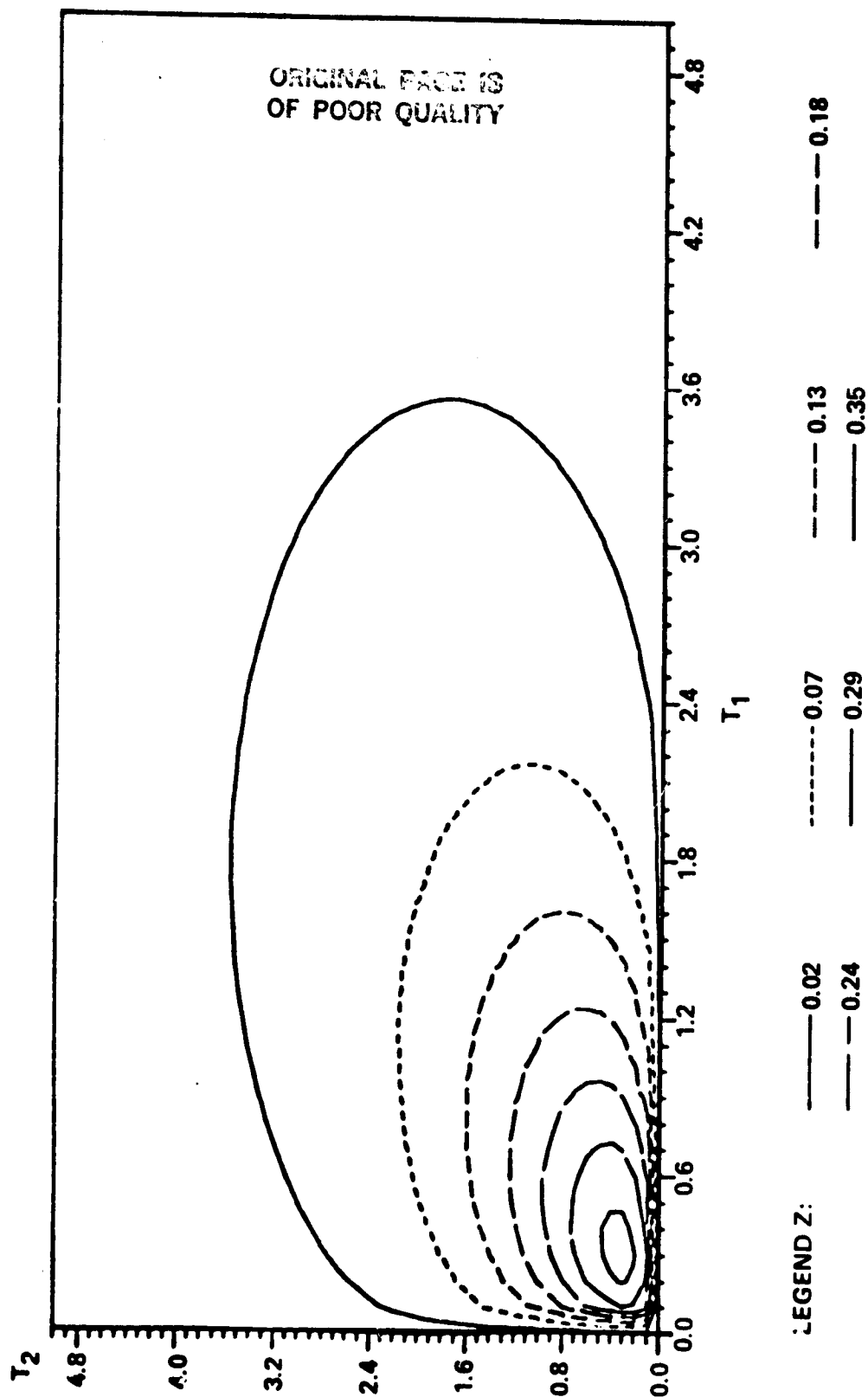


FIGURE A20 BIVARIATE GAMMA DENSITY CONTOURS, $\gamma_1 = \gamma_2 = 1.5$, $\rho = 0.50$

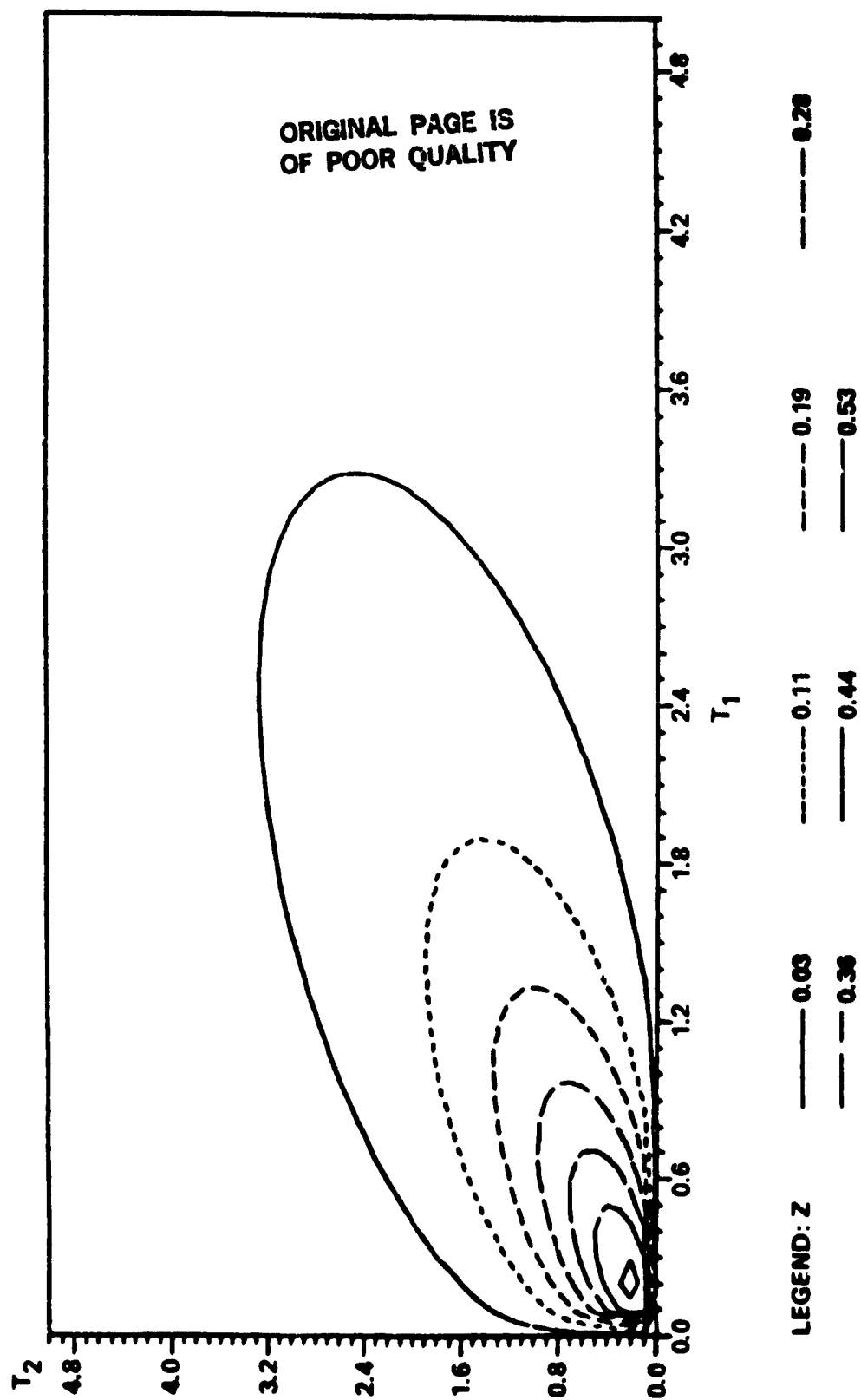


FIGURE A21. BIVARIATE GAMMA DENSITY CONTOURS, $\gamma_1 = 1.5$, $\rho = 0.75$

ORIGINAL PAGE IS
OF POOR QUALITY

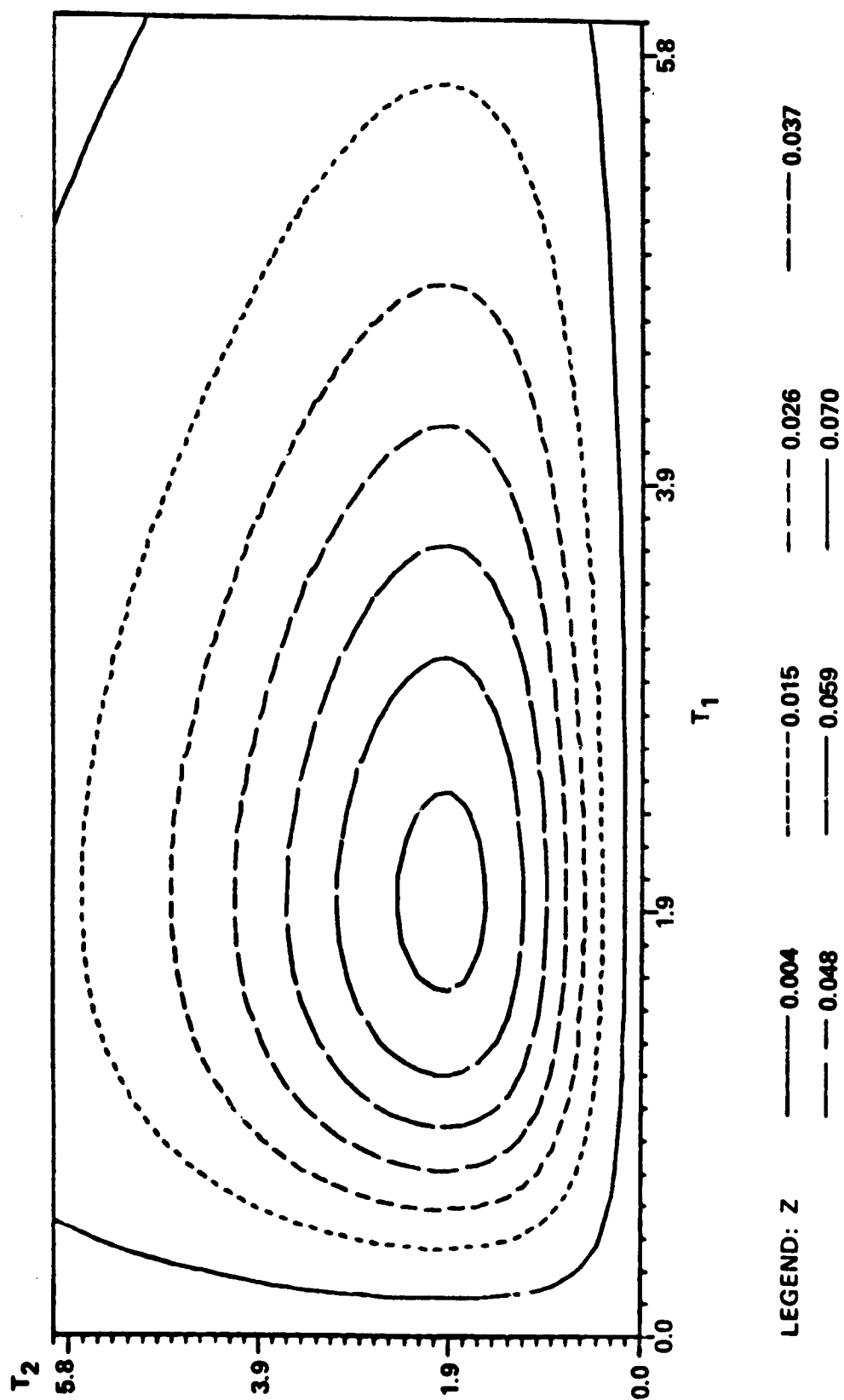


FIGURE A22 BIVARIATE GAMMA DENSITY CONTOURS, $\gamma_1 = \gamma_2 = 3.0$, $\rho = 0$

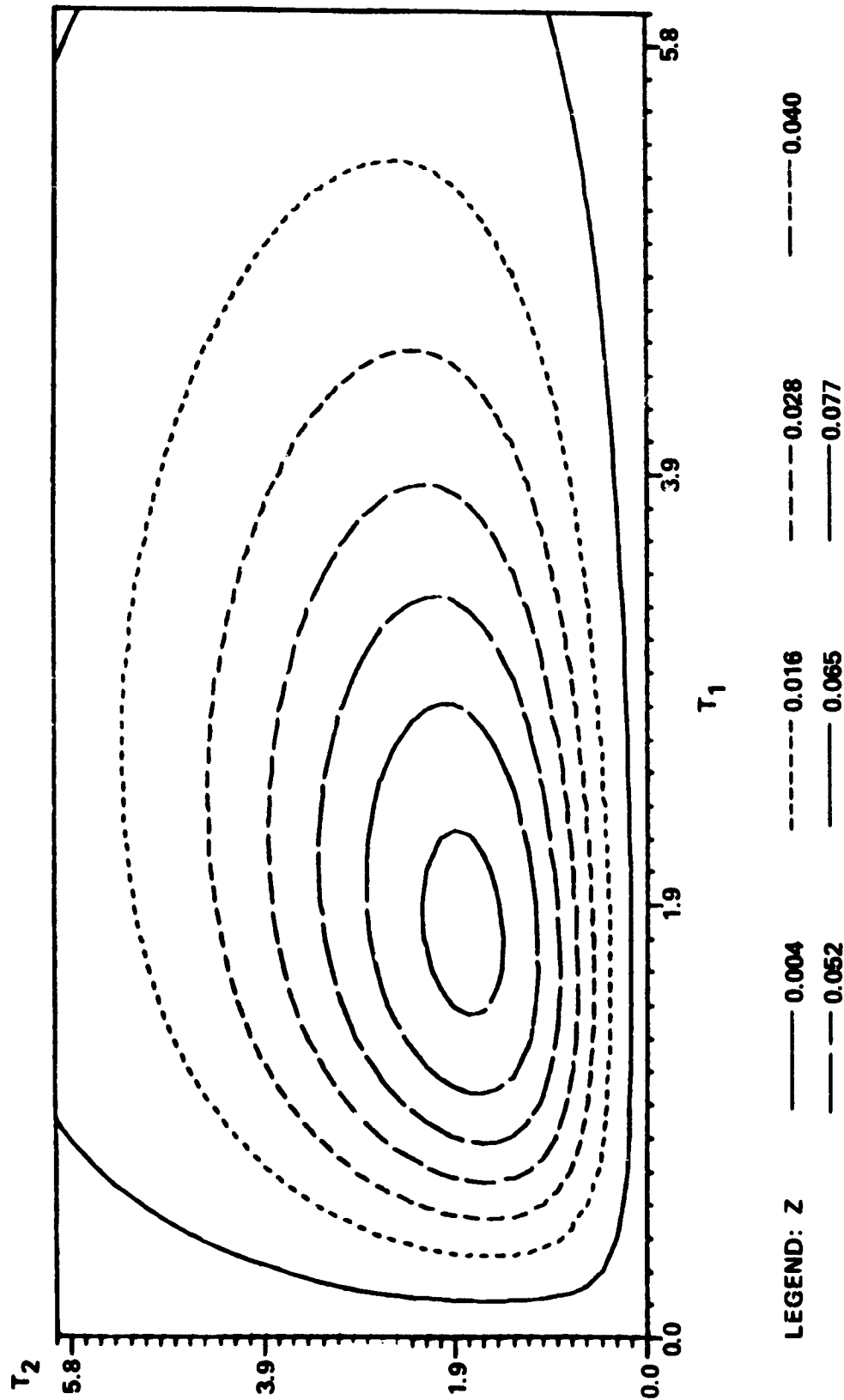


FIGURE A23. BIVARIATE GAMMA DENSITY CONTOURS, $\gamma_1 = \gamma_2 = 3.0$, $\rho = 0.25$

ORIGINAL PAGE IS
OF POOR QUALITY

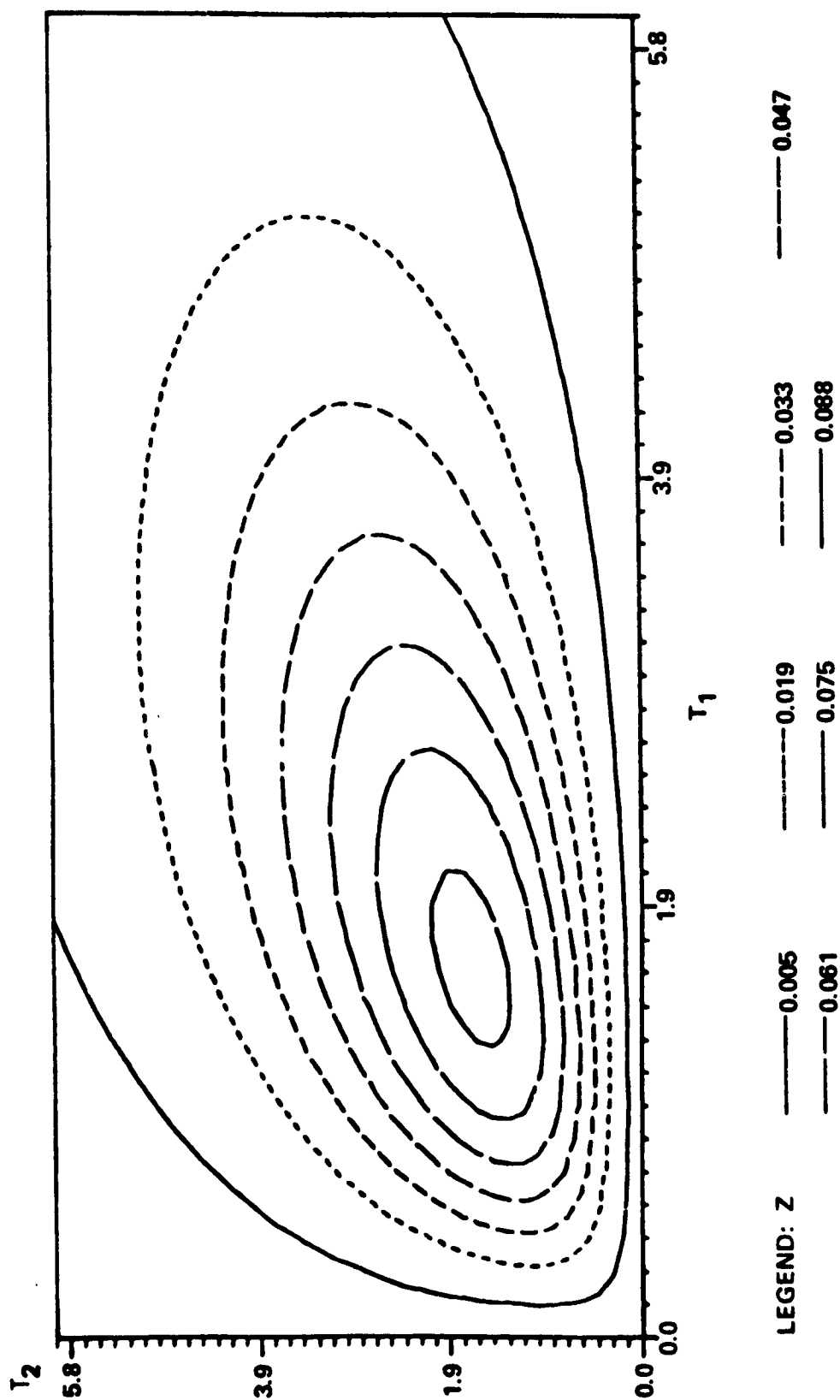


FIGURE A24. BIVARIATE GAMMA DENSITY CONTOURS, $\gamma_1 = \gamma_2 = 3$, $\rho = 0.50$

ORIGINAL PAGE IS
OF POOR QUALITY

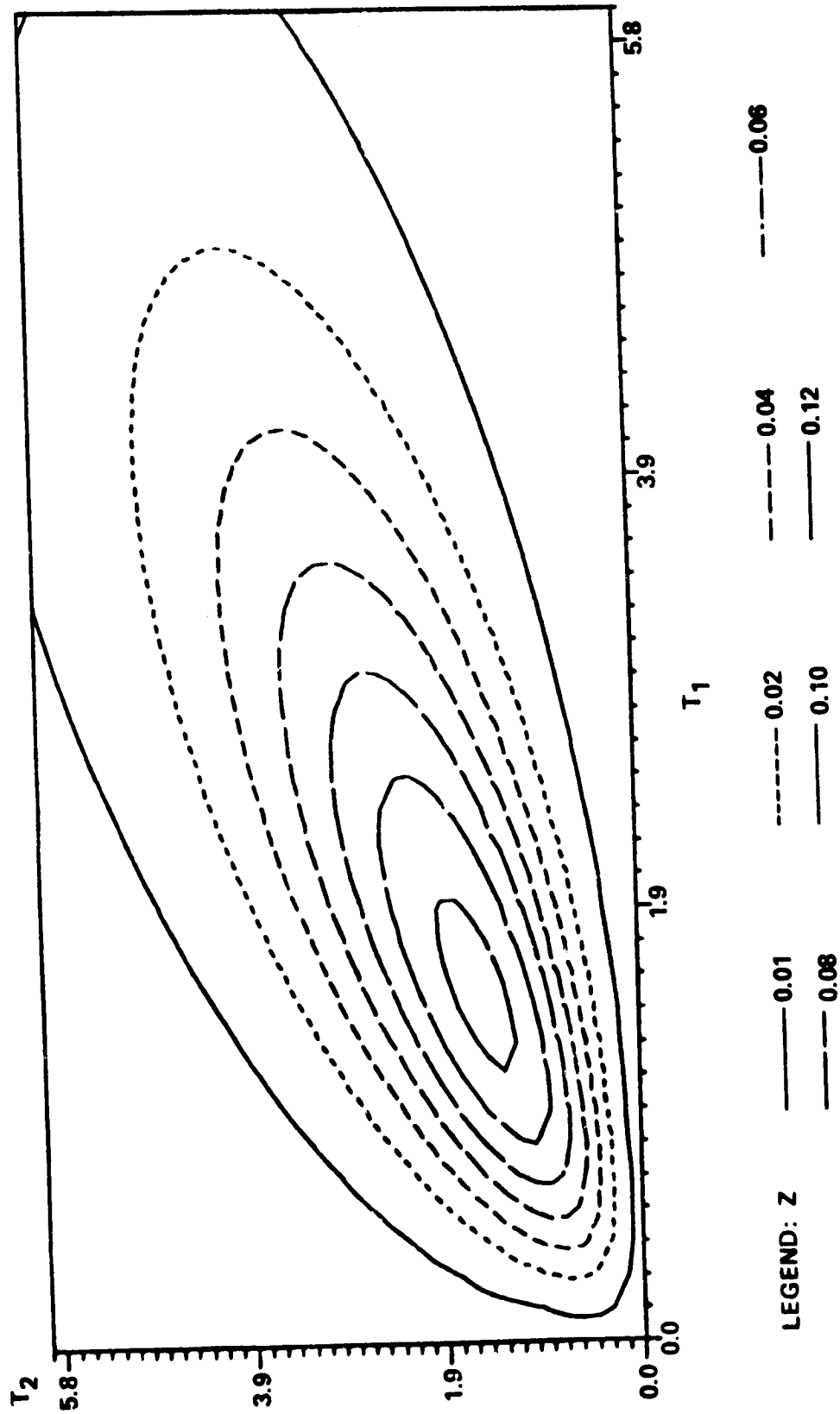


FIGURE A25. BIVARIATE GAMMA DENSITY CONTOURS, $\gamma_1 = \gamma_2 = 3.0$, $\rho = 0.75$

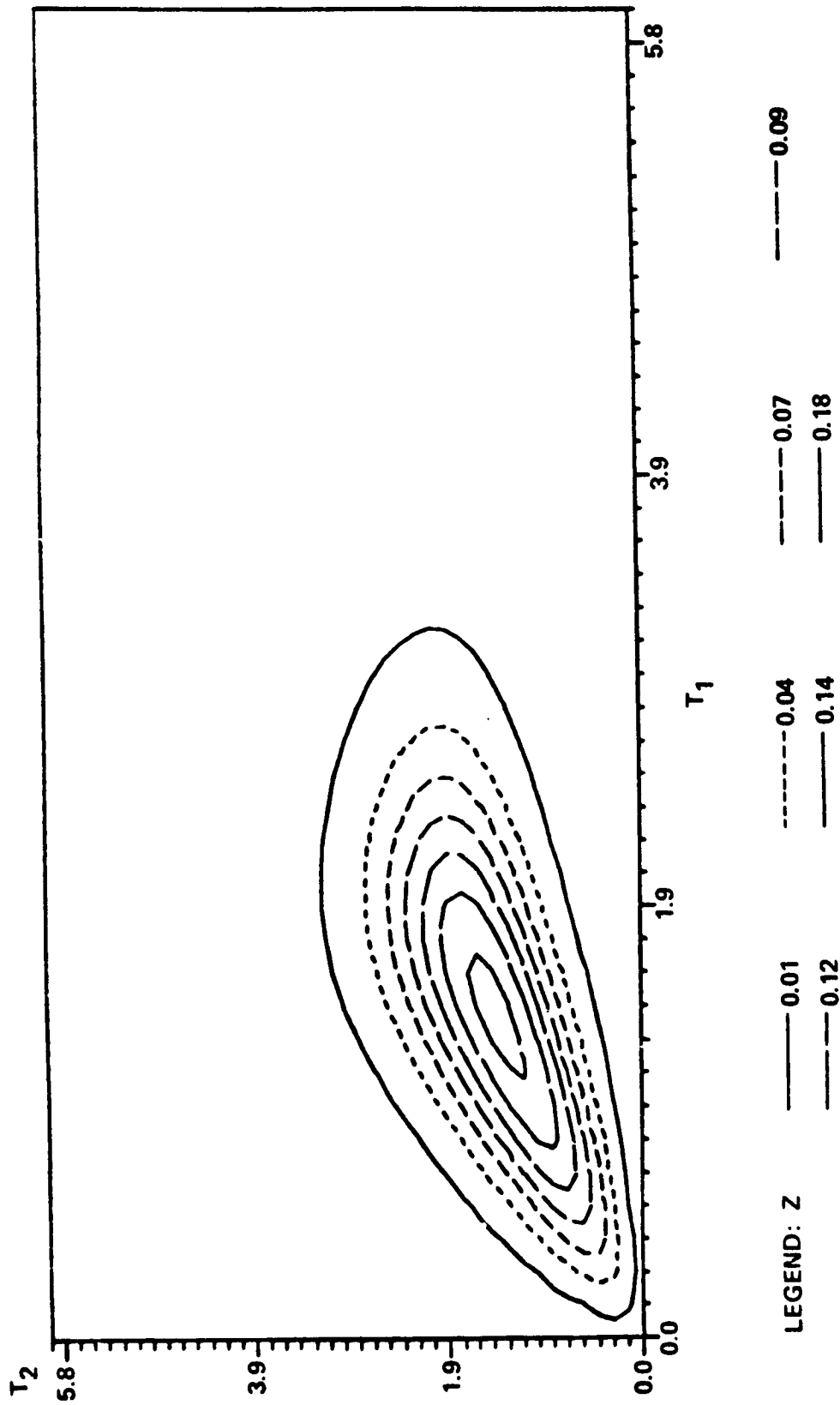


FIGURE A26. BIVARIATE GAMMA DENSITY CONTOURS, $\gamma_1 = \gamma_2 = 3.0$, $\rho = 0.90$

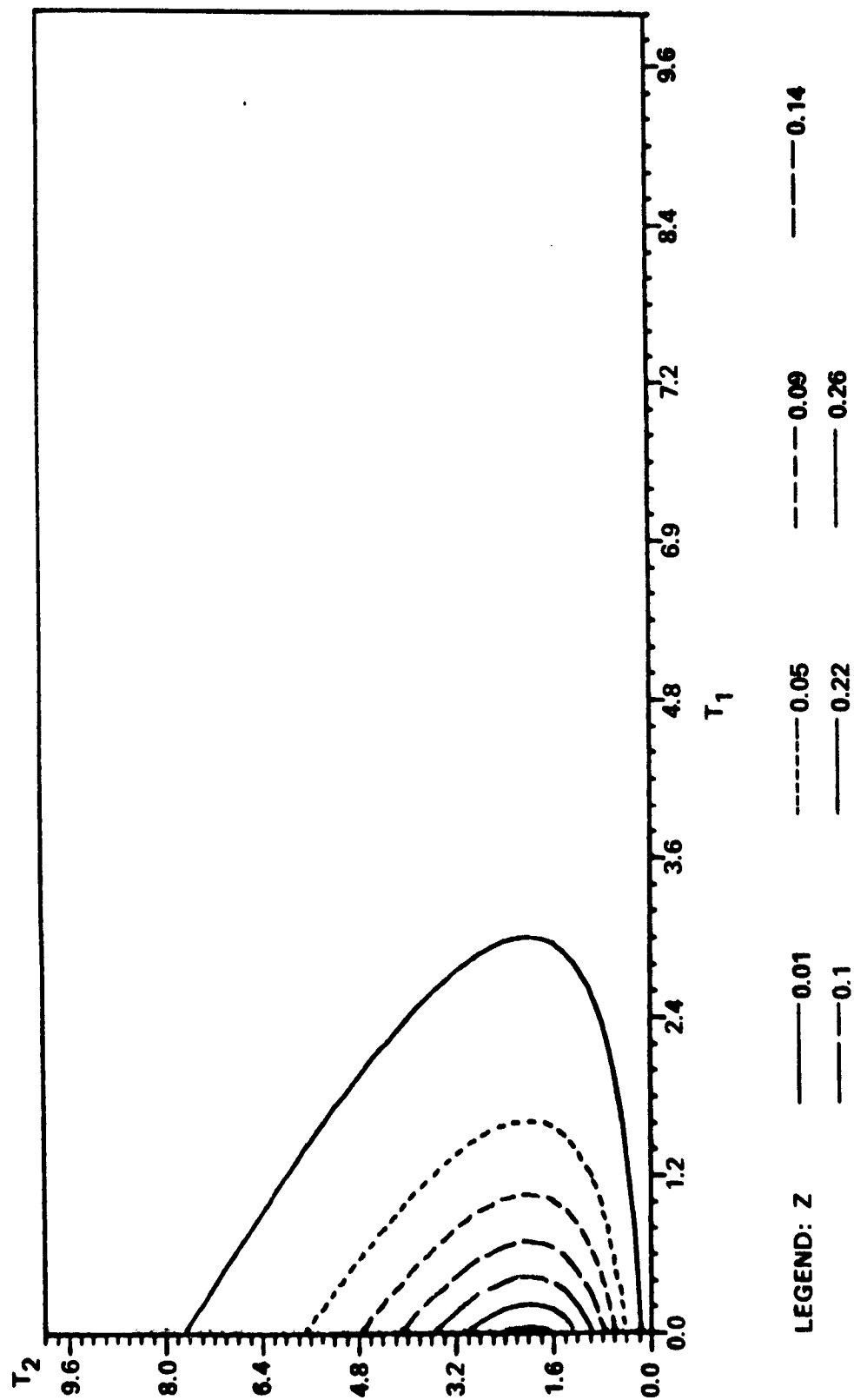


FIGURE A27. BIVARIATE GAMMA DENSITY CONTOURS, $\gamma_1 = 1.0$, $\gamma_2 = 3.0$, $\eta = 0.0$

ORIGINAL PAGE IS
OF POOR QUALITY.

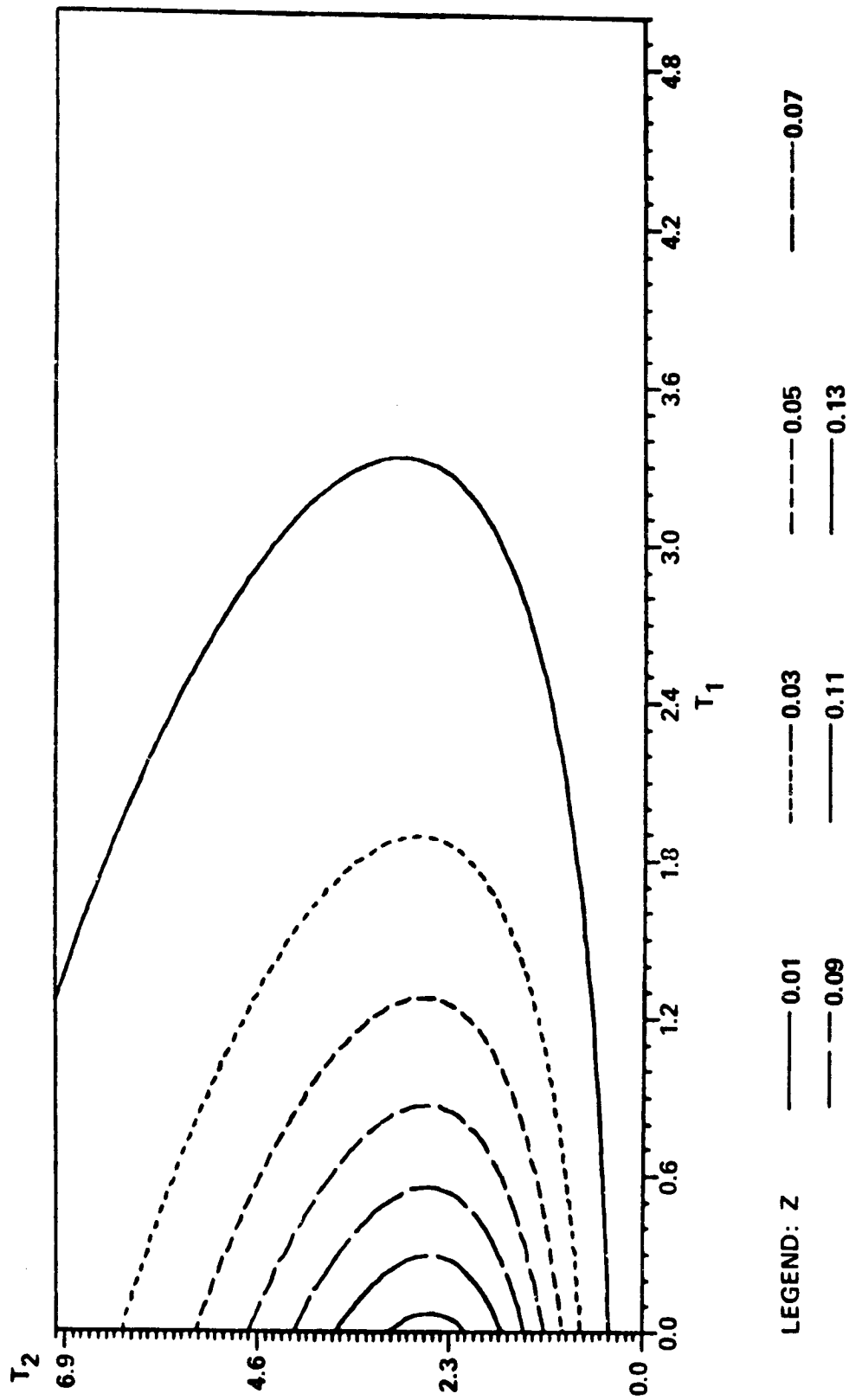


FIGURE A28. BIVARIATE GAMMA DENSITY CONTOURS, $\gamma_1 = 1$, $\gamma_2 = 3$, $\eta = 0.25$

ORIGINAL PAGE IS
OF POOR QUALITY

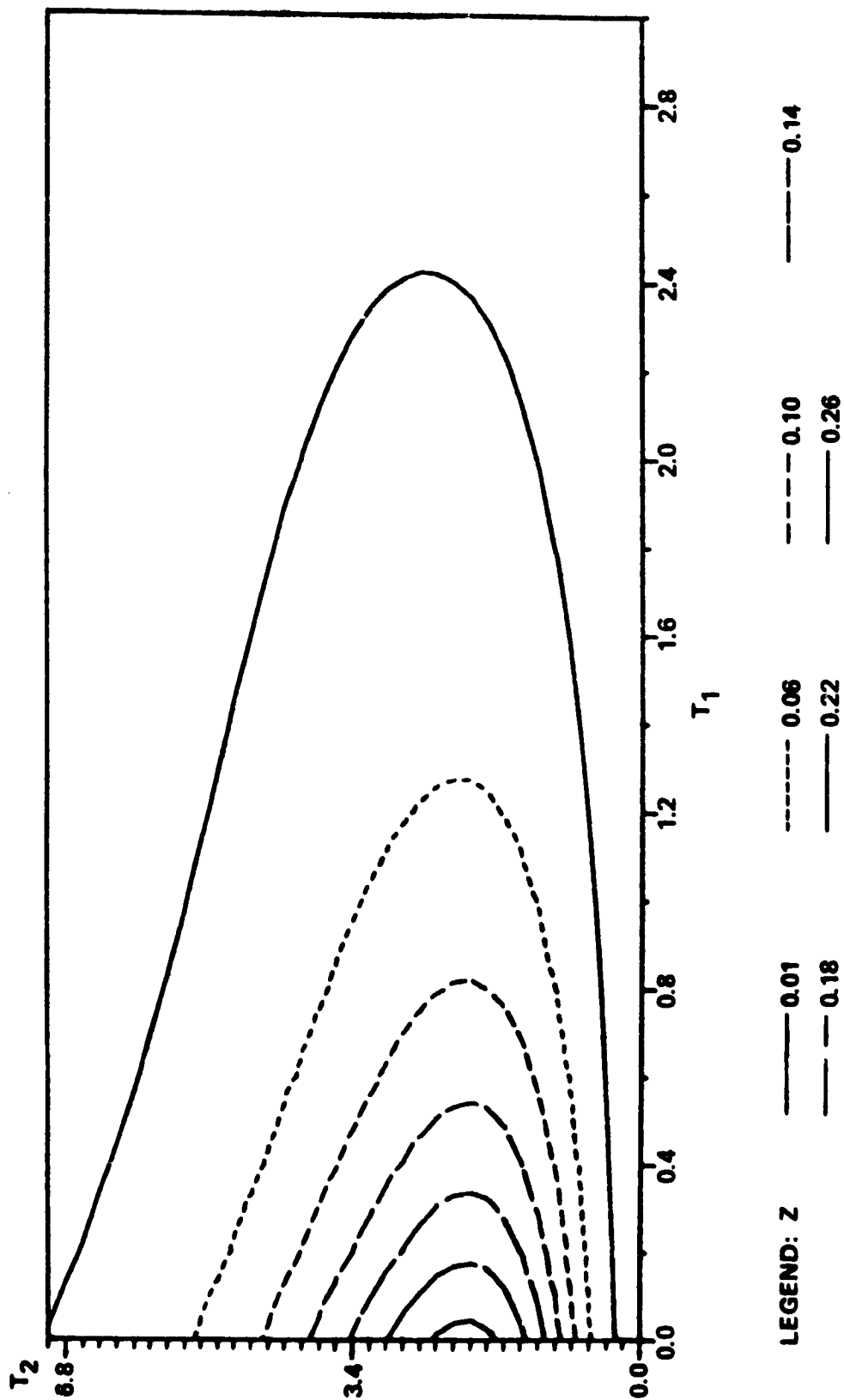


FIGURE A29. BIVARIATE GAMMA DENSITY CONTOURS, $\gamma_1 = 1$, $\gamma_2 = 3$, $\eta = 0.50$

ORIGINAL PAGE IS
OF POOR QUALITY

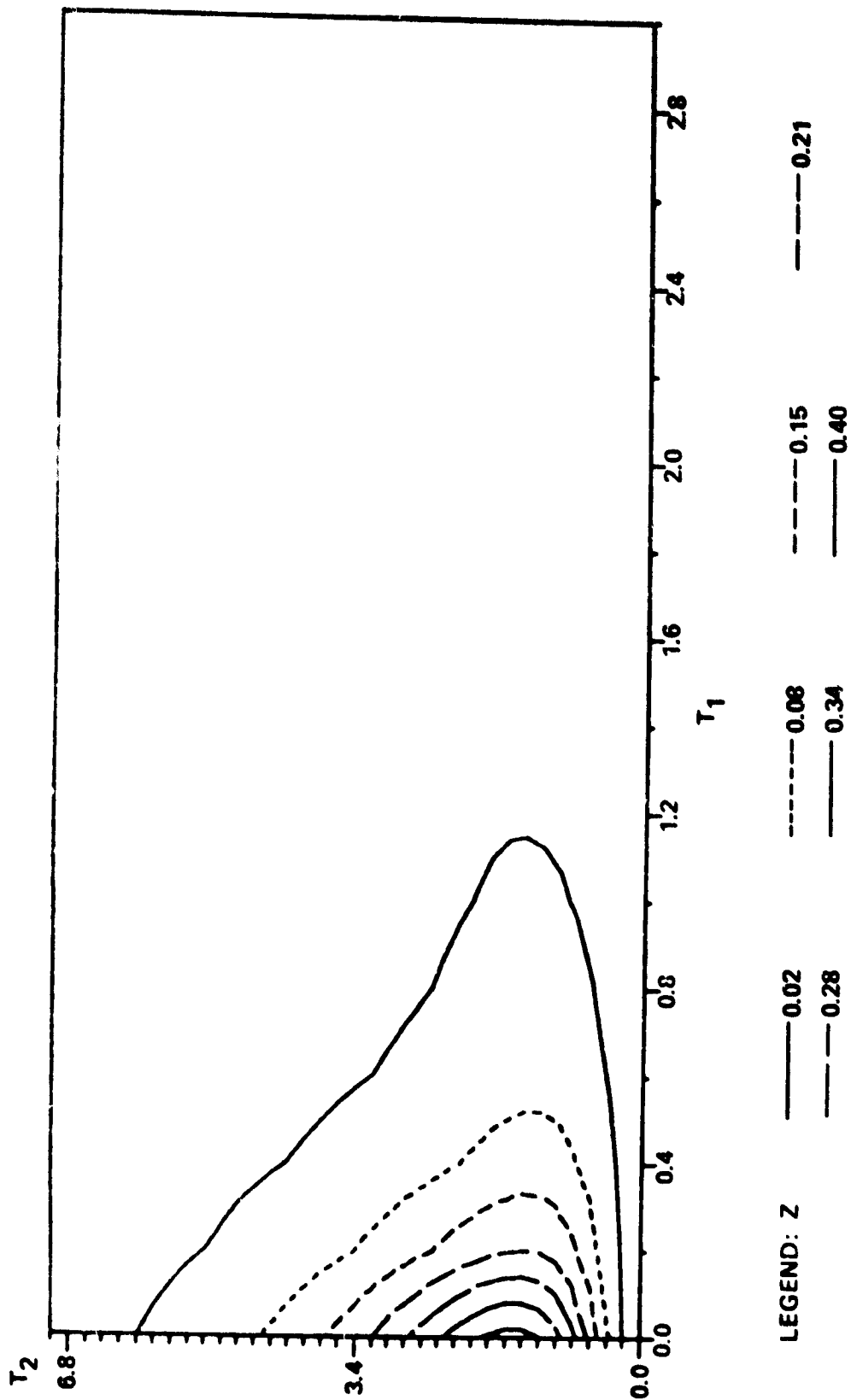


FIGURE A30. BIVARIATE GAMMA DENSITY CONTOURS, $\gamma_1 = 1$, $\gamma_2 = 3$, $\eta = 0.75$

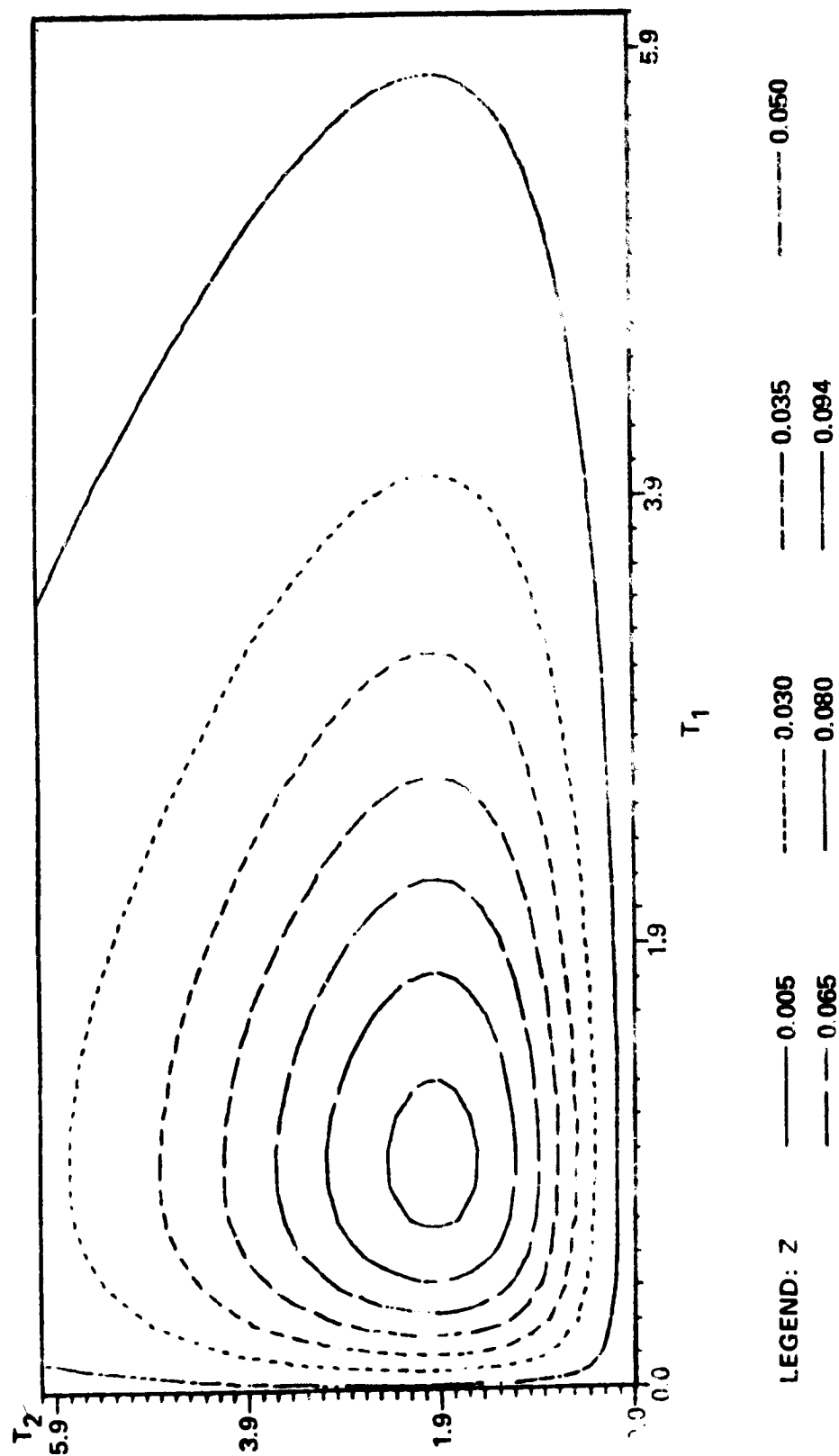


FIGURE 2.2. BIVARIATE GAMMA DENSITY CONTOURS, $\gamma_1 = 2$, $\gamma_2 = 3$, $\eta = 0$

ORIGINAL PAGE IS
OF POOR QUALITY

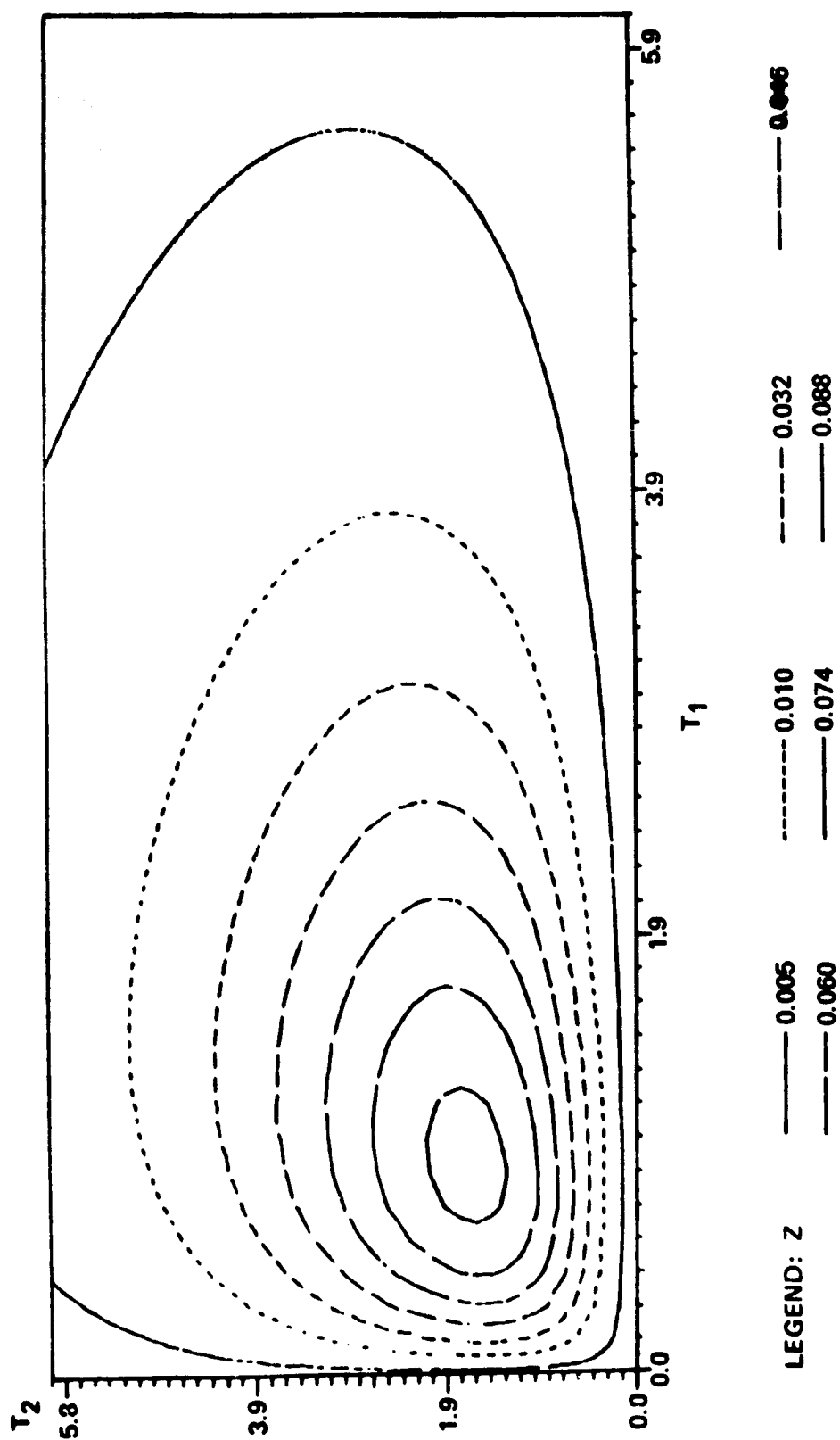


FIGURE A32 BIVARIATE GAMMA DENSITY CONTOURS, $\gamma_1 = 2$, $\gamma_2 = 3$, $\eta = 0.25$

ORIGINAL PAGE IS
OF POOR QUALITY

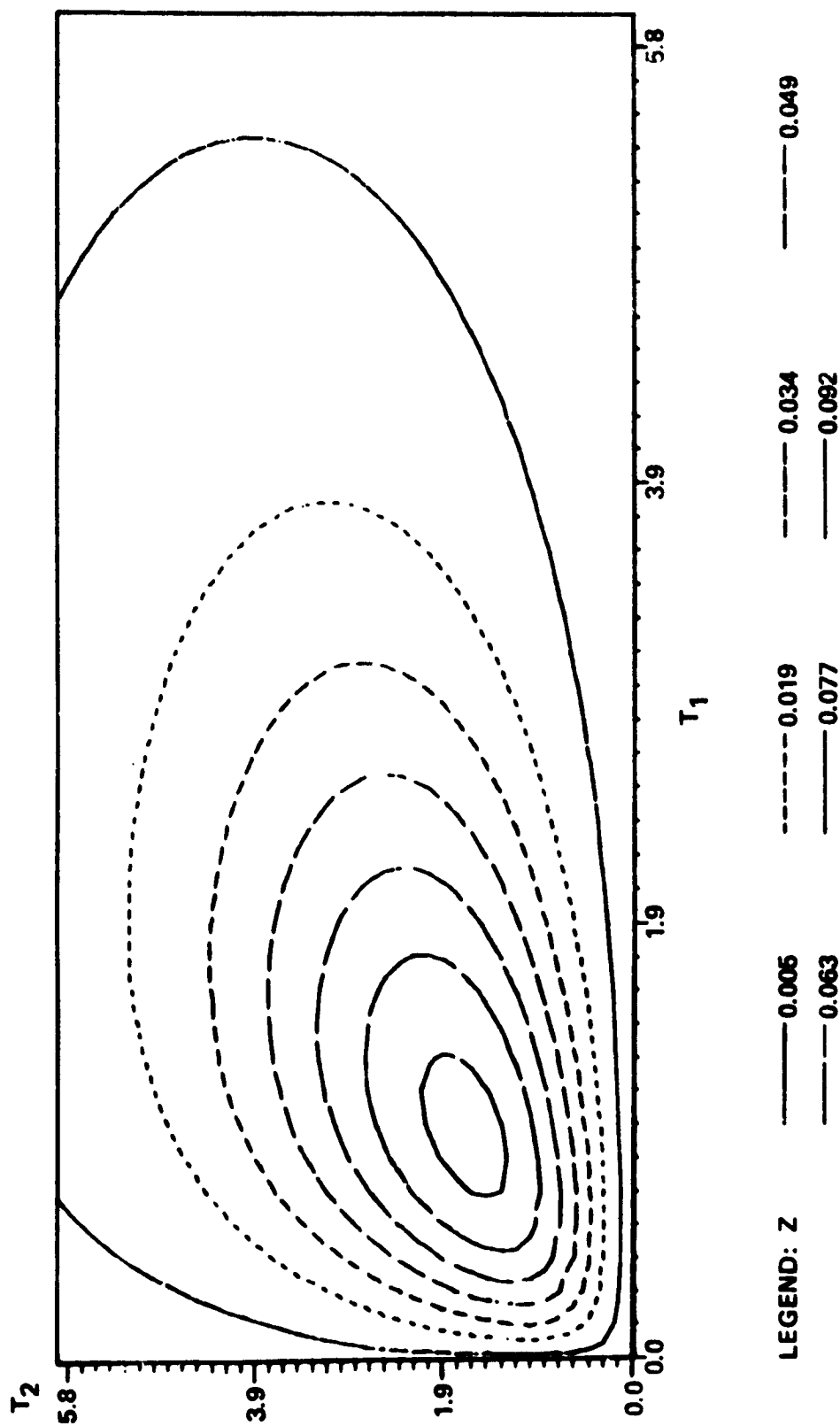


FIGURE A3.1 BIVARIATE GAMMA DENSITY CONTOURS, $\gamma_1 = 2$, $\gamma_2 = 3$, $\eta = 0.50$

ORIGINAL PAGE IS
OF POOR QUALITY

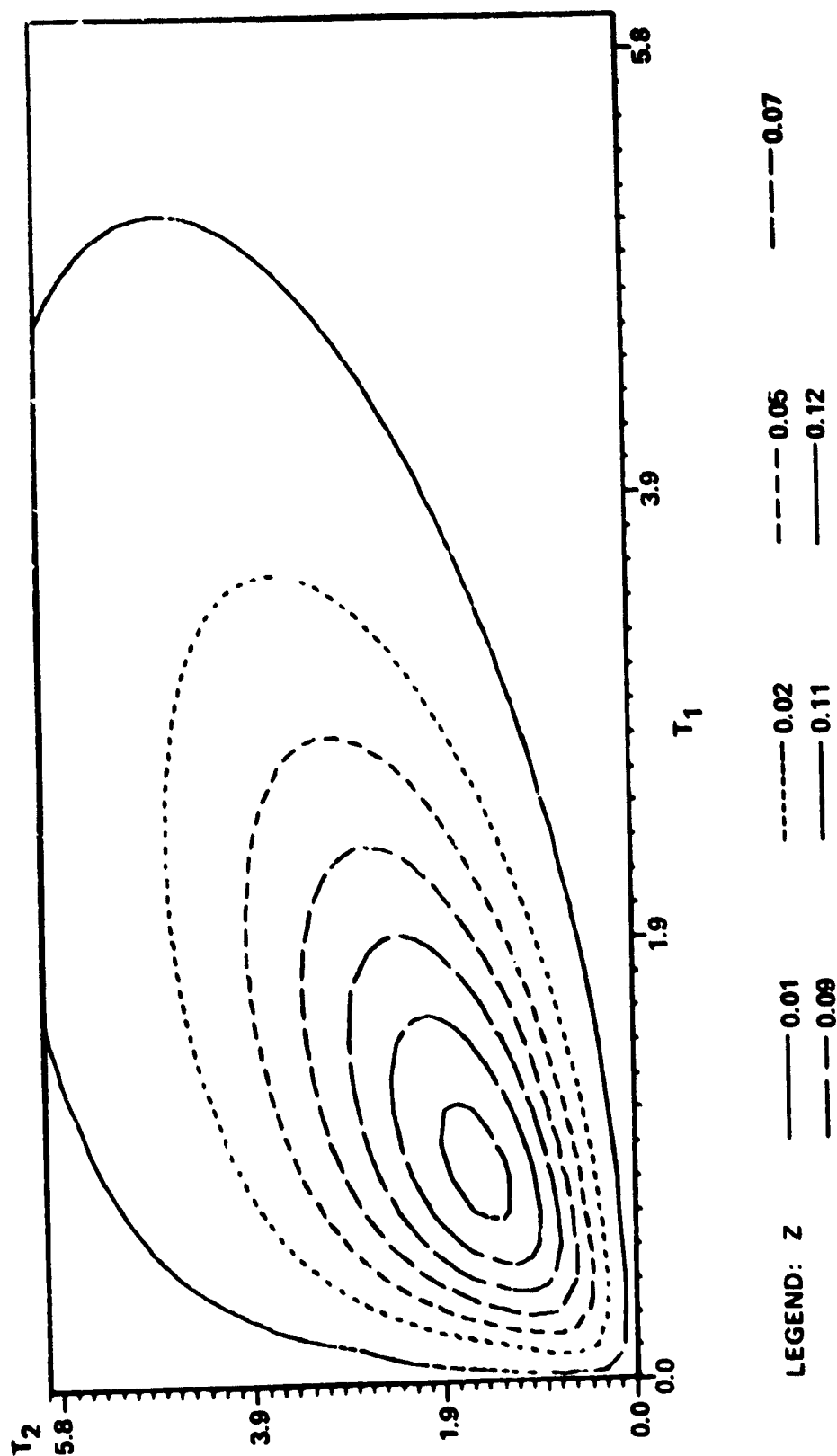


FIGURE A34 BIVARIATE GAMMA DENSITY CONTOURS, $\gamma_1 = 2$, $\gamma_2 = 3$, $\eta = 0.75$

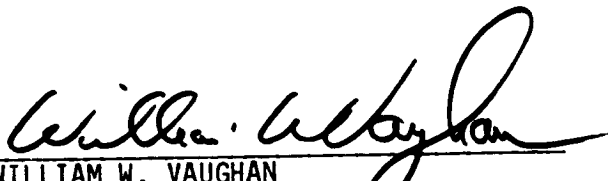
ORIGINAL PAGE IS
OF POOR QUALITY


APPROVAL

A BIVARIATE GAMMA PROBABILITY DISTRIBUTION
WITH APPLICATION TO GUST MODELING

By O. E. Smith, S. I. Adelfang,
and J. D. Tubbs

The information in this report has been reviewed for technical content. Review of any information concerning Department of Defense or nuclear energy activities or programs has been made by the MSFC Security Classification Officer. This report, in its entirety, has been determined to be unclassified.


WILLIAM W. VAUGHAN
Chief, Atmospheric Sciences Division


A. J. DESBLER
Director, Space Sciences Laboratory